Characterizing the role of NuA4 in glucose deprivation stress granule assembly and acetyl-CoA signaling in yeast

By

Meaghen Rollins

A Thesis submitted to the Faculty of Graduate and Postdoctoral Studies

In partial fulfillment of the requirements for the degree of MSc of Biochemistry

Department of Biochemistry, Microbiology and Immunology

Faculty of Medicine

University of Ottawa

ABSTRACT

A conserved mechanism of the cellular stress response is the formation of stress granules (SGs), cytoplasmic ribonucleoprotein (RNP) granules that contain translationally repressed messenger RNA (mRNA), translation initiation factors and numerous other proteins. Despite the strengthening association between SG assembly and cellular survival, the mechanisms regulating SG formation remain uncharacterized. Our lab identified a physical interaction between the lysine acetyltransferase (KAT) NuA4 and SG complex proteins (Pab1, Lsm12, Pbp1, and Pbp4) in *Saccharomyces cerevisiae*; which led us to hypothesize that lysine acetylation contributes to SG dynamics. Pab1 is a substrate for NuA4 *in-vitro* and the *in-vivo* acetylation state of Pab1 is dependent on NuA4. Further, we have determined that SG assembly upon glucose deprivation (GD) is dependent on NuA4. Thus, the objective of this project is to better define the role of NuA4 and other KATs and lysine deacetylases (KDACs) in GD SG dynamics. In addition to NuA4, the KAT Gcn5 and KDAC Rpd3 were implicated in the regulation of GD SG dynamics. It was also determined that cellular acetyl-CoA, a co-factor necessary for KAT activity, may serve as a regulator of GD SG assembly. Increasing levels of acetyl-CoA by either genetic or chemical means suppresses GD SG formation. Further, in order to identify downstream protein targets of NuA4 that may impact GD SG formation, a NuA4-dependent Pab1 protein interaction network was established under GD and non-stressed conditions. This interactome demonstrates that NuA4 impacts Acetyl-CoA Carboxylase 1 (Acc1). As Acc1 influences acetyl-CoA levels within the cell, and as acetyl-CoA impacts SG formation, this work has potentially uncovered a mechanism by which NuA4 regulates GD SG dynamics. Together this work reveals that acetyl-CoA, a metabolic readout of glucose availability, along with KAT/KDACs is a signalling pathway regulating GD SG dynamics.

ACKNOWLEDGEMENTS

Firstly, I would like to thank my supervisor Dr. Kristin Baetz for her continual support and advice throughout the completion of my studies.

I would like to express my thanks to Dr. Sylvain Huard for his guidance and help in conducting experiments and analyzing results essential to the completion of the work within this thesis.

Thank you to Jingwen Du, Jennifer Takuski, Amanda Defela, Dr. Mila Tepliakova, Mike Cotrut, Dr. Sylvain Huard, Dr. Mike Kennedy, Dr. Bo Liao, David Czosniak, and Louis Dacquay for their guidance and friendship over the entirety of my studies.

I would also like to thank Dr. Daniel Figeys for providing mass spectrometry analysis and Dr. Fullerton and his lab for conducting Acc1 activity assays and for providing me with Acetyl-CoA Carboxylase Antibody.

Finally, thank you to my family and friends for their unwavering support and love.

TABLE OF CONTENTS

LIST OF ABBREVIATIONS

Acetyl-CoA	Acetyl Coenzyme-A
Ac-K	Acetyl-Lysine
ALS	Amyotrophic Lateral Sclerosis
AMPK	AMP Kinase
ANOVA	Analysis of Variance
BF	Bright Field
BME	2-β-mercaptoethanol
CEN	Centromere (Low copy plasmid)
cDNA	Complementary deoxyribonucleic acid
Co-IP	Co-immunoprecipitation
DEPC	Diethylpyrocarbonate
DNA	Deoxyribonucleic Acid
DNase	Deoxyribonuclease
DTT	Dichlorodiphenyltrichloroethane
EDTA	Ethylenediaminetetraacetic acid
EGTA	Ethylene Glycol Tetraacetic acid
EtOH	Ethanol
FAB	Fatty Acid Biosynthesis
FITC	Fluorescein isothiocyanate
G6PDH	Glucose-6-phosphate dehydrogenase
GD	Glucose Deprivation
+ Glucose	Media Containing 2% Glucose
GFP	Green Fluorescent Protein
GNAT	Gcn5-related N-acetyltransferases
H3	Histone 3
H4	Histone 4
HAT	Histone Acetyltransferase
HCl	Hydrochloric acid
HEPEs	4-(2-hydroxyethyl)-1-piperazineethanesulfonic acid
HPR	Horseradish Peroxidase
Icl1	Immunoglobulin G
IgG	IsoCitrate Lyase 1
Interactome	Protein Interaction Network
IP	Immunoprecipitation
KAT	Lysine Acetyltransferase
KDAC	Lysine Deacetylase
LC-MS/MS	Liquid Chromatography–Mass Spectrometry
Malonyl-CoA	Malonyl-Coenzyme A
MS	Mass Spectrometry
mChIP	Modified Chromatin Immunoprecipitation
mRNA	Messenger ribonucleic acid
MYST	MOZ, Ybf2/Sas3, Sas2, and Tip60
NAD+	Nicotinamide adenine dinucleotide
NP-40	Nonidet P-40
OD600	Optical Density at 600nm
PAGE	Polyacrylamide gel electrophoresis
P-bodies	Processing Bodies

PCR	Polymerase Chain Reaction
PicNuA4	piccolo NuA4 sub-complex
PKA	Protein Kinase A
PTM	Post-translational Modification
qPCR	Quantitative Polymerase Chain Reaction
RNA	Ribonucleic Acid
RNase	Ribonuclease
RNP	Ribonucleoprotein
RPM	Rotations per minute
RT-PCR	Reverse Transcriptase Polymerase Chain Reaction
SC	Synthetic Complete
SD	Standard Deviation
SDS	Sodium monododecyl sulfate
SG	Stress Granule
TAP	Tandem Affinity Purification
TCA	Trichloroacetic acid
TRIS	Tris(hydroxymethyl)aminomethane
T-test	Students t-test
TxRed	Texas Red
WCE	Whole Cell Extract
WT	Wild type
YP	Yeast Peptone
YPD	Yeast Peptone Dextrose
Tet07	Tetracycline Repressible Promoter
tTA	Tetracycline Transactivator

LIST OF FIGURES

LIST OF TABLES

1. INTRODUCTION

Upon exposure to an environmental stress, eukaryotic cells implement a cellular response in order to promote survival. Stress granule formation is one of the mechanisms of this survival response. Under conditions of stress such as GD, this dynamic process involves the formation of cytoplasmic ribonucleoprotein granules which sequester and protect translationally repressed mRNA from degradation (Teixeira, Sheth et al. 2005, Buchan and Parker 2009, Swisher and Parker 2010). Despite the strengthening association between SG assembly and neurodegenerative disease (Ginsberg, Galvin et al. 1998, Nonhoff, Ralser et al. 2007, Ito and Suzuki 2011) and the implication of SGs as contributors to chemotherapy resistance (Arimoto, Fukuda et al. 2008, Fournier, Gareau et al. 2010, Fournier, Coudert et al. 2013, Thedieck, Holzwarth et al. 2013), the mechanisms regulating SG formation remain uncharacterized.

Many of the core SG proteins in humans possess homologues that exhibit the same function in yeast (**Table 1**) (Buchan, Nissan et al. 2010). Thus, this study uses *Saccharomyces cerevisiae* as a model to characterize the role of KATs and KDACs as well as acetyl-CoA in SG dynamics. Additionally, Acc1 is determined to be a novel target of NuA4, identifying a potential mechanism of GD SG regulation.

Yeast Protein	Mammalian Homologue	Reference
Ded1	DDX3	(Hilliker, Gao et al. 2011)
Lsm12	LSM12	(Swisher and Parker 2010)
Ngr1	TIAR	(Buchan, Muhlrad et al. 2008)
Pab1	PABP	(Hoyle, Castelli et al. 2007)
Pbp1	ATAXIN-2	(Buchan, Muhlrad et al. 2008)
Pub1	TIA-1	(Buchan, Muhlrad et al. 2008)

Table 1: Human homologues of core yeast stress granule proteins have also been localized to stress granules.

1.1 Lysine Acetylation, KATs/KDACs, and NuA4

Lysine Acetylation and KATs/KDACs

Lysine acetylation is a post translational modification (PTM) involving the addition of an acetyl group to the ε-amino-group of a lysine residue by KATs (Polevoda and Sherman 2002) (**Figure 1**; modified from Kim et al. 2010). This modification can be reversed, and the acetyl group on the lysine residue removed by KDACs (Bernstein, Tong et al. 2000) (**Figure 1**; modified from Kim et al. 2010).

Presently, 11 KATs have been identified in *S.cerevisiae*. Lysine acetyltransferases have been organized into 3 families based on structural motifs similarities (Arany Z et al. 1994, Neuwald et al. 1997, Reifsnyder et al. 1996). GNAT (Gcn5-related N-acetyltransferases), is the largest family of nuclear KATs that contain a highly conserved HAT domain along with an amino-terminal domain, an Ada2p interaction domain, and a carboxy-terminal bromodomain (Xu et al. 1998, Candau et al. 1997, Candau et al. 1996, Reviewed in: Roth, Denu et al. 2001). The GNAT family within yeast consists of Gcn5, Hat1, Elp3, Eco1, and Hpa2 (Roth, Denu et al. 2001). The MYST (MOZ, Ybf2/Sas3, Sas2, and Tip60) family in yeast have been implicated in a diverse range of cellular processes. Despite the proteins in this family having the highly conserved HAT domain described above for the GNAT family, sequences for the proteins within this family are more diverse (Roth, Denu et al. 2001). MYST family proteins include Sas3, Sas2, and Esa1 (Roth, Denu et al. 2001). Finally, p300/CBP proteins possess a highly conserved bromodomain, cysteine histidine rich module, Ada2p interaction domain and HAT domain (Arany Z et al. 1994). In yeast, the p300/CBP family consists of Rtt109, Taf1, and Spt10 (Steger, Eberharter et al. 1998, Roth, Denu et al. 2001, Lee and Workman 2007).

There are currently 10 KDACs that have been classified in *S. cerevisiae*. Lysine deacetylases are organized into 3 families based on sequence homology (Gregoretti, Lee et al. 2004). Both Class 1 KDACs (Rpd3, Hos1, and Hos2) and Class 2 KDACs (Hda1 and Hos3) are zinc-dependent. Class III KDACs (Sirtuins) in yeast include Sir2 and Hst1-4. The Sirtuins require NAD+ for deacetylation to occur (Shore 2000, Smith, Avalos et al. 2002).

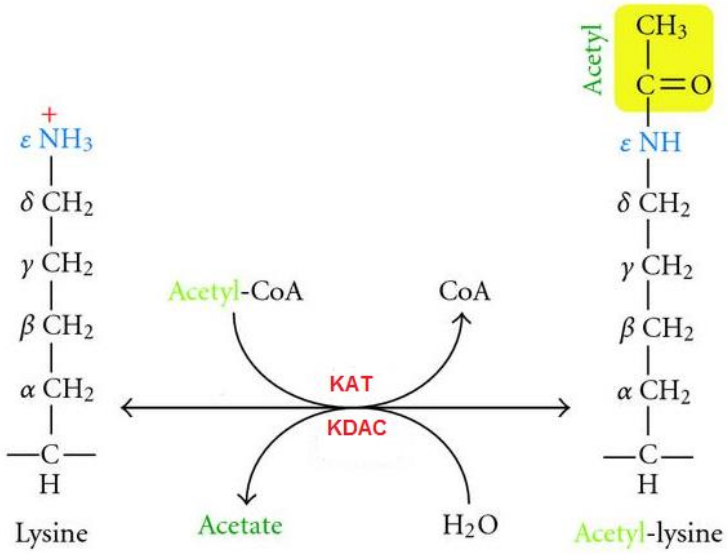

Figure 1: Schematic illustrating forward and reverse lysine acetylation reaction (modified from: Kim et al. 2010).

Impact of lysine acetylation on the cell

Traditionally, it was thought that lysine acetylation took place exclusively on histones as a means of transcriptional regulation (Reviewed in: Oliver and Denu 2011). Dynamic acetylation and deacetylation of histones, respectively eliminates or restores the positive charge of a lysine residue allowing for the conversion between heterochromatin and euchromatin (Reviewed in: Oliver and Denu 2011). Recent acetylome studies have identified acetylation sites on thousands of non-histone protein targets, indicating that the cellular role of acetylation is not limited to transcriptional events (Choudhary, Kumar et al. 2009, Wang, Zhang et al. 2010, Henriksen, Wagner et al. 2012). As described below, using targets of NuA4 as examples, acetylation can have great impact on many essential cellular processes.

Targets of the Lysine Acetyltransferase Complex, NuA4

Nucleosome acetyltransferase histone H4 (NuA4) is the yeast homologue of the human lysine acetyltransferase Tip60. NuA4 is implicated in a wide range of cellular processes such as the stress response (Lindstrom, Vary et al. 2006), septin dynamics (Mitchell, Lau et al. 2011), cell cycle (Clarke, Lowell et al. 1999) and autophagy (Yi, Ma et al. 2012). Though the most characterized targets of NuA4 include histone proteins H4 and Htz1 (Allard, Utley et al. 1999, Keogh, Mennella et al. 2006, Cheng et al. 2015, Krogan, et al. 2004), studies have shown that the impact of NuA4 on the regulation of gene expression is minor (Choy, Tobe et al. 2001, Krogan, Baetz et al. 2004, Zhang, Richardson et al. 2004, Lindstrom, Vary et al. 2006). This suggests that the acetylation of non-histone targets may explain some of the diverse cellular functions of NuA4. In fact, protein microarrays and proteome studies have identified over 200 *in-vitro* targets of NuA4 (Lin, Lu et al. 2009, Fournier, Gareau et al. 2010, Mitchell, Huard et al. 2013) whereby many of these targets are implicated in the cellular metabolism and stress response (Yi, 2012, Lu,

Lin et al. 2011, Lindstrom, Vary et al. 2006). The following examples of NuA4 targets describe the various mechanisms in which acetylation impacts diverse cellular processes. 1) Acetylation can regulate protein stabilization. For instance, NuA4 auto-acetylates Yng2, a component of the piccolo catalytic sub-complex of NuA4 itself which leads to protein stability (Lin, Qi et al. 2008). When this site is deacetylated by the KDAC Rpd3 the protein is targeted for degradation (Lin, Qi et al. 2008). 2) Acetylation can impact cellular protein levels through regulation of autophagy. For example, NuA4 is required for Atg8 translocation into vacuoles. This relocalization is necessary for proper autophagy function upon stresses such as nitrogen starvation (Yi, 2012). 3) Acetylation can act as a molecular switch. Pck1's enzymatic activity, responsible for the conversion of non-fermentable carbon sources to glucose, is dependent on acetylation by NuA4 (Lin, Lu et al. 2009). 4) Acetylation can regulate protein interactions. NuA4-dependent acetylation of Sip2 enhances the Sip2-Snf1 interaction. This causes inhibition of Snf1 kinase activity (AMPK homology); a key kinase required for response to starvation (i.e. for transcription of glucose repressed genes) (Lu, Lin et al. 2011). Further, lysine acetylation may influence protein-protein interactions by establishing binding sites on a protein, thus allowing for interactions with bromodomains (Mujtaba, He et al. 2004).

NuA4 Structure and Function

NuA4 is a modular KAT complex that is composed of the essential acetyltransferase catalytic subunit Esa1 along with 12 additional subunits (**Figure 2**; obtained from Chittuluru et al. 2011).

The acetyltransferase activity of NuA4 is attributed to the piccolo complex containing Epl1/Yng2/Eaf6, and Esa1 which is known to acetylate histone H4 (**Figure 2**; obtained from Chittuluru et al. 2011) (Boudreault, Cronier et al. 2003). The piccolo complex (PicNuA4) can exist independent from the additional recruitment module subunits (Boudreault, 2003). In fact,

PicNuA4 can acetylate histone H4 in an unregulated manner when not associated to recruitment modules (Boudreault, 2003). As Esa1 is essential, an Esa1 temperature-sensitive allele is use to study the effect of NuA4 catalytic activity on a specific pathway or process within the cell. Upon temperature shift to 37^{o}C, the *esa1-L254P* mutant loses *in-vivo* catalytic activity and eventually leads to the cell being inviable.

Molecular dissection has shown that NuA4 is a multi-subunit complex that requires the Eaf1 scaffolding protein for its assembly. Knocking-out *EAF1*causes the piccolo NuA4 sub-complex and the recruitment modules to separate (Auger, Galarneau et al. 2008, Mitchell, Lambert et al. 2008). This dissociation results in defects in global histone acetylation (Auger, Galarneau et al. 2008, Cheng et al. 2015, Huang and Tan 2013) and ultimately results in fitness deficiencies that reflect a loss in function of the NuA4 complex (Dudley, Janse et al. 2005, Auger, Galarneau et al. 2008, Mitchell, Lambert et al. 2008, Sinha, David et al. 2008).

The recruitment module sub-complexes consist of Eaf3/Eaf5/Eaf7, Act1/Arp4/Swc4/Yaf9, and Tra1. These sub-complexes direct NuA4 to non-histone protein targets and other specific genomic loci. For example, overexpression of septin genes *CDC11* and *SHS1* is toxic in *EAF5* and *EAF7* mutants (Mitchell et al. 2011), suggesting a role for recruitment module sub-complexes in NuA4's regulation of these targets. Deletion of sub complexes Eaf3/5/7 does not disrupt the full NuA4 complex and these mutants appear to display only a subset of *esa1-ts* or *eaf1Δ* cellular defects or genetic interactions (Mitchell et al. 2008, Rossetto, Cramet et al. 2014). As deletion of *EAF1* possesses severe fitness defects, *eaf7Δ* is used to confirm data and to eliminate the possibility that phenotypes are a reflection of *eaf1Δ* growth defects.

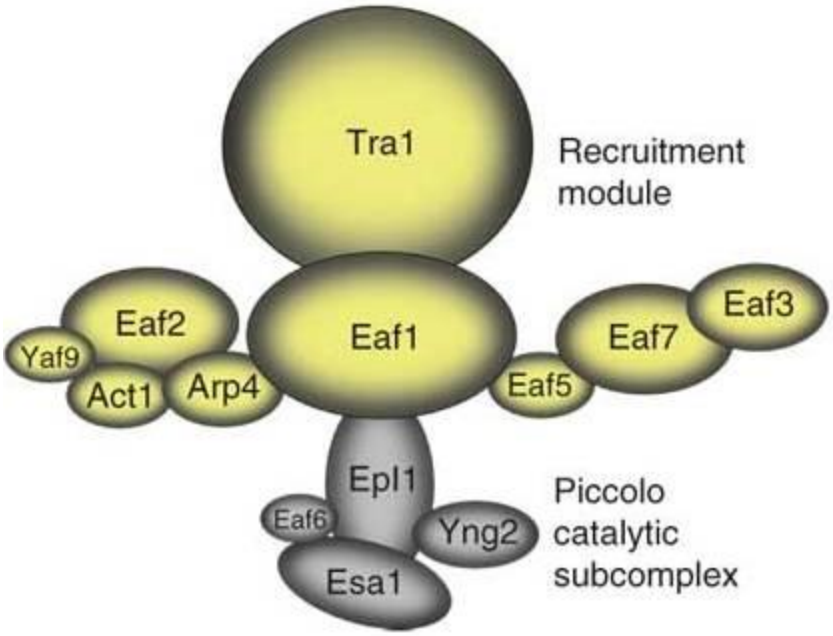

Figure 2: Schematic of the NuA4 complex (Chittuluru et al. 2011). Components of NuA4 indicated on figure.

1.2 Stress Granules

Stress Granules and Disease

A conserved mechanism of the cellular stress response is the formation of SGs, cytoplasmic RNP granules that contain translationally repressed mRNA, translation initiation factors and numerous other proteins (Buchan, Nissan et al. 2010). These mRNPs are thought to serve as sites of storage, responsible for retaining mRNA in a non-translating state before being returned to translation or sorted to processing bodies (p-bodies) for degradation (Buchan, Nissan et al. 2010) (**Figure 3;** obtained from Jennifer Takuski Baetz Lab, MSc Thesis 2014). Stress granules are also considered sites for sequestering key cell signalling pathways. Stress granules sequester pro-apoptosis factors thus preventing cell initiated death in times of stress (Arimoto, Fukuda et al. 2008, Thedieck, Holzwarth et al. 2013). For instance, upon stress, the mTORC1 component raptor is sorted to SGs thus suppressing mTORC1- induced apoptosis (Thedieck, Holzwarth et al. 2013). The sequestration of pro-apoptosis proteins, such as raptor, has been shown to contribute to resistance to chemotherapy treatment as sequestration of pro-apoptosis factors promotes cancer cell survival (Arimoto, Fukuda et al. 2008, Fournier, Gareau et al. 2010, Gareau, Fournier et al. 2011, Fournier, Coudert et al. 2013, Thedieck, Holzwarth et al. 2013). Stress granules are also defined as phenotypic markers of neurodegenerative diseases such as Alzheimer's, ALS, multisystem proteinopathy and frontotemporal lobar degeneration (Castellani, Gupta et al. 2011, Ito and Suzuki 2011, Kim, Tresse et al. 2013). Despite the strengthening association between SG formation and diseases as well as chemotherapy resistance, the regulation of SG formation remains uncharacterized. It is crucial to resolve the mechanisms regulating SG assembly to better understand their role in numerous diseases.

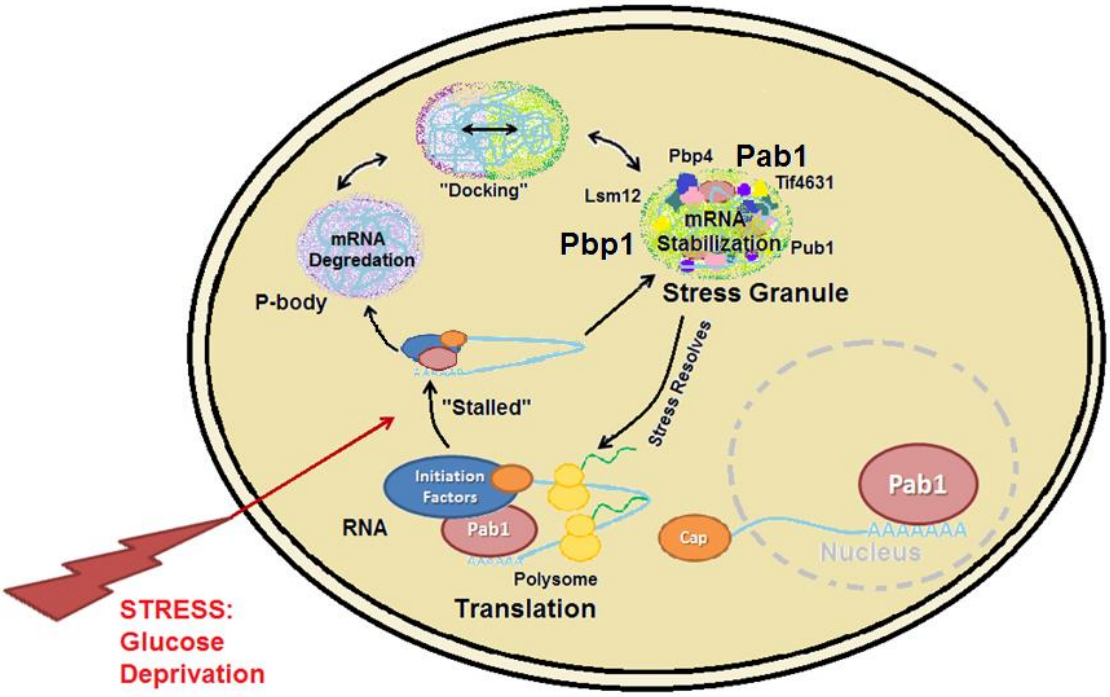

Figure 3: Lifecycle of mRNA. Following transcription of mRNA Pab1 binds to its poly-A tail. Pab1 binds with translation initiation factors and other proteins to form a closed loop structure allowing for translation to occur (binding of polysomes). Upon stress, such as GD, translation is inhibited and mRNAs are sorted to either P-bodies (for degradation) or to SGs. (Obtained from: Jennifer Takuski Baetz Lab, MSc Thesis 2014).

Stress Granule Composition

Stress granules are highly conserved. In fact, the human homologues of yeast SG proteins have also been localized to SGs (**Table 1**) (Buchan, Nissan et al. 2010). The *S. cerevisiae* Poly (A) Binding Protein 1 (Pab1) is an essential protein that possesses a high affinity to the poly-A tail at the 3' end of mRNA (Sachs, Davis et al. 1987). Under stress conditions, initiation of translation is inhibited and a subset of Pab1 and its associated mRNA localizes to SGs where it is likely protected from degradation. Pab1 is a component of both yeast and mammalian SGs and is commonly used as a marker when quantifying SG formation under various stresses such as GD (Swisher and Parker 2010). It is essential to acknowledge that the mRNA and protein composition within SGs is dependent on the type of stress that the cell is exposed to. In yeast, eIF3 is present in SGs during heat shock but not during GD stress (Grousl, Ivanov et al. 2009). Presently the mechanisms regulating the stress-dependent composition of SGs are not known.

Stress Granules and Lysine Acetylation

Lysine acetylation is a conserved process that can be found on core SG proteins in both yeast and mammals (Choudhary, Kumar et al. 2009, Henriksen, Wagner et al. 2012, Mitchell, Huard et al. 2013). In mammals, the lysine deacetylase HDAC6 has been implicated in the regulation of SG formation (Kwon, Zhang et al. 2007). Not only has this KDAC been localized to SGs but a reduction in HDAC6 function results in a significant reduction of the number of SGs that form under stress (Kwon, Zhang et al. 2007). Further, a high content microscopy screen identified over 100 deletion mutants that exhibited constitutive SG formation under non-stress-conditions. These deletion mutants included the KAT Gcn5 and KDACs Hst1 and Sir2 which suggests either that these KATs and KDACs have a role in SG disassembly/inhibition or that these strains are naturally in a semi-stressed state (Buchan, Kolaitis et al. 2013). Data from the Baetz lab has established that NuA4 physically co-purifies with SG complex proteins (Pab1, Lsm12, Pbp1, and Pbp4) and that at least Pab1 is a substrate for NuA4 *in-vitro* (Mitchell, Huard et al. 2013). Further, microscopy analysis performed by the Baetz lab has determined that GD SG formation is decreased in NuA4 mutant cells (**Figure 4;** obtained from: Jennifer Takuski Baetz Lab, MSc Thesis 2014). This demonstrates the possible role of KATs and KDACs, particularly NuA4, in the regulation of GD SG formation and function.

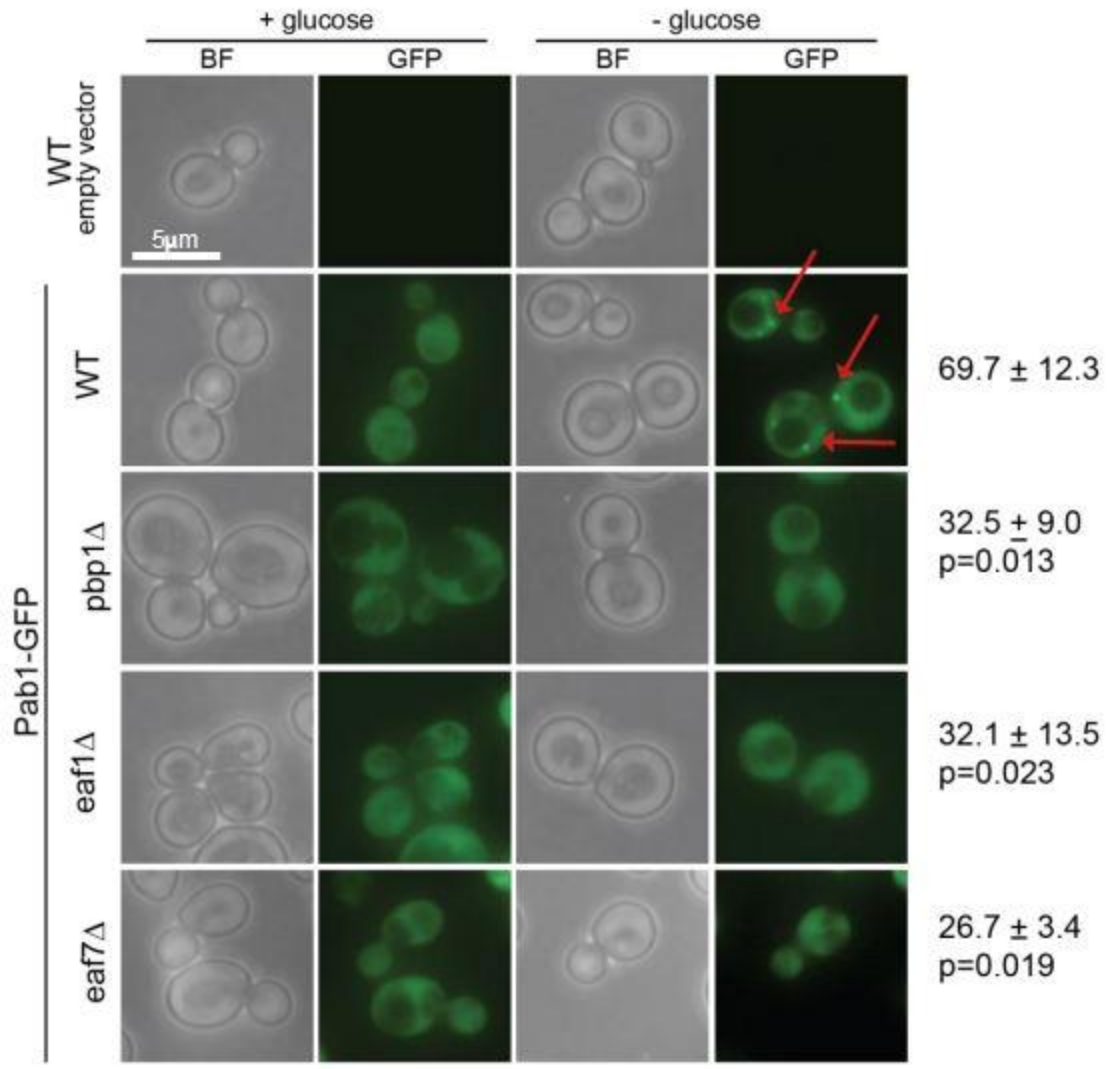

Figure 4: Stress granule formation is decreased in NuA4 mutant cells following 10 minutes of glucose deprivation. Exponential-phase (+ glucose) wild type, *eaf7Δ, eaf1Δ* and *pbp1Δ* cells transformed with *PAB1-GFP::URA::CEN* plasmid were subjected to GD (-glucose) for 10 minutes. Stress granules (Pab1-GFP foci) were quantified in three independent experiments with minimum of 300 cells per replicate. Data indicate the average percent of cells with SG foci and +/- standard deviation (Significance [$p<0.05$] determined using One Way ANOVA).Work performed by Jennifer Takuski MSc student in the Baetz Lab (Obtained from: Jennifer Takuski Baetz Lab, MSc Thesis 2014).

1.3 Glucose availability, Acetyl-CoA and Lysine Acetylation

Acetyl-CoA is a product of glucose (**Figure 5**). During prolonged GD, acetyl-CoA levels within the cell are reduced (Sandmeier, French et al. 2002). Interestingly, following only an hour of GD conditions, acetyl-CoA levels have been shown to increase 1.7 fold compared to glucose conditions (Zhang, Galdieri et al. 2013). Additionally, acetyl-CoA represents a cofactor necessary for lysine acetylation to occur (**Figure 5**). Decrease in the synthesis of acetyl-CoA, through inhibition of the two acetyl-CoA synthetases (Acs) in yeast, has been shown to rapidly decrease histone acetylation (**Figure 5**) (Takahashi, McCaffery et al. 2006). Further, an increase in cellular acetyl-CoA levels has been shown to increase global histone acetylation, alter transcriptional regulation, and increase acetylation of non-histone proteins (Galdieri and Vancura 2012). Thus, a change in cellular acetyl-CoA pools depending on glucose availability may represent a mechanism of KAT/KDAC regulation and in turn the regulation of diverse cellular processes such as GD SG formation.

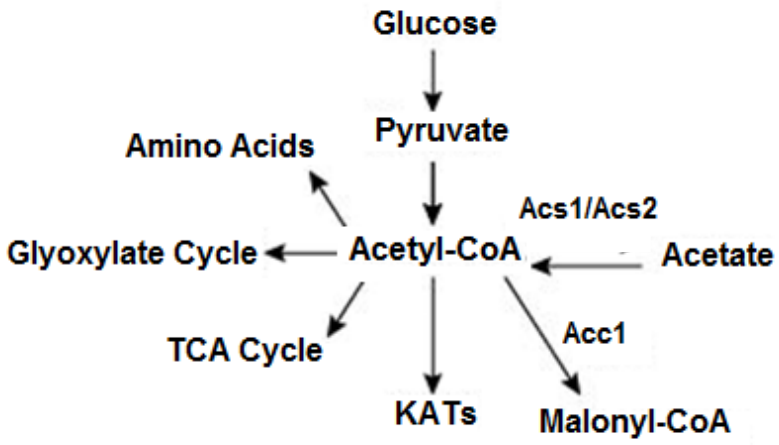

Figure 5: Schematic illustrating acetyl-CoA biosynthesis pathways.

1.4 Fatty Acid Biosynthesis Pathway and Acetyl-CoA Carboxylase (Acc1)

Fatty Acid Biosynthesis Pathway

Fatty acid biosynthesis (FAB) is an essential process that requires cellular acetyl-CoA pools (Kim, Lopez-Casillas et al. 1989). The unique properties of fatty acids are utilized in an array of cellular structures and processes including but not limited to: effective storage of metabolic energy, subcellular compartmentalization within a cell by establishing membrane bilayers, and employment of signalling functions through modifications of proteins and other means (Reviewed in: Tehlivets, Scheuringer et al. 2007).

In *S. cerevisiae*, cellular fatty acids are obtained from 3 major sources including external supply such as yeast media, endogenous lipid or protein turnover into fatty acids, and de novo synthesis (Reviewed in: Tehlivets, Scheuringer et al. 2007). As most yeast media in a laboratory does not contain fatty acids, fatty acid production is largely dependent on de novo synthesis.

Acetyl-CoA Carboxylase (Acc1)

In the initial step of FAB, acetyl-CoA is carboxylated to form malonyl-CoA (Lynen 1959) (**Figure 6;** modified from Li et al. 2014). The malonyl-CoA product functions as a building block in the proceeding steps of the FAB process by extending the fatty acid chain two carbons at a time. This initial process of malonyl-CoA production is the rate limiting step of the biosynthesis pathway and is carried out by the essential enzyme Acc1 (Obermayer 1976, Kim, Lopez-Casillas et al. 1989). Acc1 possesses 3 domains. Firstly, the biotin carboxyl carrier protein domain is responsible for covalently linking biotin, an essential co-factor necessary for acetyl-coA carboxylation to occur (Obermayer 1976). Secondly, the biotin-carboxylase domain responsible for catalyzing the ATP-dependent carboxylation of a biotin group, the first step of acetyl-CoA carboxylation (Obermayer 1976). Finally, the carboxyl-transferase domain is

responsible for transferring of the carboxyl group to the acetyl-CoA molecule, the second step of acetyl-CoA carboxylation (Obermayer 1976) (**Figure 7**). Lysine acetylation sites have been found on all 3 domains (Henriksen, Wagner et al. 2012, Downey, Johnson et al. 2015) (**Figure 7**). Specifically, conserved lysine residues 1764 and 2034 have been shown to be acetylated in the carboxyl-transferase domain and the binding pocket of the carboxyl-transferase domain respectively (Henriksen, Wagner et al. 2012, Downey, Johnson et al. 2015). These lysine residues represent potential sites of dynamic post translational modifications which may be implicated in the regulation of Acc1 activity.

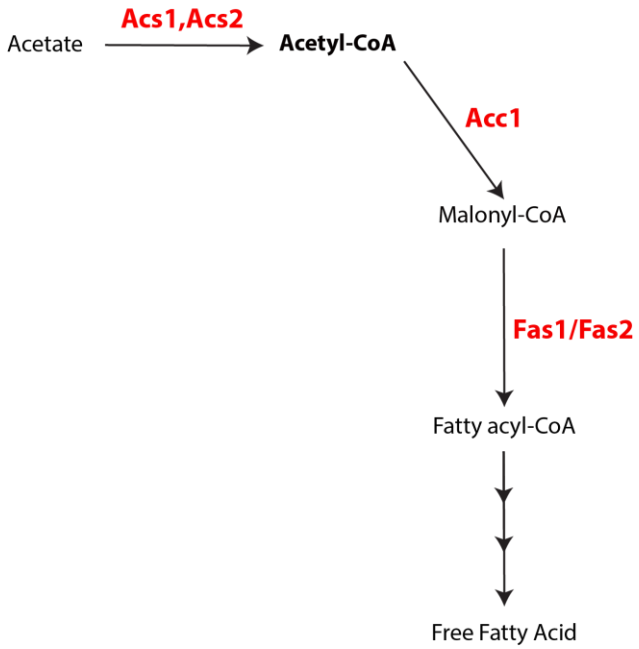

Figure 6: Schematic illustrating fatty acid biosynthesis pathway (modified from: Li et al. 2014). Enzymes and reaction substrates and products of the fatty acid biosynthesis pathway are indicated.

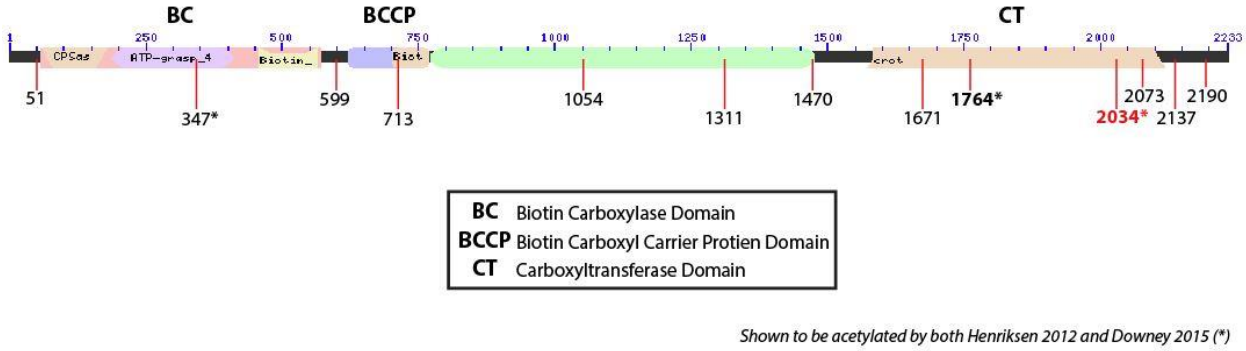

Figure 7: Schematic of Acc1 protein domains and acetylation sites. 3 domains of Acc1: biotin carboxyl carrier protein domain, biotin-carboxylase domain, and carboxyl-transferase domain.

Regulation of Acc1

Similar to its analogous protein in humans, Acc1 is inactivated by Snf1/AMPK phosphorylation (Woods, Munday et al. 1994). Snf1, the AMP-activated protein kinase in yeast plays a significant role in regulating metabolism in response to glucose changes within a cell (Carlson, Osmond et al. 1981). Serine 1157 was identified as the regulatory phosphorylation site on Acc1 (Ficarro 2002) – however if analogous to the mammalian protein, more sites and mechanisms of regulation likely exist (Witters and Watts 1990, Woods, Munday et al. 1994).

Acc1 and Lysine Acetylation

Studies in *S. cerevisiae* have shown that synthesis of fatty acids and histone acetylation compete for the same acetyl-CoA pool (Galdieri and Vancura 2012). In fact, FAB use of acetyl-CoA pools has the ability to alter acetylation of global histone and non-histone protein targets (Galdieri and Vancura 2012). A decreased expression of *ACC1* results in an increase histone acetylation and an alteration of transcriptional regulation on a global scale (**Figure 8**) (Galdieri and Vancura 2012). This result suggests there is an interdependence between FAB, KATs/KDACs and the regulation of acetyl-CoA levels in the cell, an effect that may contribute to GD SG dynamics.

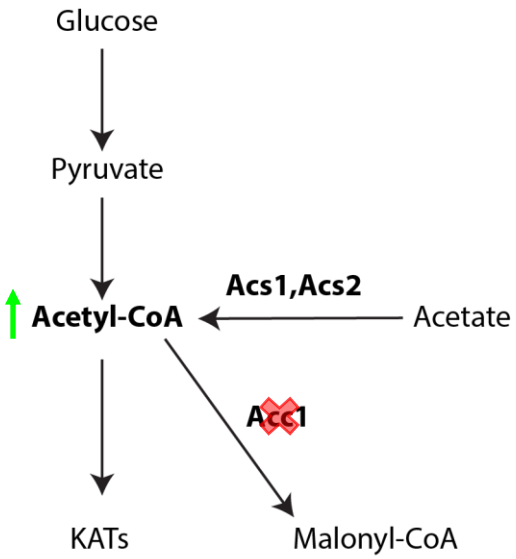

Figure 8: Schematic illustrating acetyl-CoA biosynthesis pathway. Increase of acetyl-CoA is a product of inhibiting Acc1 activity. Increase in acetyl-CoA causes increase in global histone acetylation and acetylation of non-histone proteins.

HYPOTHESIS:

Glucose deprived stress granule assembly is regulated by KATs/KDACs and the glucose rheostat acetyl-CoA **(Figure 9).**

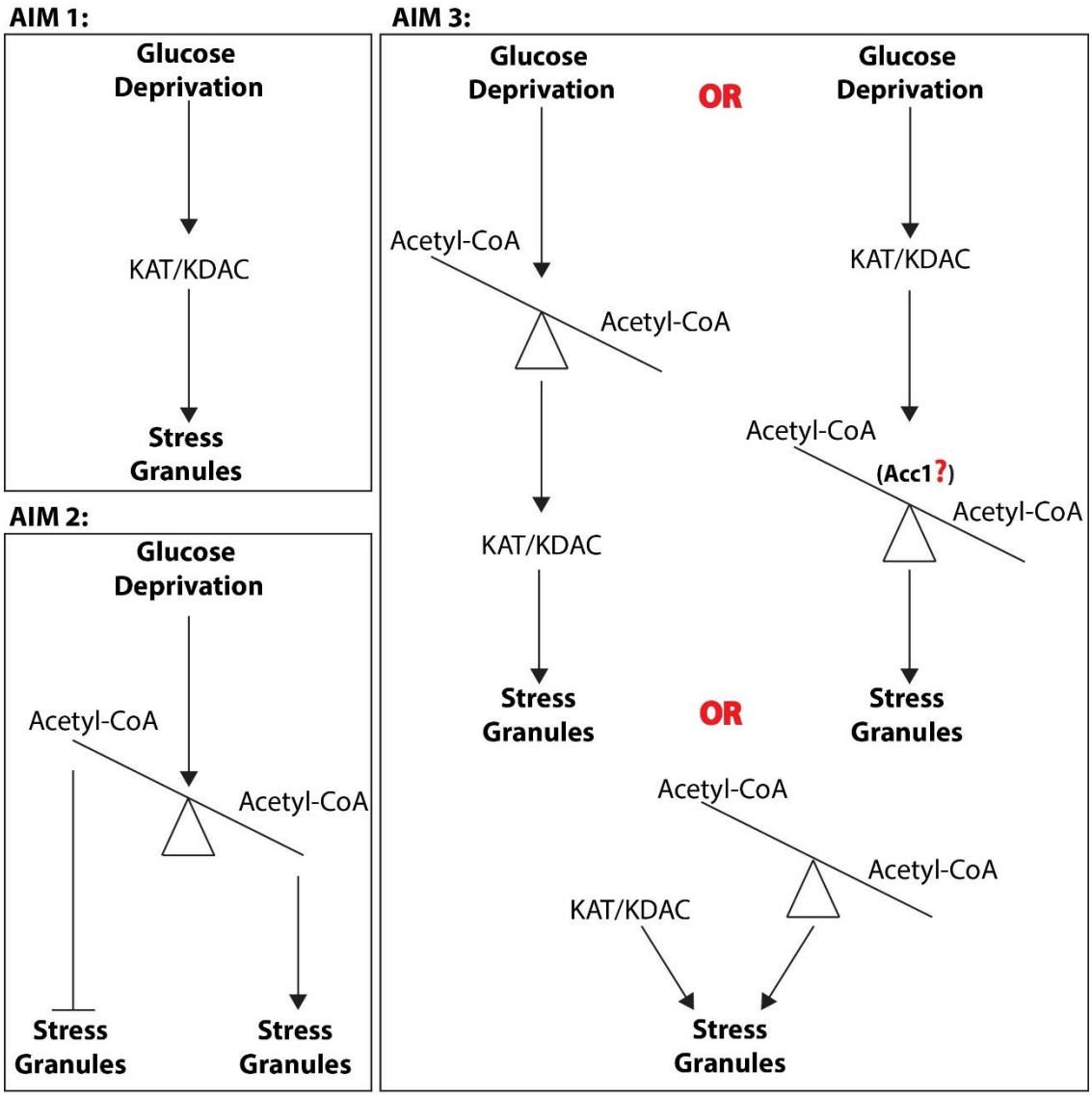

Figure 9: Schematic representing hypothesized models of glucose deprived stress granule regulation.

Specific Aims:

Aim 1: Characterize the role of KATs and KDACs in glucose deprived stress granule dynamics

Aim 2: Determine if acetyl-CoA is the metabolic signal regulating stress granule dynamics

Aim3: Determine if NuA4 impacts Acetyl-CoA Carboxylase 1

2. MATERIALS AND METHODS

2.1 Yeast Strains

Yeast strains and plasmids used throughout this thesis are listed in **Appendix B** (Tables **B4** and **B5**).

Genomic deletion or epitope tag integrations made for this study were designed with PCR-amplified cassettes as previously described (Longtine, McKenzie et al. 1998) and confirmed by PCR and/or western blot.

2.2 Strain growth and application of stress

Cells were grown in yeast, peptone, dextrose (YPD) or synthetically defined (SD) medium that was prepared using standard methods unless modifications were specified. For glucose deprivation conditions, culture were grown in YPD or SD media with 2% glucose as indicated until mid-log phase (OD_{600}~0.5-0.8) and centrifuged mildly (3000rpm for 3 minutes at room temperature). Cells were washed by resuspending pellets in YP or SD media without glucose (GD) followed by another mild centrifugation (3000rpm for 3 minutes at room temperature) prior to being resuspended in the same GD media. Cells were grown at 30^{o}C unless otherwise indicated and harvested for analysis following experiment specific incubation times.

For activation of the tetracycline repressible promoter ($tet0_7$), cultures were grown in YPD or SD media with 2% glucose as indicated until mid-log phase (OD_{600}~0.5). Doxycycline (Sigma-Aldrich, USA; Cat. #: D3447-500MG; Doxycycline was resuspended in DMSO) was added to cell cultures to a final concentration of 10uM for a 2.5 hour incubation period before being harvested. Cells were grown at 30^{o}C.

For exogenous acetate conditions, cultures were grown in YPD or SD media with 2% glucose as indicated until mid-log phase (OD_{600}~0.5-0.8). Acetate (Sigma-Aldrich, USA; Cat. #: 3863-

50mL) was added to cell cultures to a final concentration of 100mM for a 10 minute incubation period before being harvested. Cultures were grown at 30^{o}C.

2.3 Fluorescent Microscopy

Microscopy was completed using a Leica DMI 6000 florescent microscope (Leica Microsystems GmbH, Wetzler Germany). Images were captured using a Hamamatsu Orca AG camera (Hamamatsu Photonics, Herrsching am Ammersee, Germany). [Microscope features: Sutter DG4 light source (Sutter Instruments, USA), Ludl emission filter wheel equipped with Chroma bandpass emission filters (Ludl Electronic Products Ltd., USA)].

In preparation for microscopy, cells were grown in YPD or SD media with 2% glucose as indicated until mid-log phase (OD_{600}~0.5-0.8). 10mL of culture was centrifuged at 3000rpm for 3 minutes at room temperature. Following centrifugation, cells were re-suspended in 100µl of SD media. 15µl of cells were spotted onto a glass plate and live imaged immediately. Following live-cell imaging under non-stressed conditions cells were exposed to stress (GD) or drug treatment as previously described. Following incubation, the treated cultures were harvested and imaged as described above. Z-stacked images were obtained using Volocity 4.3.2 (Perkin Elmer) using a 63x objective without binning.

For mitochondrial co-localization experiments using MitoTracker Red, cells were prepared as indicated (catalog no. M-7512, Invitrogen). Briefly, cells were grown in YPD until mid-log phase (OD_{600}~0.5-0.8). Culture were incubated with a final concentration of 100nM MitoTracker Red for 30 minutes. Following incubation, cells were mildly centrifuged at 3000rpm for 3 minutes at room temperature. Cells were washed by resuspending pellets in YPD followed by another mild centrifugation (3000rpm for 3 minutes) prior to being resuspended in 100ul of the same media. Cells were imaged as previously indicated.

2.4 Image Quantification and Analysis

Stress granule microscopy and analysis was completed as previously described (Buchan, Nissan et al. 2010) with minor modifications. Stress granule microscopy experiments were completed in triplicate and each replicate consisted of at least 100 cells. Number of total cells and number of cells that form SGs were determined by manual counting of stacked images. From these values, the percentage of cells that form SGs was determined.

Fatty acid biosynthesis microscopy was completed in triplicate and each replicate consisted of at least 100 cells. Total cells as well as protein localization was determined manually using stacked images. Cellular protein localization was characterized as: Diffuse, presence of a single foci, or rod-shape foci. From these values, the percentage of cells in each localization was determined.

MitoTracker Red co-localization microscopy was completed in triplicate and each replicate consisted of at least 100 cells. Total cells as well as Acc1 co-localization with the mitochondria (MitoTracker Red) was determined manually using single plane images to increase accuracy of co-localization determination.

Statistics for each experiment was completed using GraphPad Prism 6.0. ANOVA or unpaired t-tests were utilized based on the experiment in question, with a p-value of < 0.05 representing statistical significance.

2.5 Harvesting Yeast Cell Culture

To harvest cells for protein extraction, yeast cell cultures were grown at 30^{o}C (unless otherwise indicated) overnight to an OD_{600}~1. Overnight cultures were diluted to an OD_{600}~0.1 and grown until mid-log phase (OD_{600} 0.5-0.8). Cells were collected by centrifugation for 3 minutes at 3000 rpm at 4°C. Cells were then washed by resuspending in 20 mL of ice cold water prior to

harvesting by centrifugation for 3 minutes at 3000 rpm at 4°C. Harvested cells were stored at -80°C.

2.6 Immunoprecipitation of Tandem Affinity Purification (TAP) and Green Fluorescent Protein (GFP)- Tagged Proteins

To purify GFP and TAP tagged proteins and to prepare whole cell extracts (WCE), the modified immunoprecipitation protocol (mChIP) was utilized as previously described (Lambert, Mitchell et al. 2009). Briefly, cells were harvested and frozen as indicated above. Frozen cell pellets were resuspended in an equal volume of mChIP lysis buffer [100mM HEPES (pH 8.0), 20mM magnesium acetate, 300mM sodium acetate, 10% glycerol (vol/vol), 10mM EGTA, 0.1mM EDTA] supplemented with protease (Sigma; P8215; 1 tablet/10mL of buffer) and KDAC inhibitor (Nicotinamide: Sigma; 72340; 500ul of 1M solution /10mL of buffer and Sodium Butyrate: Sigma; B5887; 500ul of 1M solution/10mL of buffer). Glass beads (Fisher Scientific, USA; 35-535) were added until just below the surface of the buffer and samples were vortexed 5-8 times for 1 minute, with 1 minute intervals on ice in between vortexes. Whole cell extract was transferred to a fresh 1.5 mL Eppendorf tube by poking a hole in the bottom of the old tube containing the lysed cells and gently centrifuging lysate into a fresh tube (1 min at 1000 rpm at 4°C). Whole cell extracts were sonicated for a single 20 second pulse at setting 4 (Misonix Sonicator) and put back on ice. Nonidet P-40 (NP- 40) was added, at a concentration of 1% measured by volume, and each sample was rotated end over end for 10 minutes at 4°C. Lysate was clarified by centrifugation at 3000 rpm for 15 minutes at 4°C. The resulting lysate was transferred to a new 1.5mL Eppendorf tube and protein concentration was determined using Bradford reagent (Bio-Rad, USA; Cat. #: 500-0006).

As indicated, 10 to 40 mg of WCE was used for immunopurification. Purification of TAP tagged proteins required 25ul of magnetic Dynabeads (catalog no. 143-01; Dynal, Invitrogen) crossed-

linked to rabbit immunoglobulin G (IgG) (catalog no. PP64; Chemicon) while 30ul of GFP-trap magnetic beads was added to the WCE for GFP Immunopurification (Chromotek, Germany; Cat. #: GTM-20). Whole cell extracts incubated with respective beads were rotated end over end for 2 hours at 4^{o}C. Following incubation, the beads were collected using a magnet and underwent three washes with 1mL of cold wash buffer [100mM HEPES (pH 8.0), 20mM magnesium acetate, 10% glycerol (V/V), 10mM EGTA, 0.1mM EDTA, 300mM sodium acetate, 0.5% NP-40]. Lysate was transferred to new 1.5 mL Eppendorf tubes between the second and final wash. Following the 3rd wash, 40µl of 1x loading buffer [50mM Tris pH 6.8, 2% SDS, 0.1% bromophenol blue, 10% glycerol] was added to the beads. Elution of the purified proteins into the loading buffer was completed by placing the samples at 65°C for 10 minutes. Post elution, the loading buffer containing the eluted sample was transferred to a new Eppendorf tube and 2-β-mercaptoethanol was added to a concentration of 200mM.

2.7 Immunoblotting

Prepared WCE (50-200ug as indicated) and IP samples in loading buffer were boiled at 95^{o}C for 10 minutes prior to being loaded onto and separated by a SDS-PAGE gel. Following separation, proteins were transferred for 80 minutes to pure nitrocellulose blotting membranes (PALL, Pall Corporation; 66485) using a Trans-Blot SD Semi-Dry Transfer Cell (BioRad; 170-3940). Membranes were blocked in 5% milk (or bovine serum albumin (Sigma; A9418) if anti-acetyl antibodies were used) for 1 hour at room temperature. Membranes were then resuspended in 5% milk (or bovine serum albumin (Sigma; A9418) if anti-acetyl antibodies were used) and primary antibody was added. Primary antibody incubation with membranes occurred overnight at 4°C. Unless otherwise indicated, the following fusion protein/antibody pairs were used. GFP fusion protein was detected using α-GFP (Roche; Cat. #: 11814460001; dilution 1/3000), TAP fusion

protein was detected using α-TAP (Thermo Scientific, CAB1001; dilution 1/10000), and HA fusion protein was detected by using α-HA (Covance, MMS-101P; dilution 1/1000). Protein acetylation was detected using anti-acetyl lysine (Cell Signaling; Cat. #: 9681; dilution 1/500). Histone H4 acetylation was detected using anti-hyperacetylated Histone H4 (Penta) (Millipore, Cat. #06-946; Dilution 1/10000). Total histone H3 levels were determined using Histone H3 antibody (Millipore, Cat. #05-928; Dilution 1/2000). Acc1 protein was detected using anti-Acetyl-CoA Carboxylase antibody (Cell Signaling; Cat. #: 3662; dilution 1/1000). The loading control used for all WCE immunoblotting experiments was G6PDH and was detected with anti-G6PDH (Sigma, A9521 1/10,000). Secondary antibodies used for the chemiluminescence imaging were coupled with HPR and included goat anti-mouse IgG (BioRad, catalog no. 170-6516, 1:5000) and goat anti-rabbit IgG (Chemicon, catalog no. AP307P, 1:5000). Secondary antibodies were incubated with the membranes in 5% milk for two hours at room temperature. Protein blots were developed using the Western Chemiluminescent HRP Substrate Detection System (Millipore, catalog no. WBKLS0500) and images were obtained using a Molecular Imager ChemiDoc XRS System (BioRad).

2.8 Western Blot Quantification

Relative quantification of western blots was completed using ImageJ. Briefly, western blot images for the protein of interest and the loading control were converted to grey scale. The mean pixel value (mean grey value) for each protein of interest, corresponding loading control, along with a background control for each lane was individually measured using a defined frame of interest. Next, for all data, inverted pixel density was determined by subtracting the measurement for each data point from 255 (saturation). The inverted value for the background was subtracted from the inverted value for the protein band of interest and loading control. Finally a ratio of the

net protein band value over the net loading control value was determined giving the relative quantification value for each protein of interest. The relative values of each protein of interest were normalized relative to WT +glucose (unless otherwise indicated). Relative values of three independent replicates were then averaged and displayed as a bar graph.

2.9 Acetyl-CoA Assay

Acetyl-CoA levels were measured using an Acetyl-Coenzyme A Assay Kit (Sigma-Aldrich, USA; Cat. #:MAK039). Sample preparation and assay reactions were carried out as indicated (Sigma-Aldrich, USA; Cat. #:MAK039). Briefly, culture were grown in YPD until mid-log phase (OD_{600}~0.5-0.8) and harvested as previously described. From frozen, cell pellets were resuspended in an equal volume of 10% perchloric acid. Glass beads were added until just below the surface of the buffer and cells were vortexed 5-8 times for 1 minute, with 1 minute intervals on ice in between vortexes. Lysates were transferred to a fresh 1.5 mL Eppendorf tube by poking a hole in the bottom of the old tube containing the lysed cells and gently centrifuging lysate into a fresh tube (1 min at 1000 rpm at 4^{o}C). Samples were clarified by centrifugation (13000 x g for 10 min at 4^{o}C). 3M potassium bicarbonate solution was added in aliquots of 1ul per 10ul of lysate until bubble production ceased. Samples were cooled on ice for 5 minutes and pH in the range of 6-8 was confirmed by benchtop pH meter (VWR International; 89231-662). Samples were spun for 2 minutes at 3000 rpm at 4^{o}C in order to pellet potassium bicarbonate. Assay reaction mixes were prepared using materials provided by Sigma-Aldrich Acetyl-Coenzyme A Assay Kit (Sigma-Aldrich, USA; Cat. #:MAK039). 40ul Acetyl-CoA assay buffer, 2ul Acetyl-CoA Substrate Mix, 1ul Conversion Enzyme, 5 Acetyl-CoA Enzyme Mix, and 2ul Fluorescent Probe was added to a solution of 10ul of sample supplemented with 40ul of Acetyl-CoA Assay buffer. Reaction mixes were incubated at 37^{o}C for 10 minutes. A SynergyH1 Multi-Mode Plate

Reader was used to measure the fluorometric product ($\lambda_{ex}535/\lambda_{em}587$) of each assay reaction. Blanks, represented by assay reactions without the addition of conversion enzyme, were used to account for background – enabling for corrected fluorescent measurements to be obtained. Using fluorometric product measurements and the experiment specific standard curve, levels of acetyl-CoA per reaction (ng/ul) was determined.

2.10 Pab1-TAP Interactome

A Pab1-TAP protein interactome was developed from 2 experiment replicates as previously described (Mitchell, Huard et al. 2013) with minor modifications. Briefly, two litre cultures of each strain type were grown at 25^{o}C overnight to an OD_{600}~1. Overnight cultures were diluted to an OD_{600}~0.1 and grown until mid-log phase (OD_{600} 0.5-0.8). Half of each culture was harvested by centrifugation as previously described. The other half of each culture underwent GD for 30 minutes at 25^{o}C as indicated above and were subsequently harvested as previously described. Harvested cells were stored at -80°C.

Proteins were resolved on NuPAGE Novex gradient SDS/PAGE 4–12%Bis-Tris Protein Gels (Invitrogen, NP0321) and silver staining was performed to visualize Pab1-TAP and co-purified proteins. Each silver stained lane was excised into 7 bands, placed in labelled 1.5mL Eppendorf tubes, and sent for mass spectroscopy analysis. Samples were processed by Dr. Figeys Lab by LC-MS/MS using a LTQ-Orbitrap XL mass spectrometer (Thermo-Electron) using conditions previously described (Mitchell, Huard et al. 2013).

The high-confidence Pab1-TAP interactome (data obtained from dataset in **Appendix A: Table A3**) only includes proteins that were identified in both replicates with a minimum of 2 unique peptides per replicate. For each replicate, peptide counts for each protein were normalized relative to Pab1-TAP peptide counts from that mChIP (hence Pab1 relative peptide count = 1).

Next for each condition, the normalized peptide count for each peptide was averaged [averaged peptide count = (peptide count rep1/Pab1 peptide count rep1 + peptide count rep2/Pab1 peptide count rep2)/2]. The relative peptide counts calculated above, were used to develop the protein interaction networks in this thesis (WT glucose vs. GD as well as WT GD vs. *eaf1Δ* GD). Manual analysis of each protein's peptide count was performed to ensure that the trends observed (co-purification increase, decrease, remains the same) were not just a result of averaging both replicates.

2.11 Trichloroacetic Acid (TCA) Lysis

TCA lysis was performed as previously described (Kao and Osley 2003). Briefly, yeast cell cultures were grown overnight to an OD_{600}~1. Overnight cultures were diluted to an OD_{600}~0.1 and were grown in YPD at 25^{o}C until mid-log phase (OD_{600}~0.5-0.8). Cells were then centrifuged at 4000 rpm for 5 min at 4^{o}C. Cell pellets were resuspended in 10 mL of ice-cold TCA (20% solution), centrifuged again as indicated above, frozen on dry ice and stored at -80°C until ready to proceed with cell lysis. Frozen cell pellets were thawed on ice prior to resuspension in 200ul of ice-cold TCA (20% solution) and transferred to a 2mL flat bottom tube. 350uL of glass beads were added to each tube and samples were vortexed 5-8 times for 30 seconds with 1 minute intervals on ice in between vortexes. Whole cell extract was transferred to a labelled 15 mL tube by poking a hole in the bottom of the old tube containing the lysed cells and gently centrifuging lysate into a fresh 15mL tube (1 min at 4000 rpm at 4^{o}C). 500ul of ice-cold TCA (5% solution) was added to the glass beads and collected in the same 15mL tube following gentle centrifugation (1 min at 4000 rpm at 4^{o}C). The pelleted lysate was resuspended and transferred to a 1.5 mL Eppendorf tube and placed on ice for 15 minutes. Samples were centrifuged at 13200rpm for 15 minutes at 4^{o}C to precipitate proteins and the supernatant was

subsequently discarded. Cell pellets were resuspended in 350ul of SDS-Page loading buffer [9.2mL of 10% SDS, 300uL of 2M Tris pH 6.8, 500uL of 2-β-mercaptoethanol and 0.05mg of bromophenol blue] and 50ul of unbuffered 1M Tris solution was added to each tube. In preparation for loading samples onto a SDS-PAGE gel for western blot analysis, samples were boiled at 95^{o}C for 10 minutes.

2.12 Quantitative real-time PCR

Cultures were grown overnight to an OD_{600}~1. Overnight cultures were diluted to an OD_{600}~0.1 and were grown in YPD at 25^{o}C until mid-log phase (OD_{600}~0.5-0.8). 50mL of cell culture was gently centrifuged (3000rpm for 3 min at 4°C) and cells were washed two times with 10ml of ice cold water. Pellets were resuspended in 2ml of Tri-Reagent (Sigma-Aldrich, USA; Cat. #: T9424) and 1ml of glass beads were added to the cell- Tri Reagent mix (Fisher Scientific, USA; Cat. #: 35535). Samples were frozen using liquid nitrogen and stored at -80°C. Following incubation at -80°C, samples were thawed at room temperature and vortexed at maximum speed for 5min. Following vortexing, 500µl of chloroform was added. Samples were mixed for 15 seconds and then incubated for 10min at room temperature prior to centrifugation at 3200g for 20min at 4°C. The resulting aqueous layer was split in half and transferred to 2 new 1.5mL RNase free Eppendorf tubes. 1mL of isopropanol was added to each tube and samples were subsequently incubated on ice for 10 min prior to centrifugation at 12000g for 20min at 4°C. 500ul of ice cold 75% ethanol (made with DEPC water) was added to resuspend and wash the white/clear pellet in each tube. The pellet was centrifuged at 7500g for 5min at 4°C. The ethanol was removed and the samples were dried. Samples were resuspended in 20µl of nuclease-free water (Ambion, USA; Cat. #: AM9937) and the split tubes containing the same sample were recombined. Once resuspended, the sample underwent DNase treatment. 10ug of RNA (as

determined via nanodrop: ND-1000 spectrophotometer, NanoDrop Technologies, USA) was treated with DNAse as indicated by the manufacturer (RQ1 RNAse-free DNAse, Promega, USA; Cat. #: M6101). RNA was isolated by adding 400µl of Nuclease-free water and 500µl of phenol/chloroform, vortexing for 1min and then centrifuging the samples at 12000g for 5 min at 4°C. The upper aqueous layer was transferred to a new RNAse-free 1.5mL Eppendorf tube followed by the addition of 5µl of 3M sodium acetate and 1ml of ice cold 100% Ethanol. The precipitated RNA was placed at -80°C overnight. The following day, samples were centrifuged at 12000g for 30 min at 4°C. The resulting pellets were each washed with 500µl of ice cold 70% ethanol made with Nuclease-free water and centrifuged again at 7500g for 5 min at 4°C. Ethanol was removed, samples were dried and 20µl Nuclease-free water was added to resuspend each sample. The RNA concentration was determined using a NanoDrop and all samples were normalized to 200 ng/µl using Nuclease-free water. RT-PCR was performed with all samples as indicated by the manufacturer (High Capacity cDNA RT Kit, Applied Biosystems, USA; Cat. #: 4368814). Primary melting curve and standard curve experiments and the final qPCR was performed with the cDNA as per the manufacturer's instructions in a final volume 10µl (SsoFast EvaGreen Supermix; Bio-Rad, USA; Cat. #: 172-5201).

Primers used for the qPCR:

Internal Controls:

TDH3 Primers:
TDH3 forward 5'- CTGTCAAGTTGAA CAAGGAAACCAC -3'
TDH3 reverse 5'- CAACGTGTTCAACCAAGTCGACAA -3'

NADH Primers:
NADH forward 5'- GTTTAGGGGCCAAATCCAAT -3'
NADH reverse 5'- GCTTAGCACCCTGAGCAATC -3'

ACC1 Primers:

ACC1 Primer Set 1:
ACC1 forward 5'- CCGAAGGTGGTGGTGGTAA -3'
ACC1 reverse 5'- ATGAAAATGGGGGAGCCTG -3'

ACC1 Primer Set 2:
ACC1 forward 5'- TCCAGAAGATGTCGAAGCC -3'
ACC1 reverse 5'- TCAAGGCACGCAATGGTAC -3'

3. RESULTS:

The result section is organized into my three aims:

Aim 1: Characterize the role of KATs and KDACs in glucose deprived stress granule dynamics
Aim 2: Determine if acetyl-CoA is the metabolic signal regulating stress granule dynamics
Aim 3: Determine if NuA4 impacts Acetyl-CoA Carboxylase 1

Each of these aims work to characterize how glucose deprived stress granule dynamics is regulated by KATs and KDACs as well as acetyl-CoA. Further, as Acc1 influences acetyl-CoA levels within the cell, and as acetyl-CoA impacts stress granule formation, this work has potentially uncovered a mechanism by which NuA4 regulates glucose deprived stress granule dynamics.

3.1 Aim 1: Characterizing the role of lysine acetyltransferases and lysine deacetylases in glucose deprived stress granule dynamics

3.1.1 Deletion of *EAF7* results in a delay in glucose deprived stress granule formation.

The Baetz lab has established that NuA4 physically co-purifies with SG complex proteins (Pab1, Lsm12, Pbp1, and Pbp4) and that Pab1 is an *in-vitro* substrate of NuA4 (Mitchell, Huard et al. 2013). Further, microscopy-based analysis determined that that the percentage of cells that form SGs after 10 minutes of GD is decreased in NuA4 mutant cells (**Figure 4, unpublished work of Jennifer Takuski**). In order to determine whether the NuA4 mutants cause a delay or a complete inhibition of the GD SG response, SG formation was measured in exponential-phase wild type and *eaf7*Δ cells expressing Pab1-GFP in both glucose and GD conditions (10 minutes, 30 minutes and 60 minutes). The time course revealed that the percentage of *eaf7Δ* cells with SGs increase to wild type levels (70% of cells containing SGs) after 30 minutes of GD and that SGs begin to resolve at the 60 minute time point in both strains (**Figure 10**). This experiment revealed that the *eaf7Δ* defect in SG formation is a delay rather than a complete inhibition of GD SG formation. As there are minimal fitness defects in the *eaf7Δ* (**Figure 11C**) (Deutschbauer, Jaramillo et al. 2005), this work suggests that another KAT may have the ability to compensate for the loss of NuA4 function in regulating SG formation.

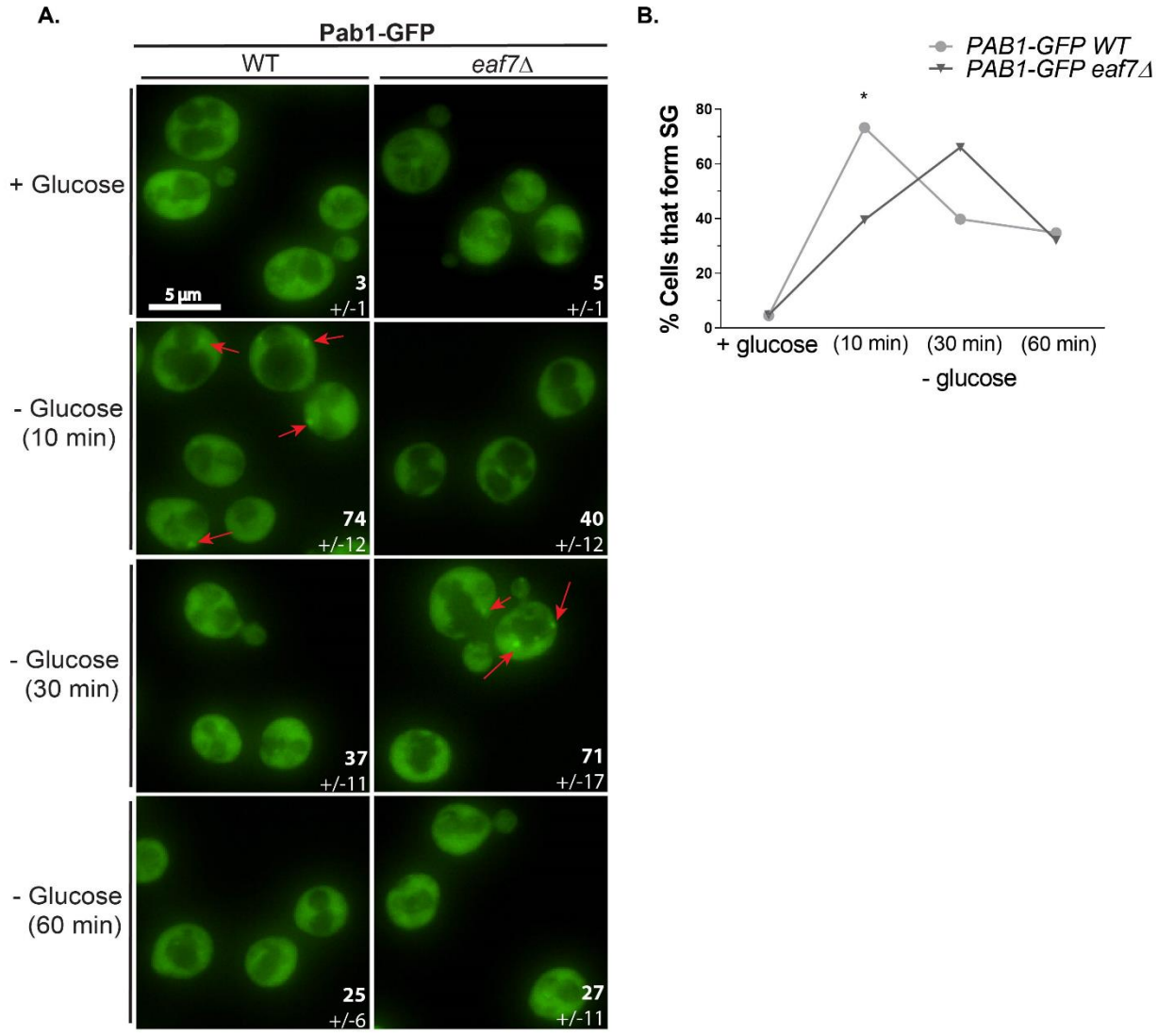

Figure 10 *eaf7Δ* mutant displays a delay in glucose deprived stress granule assembly. Exponential-phase (+ glucose) wild type (WT, YKB3114) and *eaf7Δ* (YKB3336) cells expressing endogenously tagged Pab1-GFP were subjected to GD (-glucose) for the indicated times. Stress granules (Pab1-GFP) were manually quantified in three independent experiments with minimum of 100 cells per replicate. **A.** Typical images of SGs. Numbers indicate the average percent of cells with SG foci and +/- standard deviation. **B.** Quantification of data in A. *eaf7Δ* mutant displays a delay in glucose deprived stress granule assembly compared to WT cells. Following 30 minutes of GD, *eaf7Δ* cells with SGs increase to 70% while SGs in WT cells begin to resolve (Significance determined using Two Way ANOVA* $p<0.05$).

3.1.2 EAF7 and *GCN5* are functionally redundant for glucose deprived stress granule assembly.

As *GCN5* is highly conserved and has been reported to regulate many essential stress response genes (Huisinga and Pugh 2004, Li and Shogren-Knaak 2009, Xue-Franzen, Henriksson et al. 2013, Gaupel, Begley et al. 2015), we sought to test whether Gcn5 also plays a role in GD SG dynamics and if it is functionally redundant with Eaf7 in regulating GD SG assembly. Stress granule formation was measured in wild type, *eaf7Δ, gcn5Δ,* and *eaf7Δgcn5Δ* cells expressing Pab1-GFP from its endogenous loci in both glucose and GD conditions (10 minutes, 30 minutes and 60 minutes). While *gcn5Δ* cells do not display a significant reduction in GD SG assembly compared to wild type cells, *eaf7Δgcn5Δ* cells display a significant reduction in GD SG formation compared to both wild type and single KAT mutants (**Figure 11A**). Further, in contrast to *eaf7Δ* mutant cells, the percentage of cells with SGs do not increase over the time course in *eaf7Δgcn5Δ* mutant cells (**Figure 11B**). In fact, only 25% of the double mutant cells ever display GD SGs (**Figure 11B**). As *eaf7Δgcn5Δ* cells display minimal growth defects compared to the single mutants (**Figure 11C**), it is unlikely the defects in GD SG formation reflect cell sickness; rather these results demonstrate that *EAF7* and *GCN5* are functionally redundant in GD SG regulation. Together, this data affirms that the GD SG regulatory mechanism is a dynamic process involving multiple KAT enzymes.

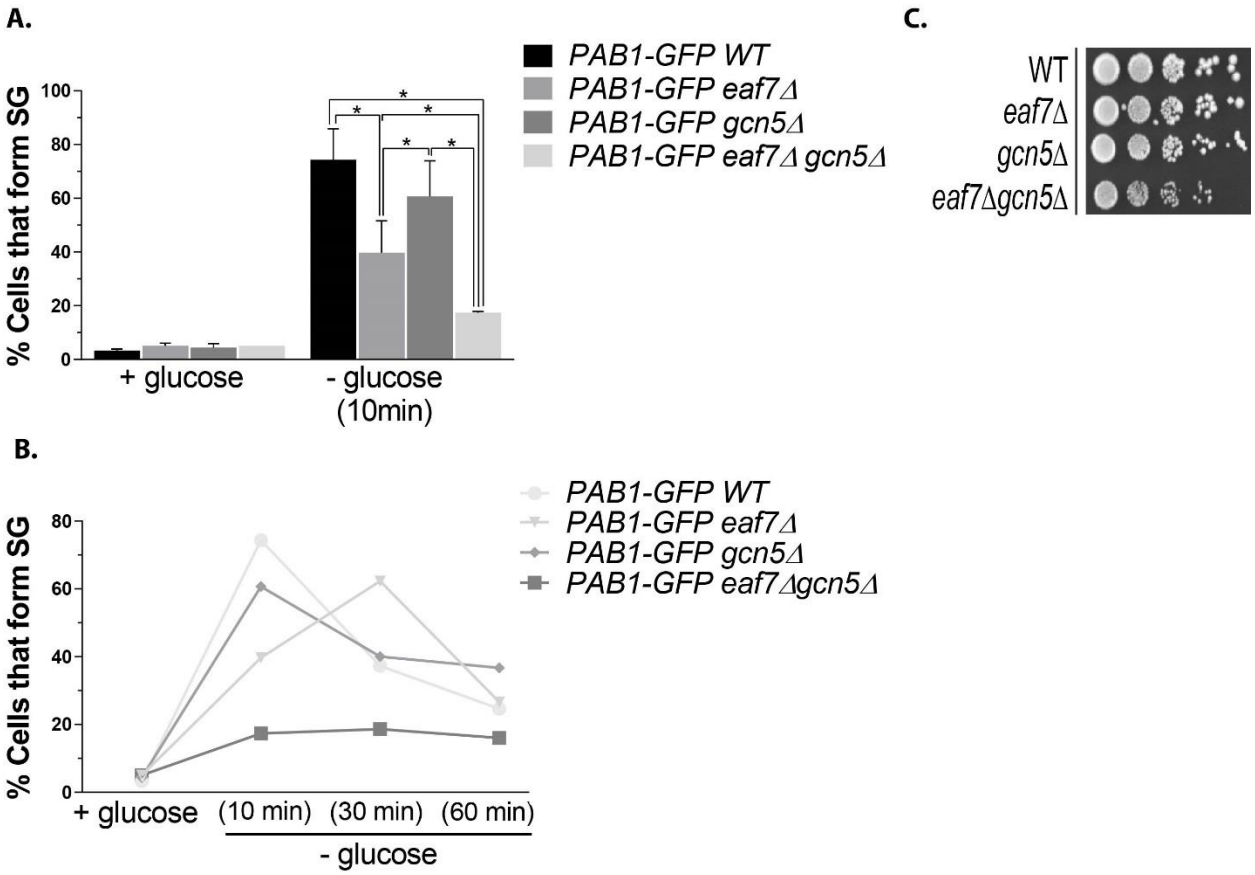

Figure 11: *EAF7* and *GCN5* are functionally redundant in regulating glucose deprived stress granule assembly. Exponential-phase (+ glucose) wild type (WT, YKB3114), *eaf7Δ* (YKB3336), *gcn5Δ* (YKB4116), and *eaf7Δgcn5Δ* (YKB4118) cells expressing endogenously tagged Pab1-GFP were subjected to GD (-glucose) for the indicated times. Stress granules (Pab1-GFP foci) were manually quantified in three independent experiments with minimum of 100 cells per replicate. Figures A and B represent results from the same data set. **A.** *eaf7Δgcn5Δ* mutants show a reduction in the percentage of cells with SG foci following 10 min of GD. Data plots indicate the average percent of cells with SG foci +/- standard deviation (Significance determined using Two Way ANOVA* $p<0.05$). **B.** *eaf7Δgcn5Δ* mutant displays an inhibition and not a delay in glucose deprived stress granule assembly over a 60 minute time course. Data indicate the average percent of cells with SG foci. **C.** *eaf7Δgcn5Δ* cells are viable and display minimal growth defects. The fitness of the mutants used in the SG study were examined by spotting 10-fold serial dilution of cells on plates containing Yeast Peptone Dextrose (YPD) media. Image is representative of three replicates.

3.1.3 EAF7 and *GCN5* impact protein levels of Pab1-GFP

As Pab1 was previously shown to be a target of NuA4 *in-vitro* (Mitchell, Huard et al. 2013), I sought to determine if *EAF7* or *GCN5* individually or together impact Pab1-GFP protein levels. To determine relative Pab1-GFP protein levels, western blot analysis was performed using the WCE of glucose and GD (10 minutes) wild type, *eaf7Δ, gcn5Δ,* and *eaf7Δgcn5Δ* exponential phase cells expressing Pab1-GFP. Interestingly, the results indicate that the *eaf7Δgcn5Δ* double mutant has lower Pab1-GFP protein levels compared to wild type and single deletion mutant strains (**Figure 12)**. However, unpublished work from Jennifer Takuski (Baetz Lab) indicates that GD SG formation is regulated independently of Pab1 protein levels (personal communication and MSc Thesis J.Takuski), suggesting that Eaf7 and Gcn5 are not impacting GD SGs through changes in Pab1-GFP protein levels.

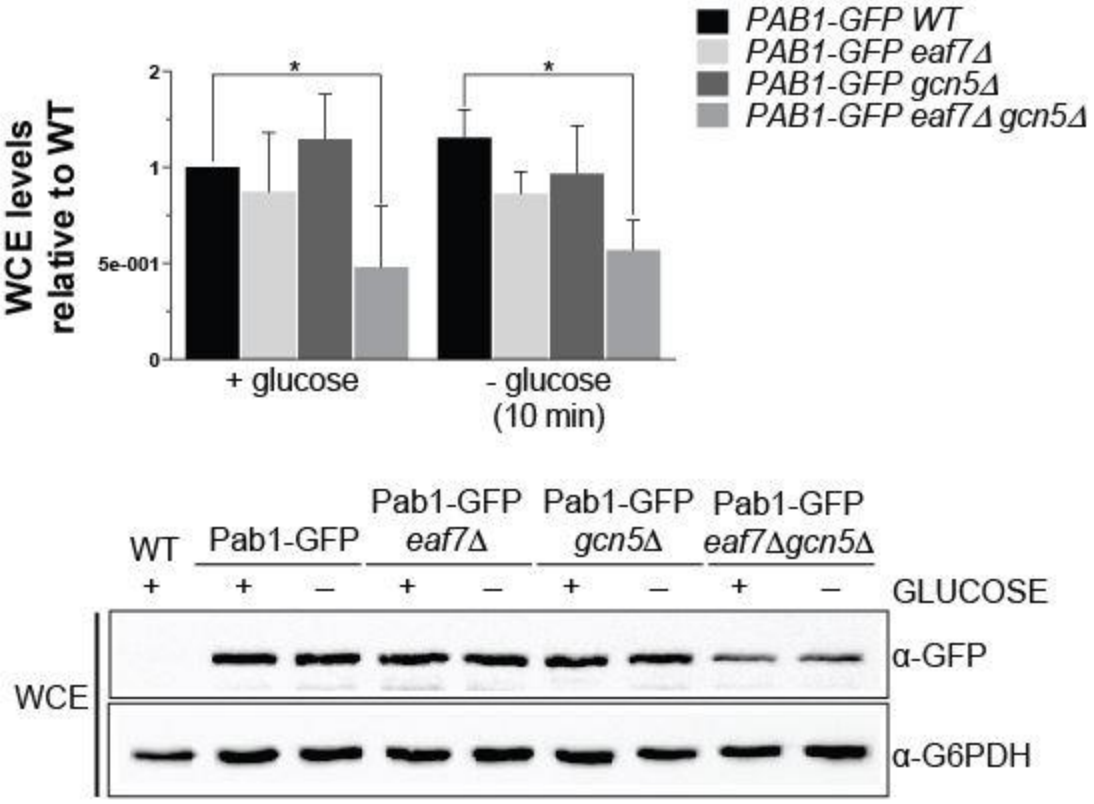

Figure 12: *EAF7 GCN5* double mutant reduces Pab1-GFP protein levels. Exponential-phase (+ glucose) wild type (WT, YKB3114), *eaf7Δ* (YKB3336), *gcn5Δ* (YKB4116), and *eaf7Δgcn5Δ* (YKB4118) cells expressing endogenously tagged Pab1-GFP were harvested both before and after GD (10 minutes). 25ug of whole cell extract was resolved by SDS-PAGE prior to western blot analysis. Antibodies are indicated on figure. Image is representative of 3 replicates. (Significance determined using Two Way ANOVA* $p<0.05$).

3.1.4 Deletion of *RPD3* rescues *EAF7 GCN5* double mutant defects in glucose deprived stress granule formation

Previous studies have shown that deletion of *RPD3* rescues numerous phenotypes of NuA4 mutants (Biswas, Takahata et al. 2008, Lin, Qi et al. 2008, Chang and Pillus 2009, Kremer and Gross 2009). Further, Rpd3 has been shown to oppose Gcn5 in a wide range of cellular processes (Burgess 1999, Perez-Martin 1998, Vogelauer 2000). This knowledge suggests that many NuA4 and Gcn5-dependent acetylation sites are also regulated by the KDAC Rpd3. Therefore, we investigated whether *rpd3Δ* can rescue the GD SG assembly phenotype of *EAF7* and *GCN5* mutants. Stress granule formation was measured in wild type, *rpd3Δ, eaf7Δgcn5Δ* and *eaf7Δgcn5Δrpd3Δ* cells expressing Pab1-GFP in both glucose and GD conditions (10 minutes, 30 minutes and 60 minutes). Deletion of *RPD3* alone does not impact SG formation under either glucose or GD conditions; however it does rescue the GD SG phenotype of *eaf7Δgcn5Δ* cells **(Figure 13A).** This data suggests that Rpd3 opposes NuA4/Gcn5-dependent SG assembly, thus implicating this KDAC in GD SG inhibition.

Next we sought to determine if Rpd3 is rescuing GD SG defects of *eaf7Δgcn5Δ* cells through the manipulation of Pab1 acetylation. The impact of Eaf7, Gcn5 and Rpd3 on Pab1-GFP acetylation was determined by immunopurifying Pab1-GFP and probing for acetylation using acetyl lysine antibodies. The *eaf7Δgcn5Δ* double mutant showed a significant reduction in Pab1-GFP acetylation compared to the wild type cells (**Figure 13C**). However, there was no increase in acetylation in the *eaf7Δgcn5Δrpd3Δ* compared to the *eaf7Δgcn5Δ* mutant **(Figure 13C)**. These results suggest that Eaf7, Gcn5, and Rpd3 may regulate SG assembly via a mechanism independent of Pab1 acetylation. Alternatively, as over 8 acetylation sites have been identified on Pab1 (Henriksen, Wagner et al. 2012, Mitchell, Huard et al. 2013), deletion of *RPD3* may

only impact the acetylation state of one or two sites, and changes might not be detected through this method. Indeed, though the *in-vivo* acetylation of Pab1 is dependent on NuA4 and Gcn5, the biological consequence of Pab1 acetylation has yet to be established and may not impact SG dynamics.

Taken together, my genetic analysis indicates that NuA4-component Eaf7, as well as Gcn5 and Rpd3 are involved in the regulation of GD SG dynamics. My analysis further suggest that these KATs and KDAC are influencing SG dynamics independently of both Pab1 protein levels and acetylation, thus suggesting regulation via another mechanism.

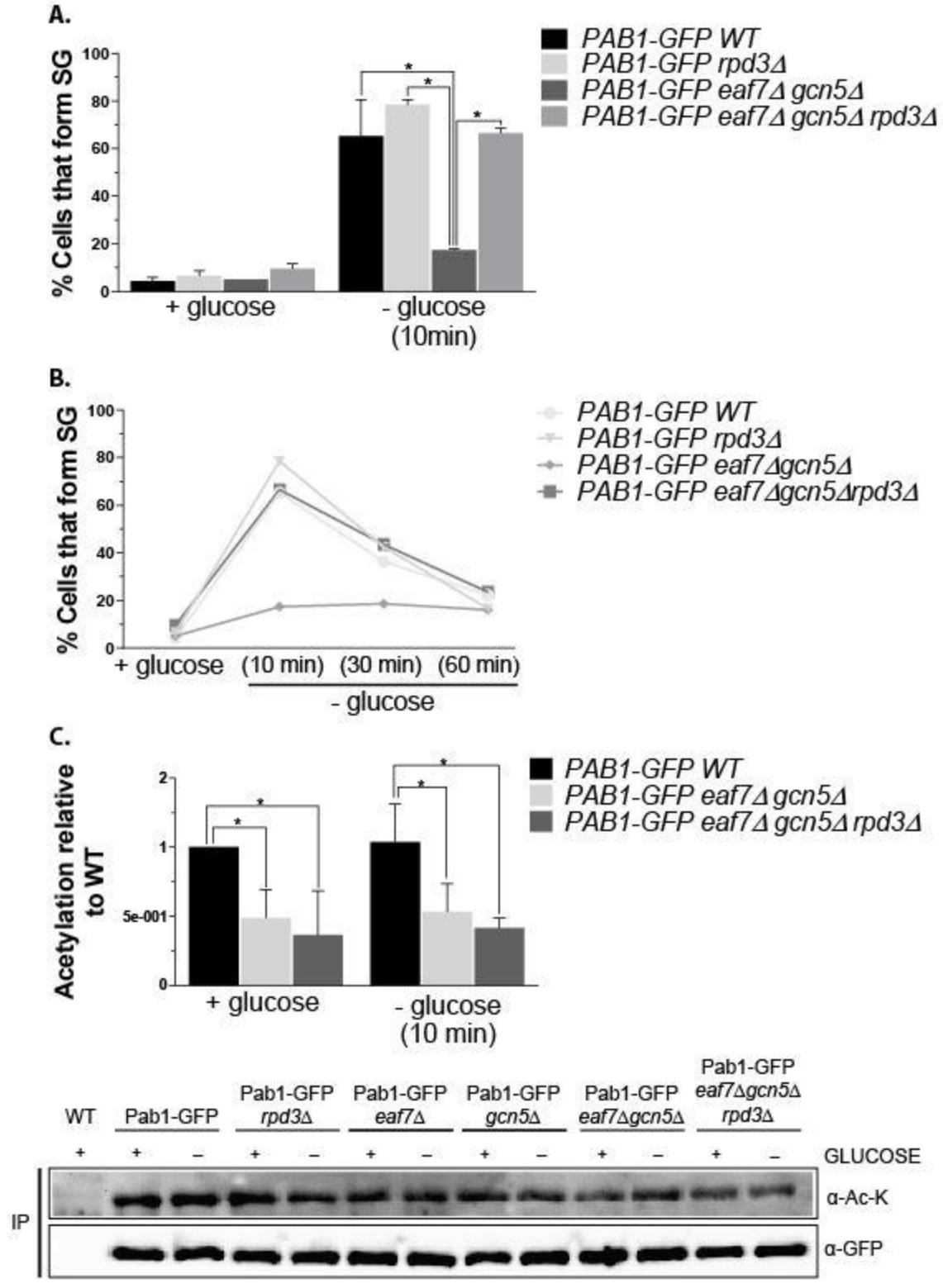
A.
% Cells that form SG
PAB1-GFP WT
PAB1-GFP rpd3Δ
PAB1-GFP eaf7Δ gcn5Δ
PAB1-GFP eaf7Δ gcn5Δ rpd3Δ
+ glucose
- glucose (10min)
B.
% Cells that form SG
PAB1-GFP WT
PAB1-GFP rpd3Δ
PAB1-GFP eaf7Δgcn5Δ
PAB1-GFP eaf7Δgcn5Δrpd3Δ
+ glucose
(10 min)
(30 min)
(60 min)
- glucose
C.
Acetylation relative to WT
PAB1-GFP WT
PAB1-GFP eaf7Δ gcn5Δ
PAB1-GFP eaf7Δ gcn5Δ rpd3Δ
+ glucose
- glucose (10 min)
WT
Pab1-GFP
Pab1-GFP rpd3Δ
Pab1-GFP eaf7Δ
Pab1-GFP gcn5Δ
Pab1-GFP eaf7Δgcn5Δ
Pab1-GFP eaf7Δgcn5Δ rpd3Δ
GLUCOSE
IP
α-Ac-K
α-GFP

Figure 13: *rpd3Δ* rescues glucose deprivation stress granule assembly defects but not Pab1 acetylation deficiency of *eaf7Δgcn5Δ* cells. Exponential-phase (+ glucose) wild type (WT, YKB3114), *rpd3Δ* (YKB3341), *eaf7Δgcn5Δ* (YKB4116), and *eaf7Δgcn5Δ rpd3Δ* (YKB4120) cells expressing endogenously tagged Pab1-GFP were subjected to GD (-glucose) for the indicated times. Stress granules (Pab1-GFP) were manually quantified in three independent experiments with minimum of 100 cells per replicate. Figures A and B represent results from the same data set. **A.** Deletion of *RPD3* significantly increases the percentage of *eaf7Δgcn5Δ* cells with stress granule foci following 10 min of glucose deprivation. Data indicate the average percent of cells with SG foci +/- standard deviation (Significance determined using Two Way ANOVA* $p<0.05$). **B.** *eaf7Δgcn5Δrpd3Δ* display glucose deprived stress granule assembly time course trend similar to WT cells. Data indicate the average percent of cells with SG foci. **C.** *rpd3Δ* does not rescue the significant decrease in Pab1 acetylation of the *eaf7Δgcn5Δ* double mutant. Exponential-phase (+ glucose) wild type (WT, YKB3114), *eaf7Δ* (YKB3336), *gcn5Δ* (YKB4116), *rpd3Δ* (YKB3341), *eaf7Δgcn5Δ* (YKB4118), and *eaf7Δgcn5Δrpd3Δ* (YKB4120) cells expressing endogenously tagged Pab1-GFP were harvested both before and after GD (10 minutes). 10 mg of WCE used for IP [40% used for acetyl blot; 4% used for Pab1-GFP IP blot]. Antibodies indicated on figure. Image is representative of 3 replicates. Quantification of 3 western blots completed using image J. Acetylation levels measured relative to WT (Significance determined using Two Way ANOVA* $p<0.05$).

3.2 Aim 2: Characterizing the role of cellular acetyl-CoA levels in the regulation of glucose deprived stress granule dynamics

3.2.1 Exogenous acetate supresses glucose deprived stress granule formation

As cellular levels of acetyl-CoA reflect glucose availability (Zhang, Galdieri et al. 2013) and as acetyl-CoA impacts global histone and non-histone protein acetylation (Takahashi, McCaffery et al. 2006, Galdieri and Vancura 2012) we next sought to determine if changes in acetyl-CoA impact GD SG formation. As exogenous acetate treatment of *S.cerevisiae* is converted to acetyl-CoA (Cai, Sutter et al. 2011) (**Figure 14A**), we sought to see if GD SG formation in wild type cells was impacted by 100mM exogenous acetate. Stress granule formation was measured in exponential-phase wild type cells expressing Pab1-GFP under glucose, GD, or GD with acetate conditions (10 min). We found that acetate treatment significantly reduces GD SG formation in wild type cells (**Figure 14C/D**). However, the repression of GD stress granule assembly by acetate might reflect conversion of acetate to glucose by the glyoxylate cycle (**Figure 14B**), rather than acetyl-CoA levels. To address this, we asked if acetate could suppress GD SG formation in *icl1Δ* cells, a mutant that inhibits the glyoxylate cycle pathway. As acetate also suppresses GD SGs in *icl1Δ* cells (**Figure 14C/D**), this data indicates that exogenous acetate is inhibiting GD SG assembly not via conversion to glucose but rather through another metabolite or mechanism.

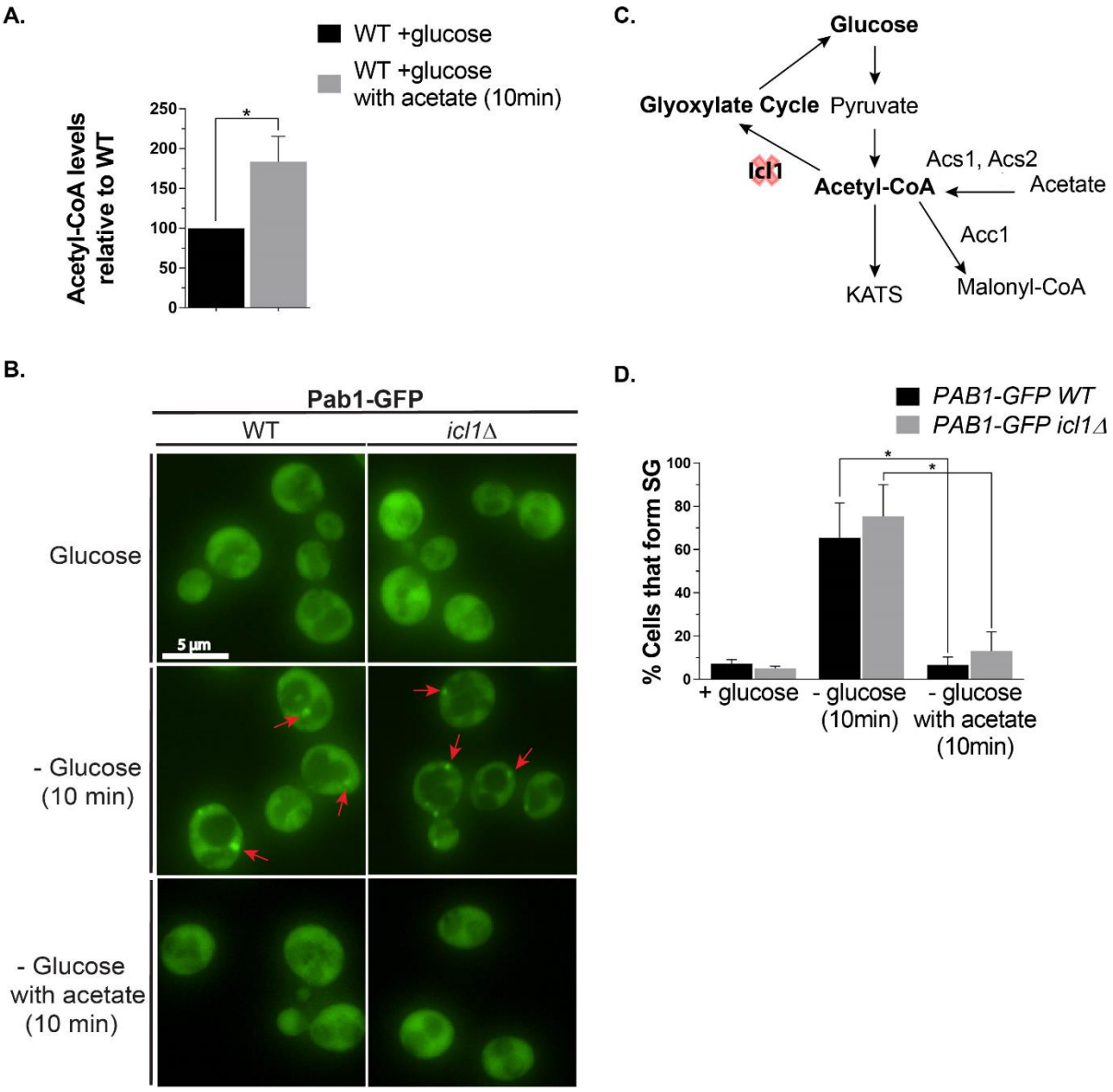
A.
WT +glucose
WT +glucose with acetate (10min)
Acetyl-CoA levels relative to WT
250
200
150
100
50
0
*
C.
Glucose
Glyoxylate Cycle
Pyruvate
Icl1
Acetyl-CoA
Acs1, Acs2
Acetate
Acc1
KATS
Malonyl-CoA
B.
Pab1-GFP
WT
icl1Δ
Glucose
- Glucose (10 min)
- Glucose with acetate (10 min)
5 µm
D.
PAB1-GFP WT
PAB1-GFP icl1Δ
% Cells that form SG
100
80
60
40
20
0
*
*
+ glucose
- glucose (10min)
- glucose with acetate (10min)

Figure 14: Exogenous acetate suppresses glucose deprived stress granule formation independent of Icl1. A. Addition of acetate to wild type cells increases cellular acetyl-CoA pools approximately 1.8 fold compared to WT cells without acetate. Exponential-phase (+ glucose) wild type (WT, YKB1079) cells were harvested before and after addition of 100mM acetate for 10 minutes. Acetyl-CoA levels measured relative to WT cells. Work of Dr. Sylvain Huard. Image is representative of 3 replicates. (Significance determined using Paired t-test * $p<0.05$) **B**. Schematic illustrating acetyl-CoA biosynthesis pathways. **C-D:** Exponential-phase (+ glucose) wild type (WT, YKB3114) and *icl1Δ* (YKB4010) cells expressing endogenously tagged Pab1-GFP were subjected to GD or GD + acetate for 10 minutes. Stress granules (Pab1-GFP foci) were manually quantified in three independent experiments with minimum of 100 cells per replicate. **C.** Typical images of glucose deprived stress granules in WT and *icl1Δ* cells, +/- acetate. **D.** Quantification of data in figure C. WT and *icl1Δ* mutant display a reduction in GD SG formation upon exposure to GD + acetate. Data indicate the average percent of cells with SG foci +/- standard deviation (Significance determined using Two Way ANOVA* $p<0.05$).

3.2.2 Exogenous acetate enhances glucose deprived stress granule recovery

We next sought to determine if exogenous acetate not only impacts assembly of GD SGs, but whether it impacts disassembly of GD SGs. Exponential-phase wild type cells expressing Pab1-GFP, underwent 30 minutes of GD followed by a 30 minute treatment with 100mM acetate, 2% glucose or continued GD prior to counting. Interestingly, the addition of acetate significantly decreased the percentage of cells with SGs compared to the GD control while the 2% glucose supplementation did not significantly recover (**Figure 15**). This result further supports that exogenous acetate, a precursor of acetyl-CoA, regulates GD SG dynamics.

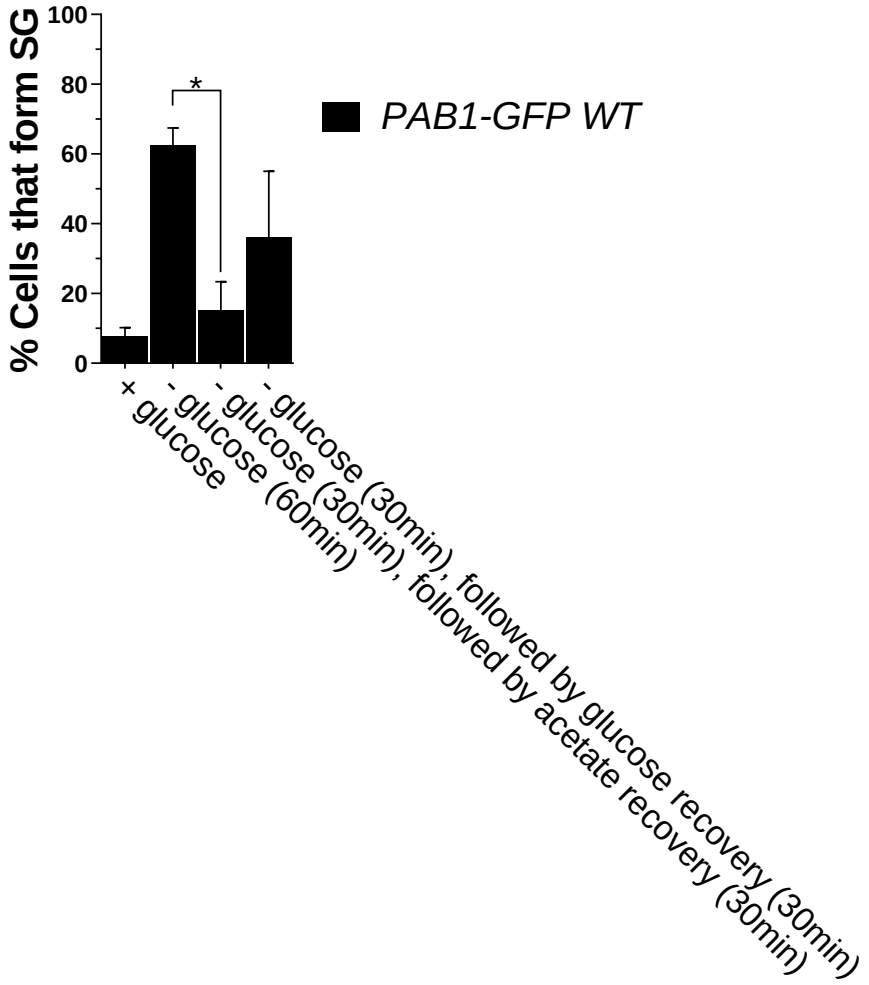

Figure 15: Addition of exogenous acetate enhances glucose deprived stress granule recovery. Exponential-phase wild type (WT, YKB3114) cells expressing Pab1-GFP (+ glucose), underwent 30 minutes of GD followed by a 30 minute treatment with 100mM acetate, 2% glucose or continued GD prior to counting of SGs. Stress granules (Pab1-GFP foci) were manually quantified in three independent experiments with minimum of 100 cells per replicate. Data indicate the average percent of cells with SG foci +/- standard deviation. WT cells +acetate recovery show a significant reduction in SG formation compared to the GD cells while the cells exposed to 2% glucose condition did not significantly recover (Significance determined using Paired t-test * $p<0.05$).

3.2.3 Exogenous acetate suppresses glucose deprived stress granules independently of NuA4 and Gcn5

As acetyl-CoA levels regulate KAT activity (Takahashi, McCaffery et al. 2006, Galdieri and Vancura 2012), we wanted to determine if exogenous acetate suppression of GD SG assembly is dependent on NuA4 (Eaf7) and/or Gcn5. Stress granule formation was measured in exponential-phase wild type, *eaf7Δ* and *eaf7Δgcn5Δ* cells expressing Pab1-GFP under glucose, GD (10 min) , or GD with 100mM acetate (10 min) conditions. The addition of acetate significantly reduced GD SG formation in *eaf7Δ* and *eaf7Δgcn5Δ* cells **(Figure 16)**, suggesting that exogenous acetate inhibition or disassembly of GD SGs is not dependent on NuA4 or Gcn5.

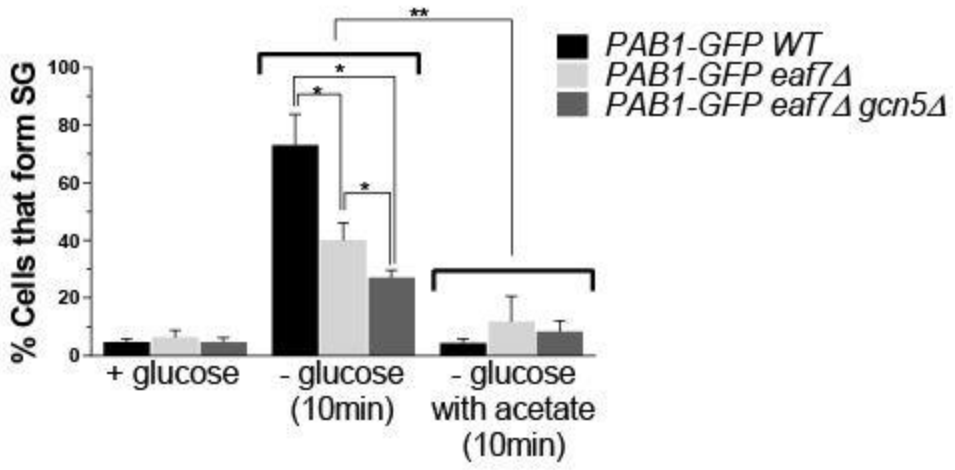

Figure 16: Exogenous acetate suppression of glucose deprived stress granule formation is independent of Eaf7 and Gcn5. Exponential-phase (+ glucose) wild type (WT, YKB3114), *eaf7Δ* (YKB3336) and *eaf7Δgcn5Δ* (YKB4118) cells expressing endogenously tagged Pab1-GFP were subjected to GD (-glucose) or GD + acetate for 10 minutes. Stress granules (Pab1-GFP foci) were manually quantified in three independent experiments with minimum of 100 cells per replicate. Data indicate the average percent of cells with SG foci +/- standard deviation (Significance determined using Two Way ANOVA* $p<0.05$). (** = $p<0.05$ comparing each strain in –glucose with acetate condition to same strain and WT in – glucose condition).

3.2.4 Reduced expression of *ACC1* reduces glucose deprived stress granule formation

To confirm that the impact of exogenous acetate on SG formation is through the metabolite acetyl-CoA, we next sought to determine if genetic manipulation of cellular acetyl-CoA levels impacts GD SGs**.** Reducing the activity of Acc1 results in an increase in cellular acetyl-CoA (**Figure 17A**) (Galdieri and Vancura 2012). Therefore, using a doxycycline regulatable $tet0_7$ repressible promoter to control the expression of *ACC1* (*$tet0_7$-ACC1*) (Shirra, Patton-Vogt et al. 2001) in a strain transformed with a Pab1-GFP expressing plasmid, we asked if reducing *ACC1* expression impacts GD SG formation.

To ensure that the addition of doxycycline reduced Acc1 activity in the *$tet0_7$-ACC1* cells, we first assessed Acc1 protein levels, cellular acetyl-coA levels, and global histone acetylation in exponential-phase *$tet0_7$-ACC1* cells before and after exposure to 10uM doxycycline for a 2.5 hour incubation period. As expected, in *$tet0_7$-ACC1* cells upon doxycycline treatment, Acc1 protein levels were reduced, while histone H4 acetylation and acetyl-CoA levels were increased (**Figure 17B-D**). Together, these experiments demonstrate that Acc1 activity is reduced and acetyl-CoA levels increased in *$tet0_7$-ACC1* cells upon doxycycline treatment.

To determine the impact that reduced Acc1 activity has on GD SG formation, exponentially grown *$tet0_7$-ACC1* cells transformed with a Pab1-GFP expressing plasmid were treated with either vehicle control or 10uM doxycycline for a 2.5 hour incubation period prior to GD. Importantly, doxycycline treatment did not induce SGs in glucose conditions (**Figure 17E**). However, reducing Acc1 activity suppressed GD SG formation (**Figure 17E**). Thus, increasing acetyl-CoA levels, by inhibiting the expression of *ACC1*, correlates with a reduction in GD SG formation.

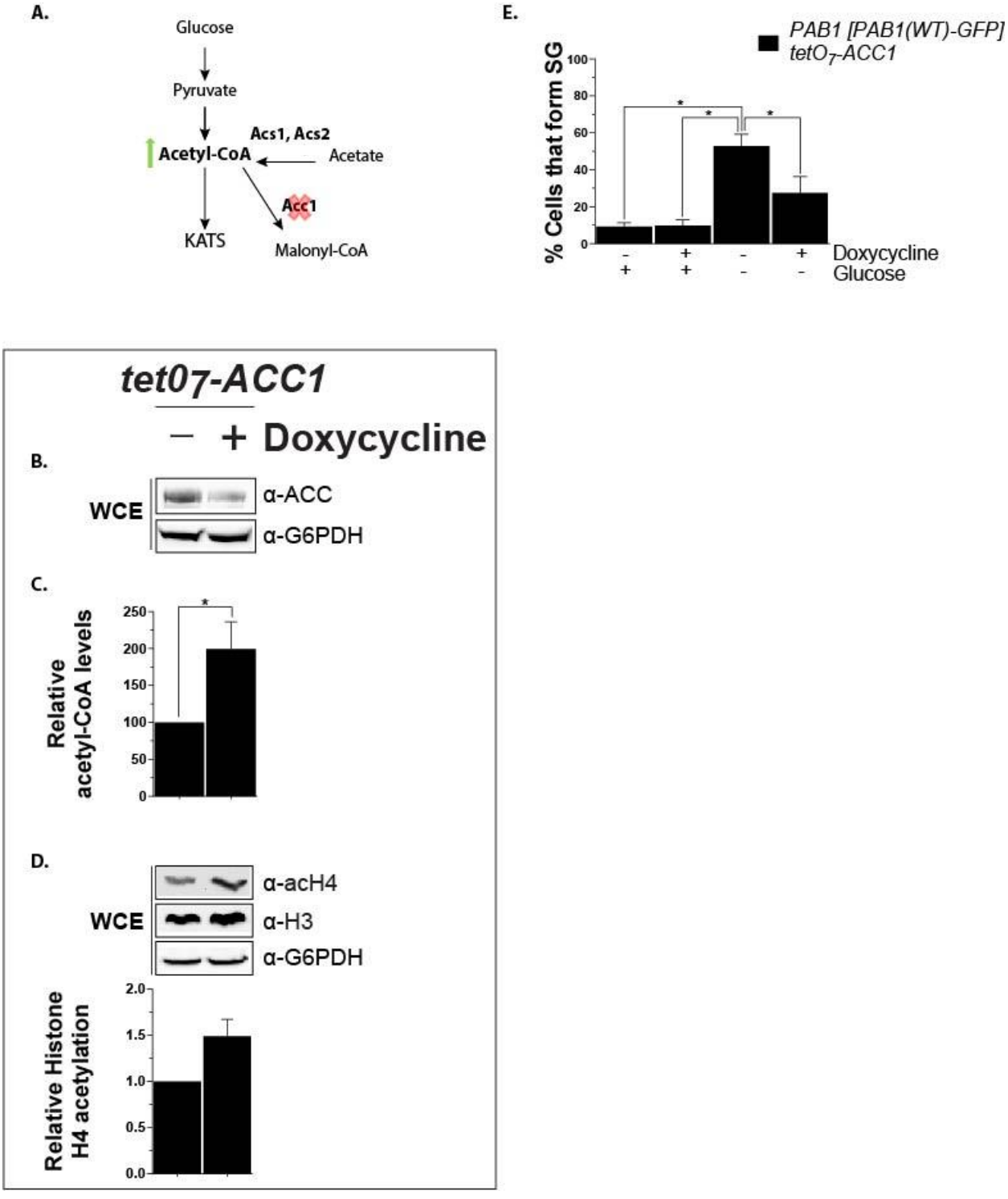
A.
Glucose
Pyruvate
Acetyl-CoA
Acs1, Acs2
Acetate
Acc1
KATS
Malonyl-CoA
E.
PAB1 [PAB1(WT)-GFP]
tetO7-ACC1
% Cells that form SG
Doxycycline
Glucose
tet07-ACC1
– + Doxycycline
B.
WCE
α-ACC
α-G6PDH
C.
Relative acetyl-CoA levels
D.
WCE
α-acH4
α-H3
α-G6PDH
Relative Histone H4 acetylation

Figure 17: Reducing Acc1 activity suppresses glucose deprived stress granule formation. A. Schematic illustrating acetyl-CoA biosynthesis pathways. **B-D:** Exponential-phase *tet0$_7$ACC1* (YKB4047) cells (+ glucose) were harvested before and after treatment with 10uM doxycycline for 2.5 hours at 30^{o}C. (Significance determined using Paired t-test* $p<0.05$). **B.** Acc1 protein levels decrease upon doxycycline treatment of *tet0$_7$-ACC1*. Whole Cell Extract was prepared using TCA lysis and 10ul of WCE was resolved by SDS-PAGE prior to western analysis using the indicated antibodies. Image is representative of 3 replicates. **C.** Cellular acetyl-CoA pools increase upon doxycycline treatment of *tet0$_7$-ACC1* cells. Work of Dr. Sylvain Huard. Image is representative of 3 replicates. Graph represents relative acetyl-CoA levels +/- standard deviation. **D.** Global acetylation of histone H4 increases upon doxycycline treatment of *tet0$_7$-ACC1* cells. 150ug of WCE was resolved by SDS-PAGE prior to Western analysis using the indicated antibodies. Image is representative of 2 replicates. Graph represents relative acetyl-CoA levels +/- standard deviation. **E.** *tet0$_7$-ACC1* cells exposed to doxycycline prior to glucose deprivation suppress stress granule formation. Exponential-phase *tet0$_7$ACC1* (YKB4048) cells (+ glucose) transformed with a *PAB1-GFP::URA::CEN* plasmid (PBK192) were subjected to 10uM doxycycline for 2.5 hours at 30^{o}C with and without GD. Stress granules (Pab1-GFP foci) were manually quantified in three independent experiments with minimum of 100 cells per replicate. Data indicate the average percent of cells with SG foci +/- standard deviation (Significance determined using Paired t-test* $p<0.05$).

3.2.5 *ACS1* deletion mutant increases glucose deprived stress granule formation

We next asked if decreasing cellular acetyl-CoA levels impacts GD SG formation. As acetyl-CoA synthetases (Acs) function to produce cellular acetyl-CoA from acetate, *ACS* mutants were used to represent a decrease cellular acetyl-CoA levels (Takahashi, McCaffery et al. 2006) (**Figure 18A**).

To determine the impact that decrease in acetyl-CoA synthetase function has on GD SG formation, SGs were measured in wild type, *acs1Δ, acs2-ts,* and *acs2-tsacs1Δ* cells expressing Pab1-GFP following a 1 hour temperature shift to 25^{o}C, 33^{o}C or 37^{o}C. Upon shift to 37^{o}C, SGs are not present in GD cells of any strain types (**Data in Appendix A: Figure S1**). This result suggests that the temperature shift prevents the GD SG response by an unknown mechanism. Thus, a 33^{o}C semi-permissive temperature shift was used to obtain a partial loss of function of *ACS2*. Shifting *acs2-ts* to 33^{o}C for 1 hour prior to 10 minutes of GD did not impact GD SG formation compared to both wild type and *acs2-ts* cells at permissive temperature (25^{o}C) (**Figure 18B**). These results indicate either that *ACS2* function is not impacted upon shift to 33^{o}C or that Acs2 does not impact GD SG formation. Interestingly, deleting *ACS1* in *acs1Δ* and *acs2-tsacs1Δ* cells significantly increases GD SG formation compared to wild type cells at both 25^{o}C and 33^{o}C (**Figure 18B/C**). These results demonstrate that there is a correlation between decreasing acetyl-CoA levels, via the deletion of *ACS1,* and increasing GD SG formation compared to wild type cells. This data further contributes to the hypothesis that cellular acetyl-CoA levels regulate GD SG response.

As Acs1 is involved in acetate to acetyl-coA conversion, microscopy was completed to determine if exogenous acetate reduction of GD SG formation is dependent on the presence of

ACS1. Stress granule formation was measured in exponential-phase wild type and *acs1Δ* cells expressing Pab1-GFP under glucose, GD (10 min), or GD with 100mM acetate (10 min) conditions. The addition of acetate significantly reduces GD SG formation compared to GD alone in the *ACS1* deletion mutant (**Figure 18C**). This suggests either that exogenous acetate is suppressing GD SG formation independently of the acetate to acetyl-coA conversion pathway, or that functionally redundant Acs2 is fully compensating for the loss of Acs1.

To corroborate that *ACS1* mutants do in fact possess a decrease in cellular acetyl-CoA levels, acetyl-CoA was measured in extracts from wild type and *acs1Δ* cells. In agreement with previous studies (van den Berg and Steensma 1995, Takahashi, McCaffery et al. 2006), *ACS1* mutants possess approximately 2 fold less cellular acetyl-CoA compared to wild type cells (**Figure 18D**).

Taken together, my analysis demonstrates that exogenous acetate and genetic manipulation of acetyl-CoA levels both impact GD SG formation. These results demonstrate that an increase in acetyl-CoA can lead to a decrease in GD SG formation, and the reverse is also confirmed. My analysis further suggests that exogenous acetate's impact on GD SG formation is not dependent on NuA4, Gcn5 or Acs1 – potentially indicating that acetyl-CoA regulation of GD SG formation is independent or downstream of these enzymes.

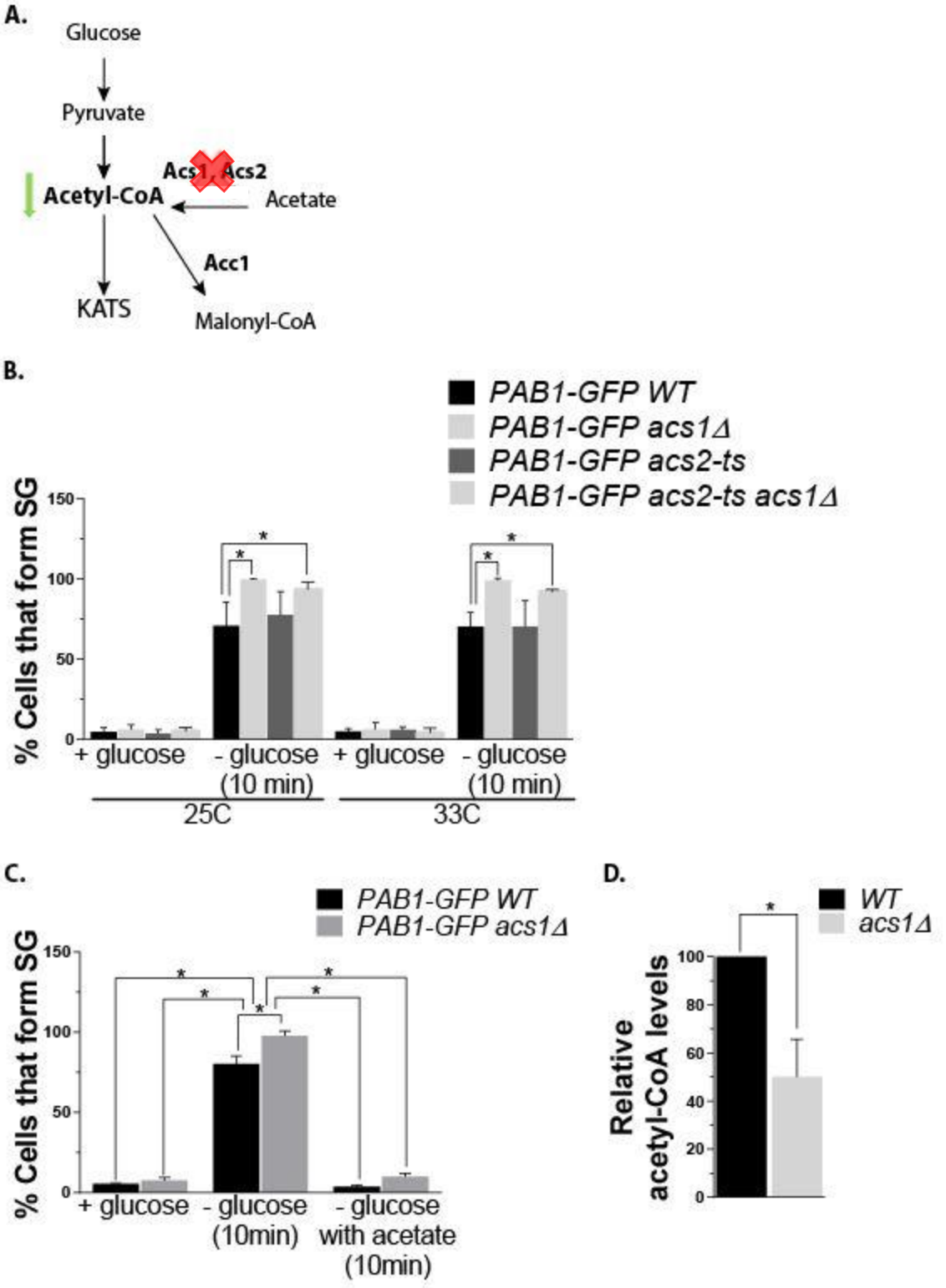
A.
Glucose
Pyruvate
Acs1, Acs2
Acetyl-CoA
Acetate
Acc1
KATS
Malonyl-CoA
B.
PAB1-GFP WT
PAB1-GFP acs1Δ
PAB1-GFP acs2-ts
PAB1-GFP acs2-ts acs1Δ
% Cells that form SG
150
100
50
0
+ glucose
- glucose (10 min)
+ glucose
- glucose (10 min)
25C
33C
C.
PAB1-GFP WT
PAB1-GFP acs1Δ
% Cells that form SG
150
100
50
0
+ glucose
- glucose (10min)
- glucose with acetate (10min)
D.
WT
acs1Δ
Relative acetyl-CoA levels
100
80
60
40
20
0

Figure 18: *ACS1* deletion mutant increases glucose deprived stress granule formation. A. Schematic illustrating acetyl-CoA biosynthesis pathway. Decrease of acetyl-CoA is a product of inhibiting Acs1/Acs2 activity. **B.** Deletion of *ACS1* increases glucose deprived stress granule formation. Exponential-phase (+glucose) wild type (WT, YKB3114), *acs1Δ* (YKB4132), *acs2-ts* (YKB4022), *and acs2-ts acs1Δ* (YKB4121), cells expressing PAB1-GFP were GD for 10 minutes following a 1 hour temperature shift to 25^{o}C and 33^{o}C. Stress granules (Pab1-GFP foci) were manually quantified in three independent experiments with minimum of 100 cells per replicate. Data indicate the average percent of cells with SG foci +/- standard deviation (Significance determined using Two Way ANOVA* $p<0.05$). **C.** Exogenous acetate can suppress glucose deprived stress granule formation in *acs1Δ* cells**.** Exponential-phase (+glucose) wild type (YKB3114) and *acs1Δ* (YKB4132) cells expressing Pab1-GFP were subjected to GD (-glucose) or GD + acetate for 10 minutes. Stress granules (Pab1-GFP foci) were manually quantified in three independent experiments with minimum of 100 cells per replicate. Data indicate the average percent of cells with SG foci +/- standard deviation (Significance determined using Two Way ANOVA* $p<0.05$). **D.** Deletion of *ACS1* decreases cellular acetyl-CoA pools more than 2 fold compared to WT cells. Exponential-phase (+glucose) wild type (WT, YKB1079), *acs1Δ* (YKB4154) were grown at 30^{o}C until harvested at OD_{600} of 0.6. Acetyl-CoA levels measured relative to WT cells. Work of Dr. Sylvain Huard. Image is representative of 3 replicates. (Significance determined using Unpaired t-test* $p<0.05$)

3.3 Aim 3: Determining if NuA4 impacts Acetyl-CoA Carboxylase 1

As we and others have implicated KATs and KDACs in SG regulation (Kwon, Zhang et al. 2007, Buchan, Kolaitis et al. 2013, Mitchell, Huard et al. 2013), one hypothesis is that acetylation of SG proteins promotes aggregation into SGs. To begin to explore this hypothesis we sought to determine if NuA4 impacts the Pab1 protein interaction network (or interactome). Exponential-phase wild type and *eaf1*Δ cells expressing Pab1-TAP were harvested before and after 30 minutes of GD and subsequently underwent Modified Chromatin Immunopurification (mChIP) (Lambert, Mitchell et al. 2009). Modified Chromatin Immunopurification was used because sonication and gentle centrifugation increases the depth of protein interactions obtained compared to a standard immunoprecipitation procedure (Lambert, Mitchell et al. 2009). *eaf1*Δ was selected as the NuA4 mutant because this deletion abolishes the NuA4 complex (Auger, Galarneau et al. 2008, Mitchell, Lambert et al. 2008) and displays defects in global histone acetylation (Auger, Galarneau et al. 2008, Cheng et al. 2015, Huang and Tan 2013). To generate a high-confidence Pab1-TAP interactome, 2 replicates were completed per condition and the Pab1-TAP protein interactors were determined by mass spectrometry as described (Mitchell, Huard et al. 2013). The high confidence dataset discussed below only includes proteins that were identified in both replicates with a minimum of 2 unique peptides per replicate. For each replicate, peptide counts for each protein were normalized relative to Pab1-TAP peptide counts from that mChIP (hence Pab1 relative peptide count = 1). Next for each condition, the normalized peptide count for each peptide was averaged and these values were used to develop the protein interaction networks described below. A complete dataset, including a comprehensive list of acetylations and protein co-purifiers, can be found in **Appendix A: Table A2/A3**.

3.3.1 Pab1-TAP Interactome Primary Comparative Analysis

Under glucose conditions, I identified 99 proteins co-purifying with Pab1-TAP. When compared to the Pab1 interaction network developed by of Richardson, Denis et al. 2012, approximately 20% of the proteins reported to co-purify with Pab1 by Richarson et al. 2012, were common between both datasets (**Figure 19**). Of the common co-purifiers, 50% were proteins involved in translation (Tif4631, Tif4632, Clu1, Yef3) while 25% were nucleolar proteins (Rrp5 and Brx1). It is important to acknowledge the difference in number of protein co-purifiers with Pab1 in this thesis vs. Richardson et al. 2012 (**Figure 19**). The screen completed by Richardson et al. 2012 omits all ribosomal proteins from their protein interaction network. The interactome in this thesis includes over 35 ribosomal protein interactors under glucose conditions. These proteins were not omitted from our dataset in an attempt to develop a more inclusive interactome. Despite the difference in number of protein co-purifiers it is still apparent that there is overlap between the interactome developed by Richardson, Denis et al. 2012 and this study (Richardson, Denis et al. 2012). Comparably, under glucose conditions, while the traditional protein immunoprecipitation method co-purified 9 non-ribosomal translational proteins (including Tif4631 and Tif4632), 11 non-ribosomal translational proteins (including Tif1/2, Tif4631 and Tif4632) were co-purified with Pab1-TAP using the mChIP method of purification. Further, the traditional protein immunoprecipitation method co-purified nucleolar proteins Nop6 and Nop77, while the mChIP method of purification used in this study co-purified Nop4, Nop56, and Nop58 under glucose replete conditions. Further, 6 of the 18 well-characterized core GD SG proteins were co-purified by Richardson, Denis et al. 2012 as well as in the Pab1 protein interaction network found in this thesis under glucose conditions (**Figure 19**). As many of the core GD SG proteins are involved in translation and RNA binding we would expect to co-purify some of these proteins with Pab1-TAP under both glucose replete and deprived conditions. This result indicates that the mChIP

procedure is able to maintain some SG and translational protein interactions throughout the purification process.

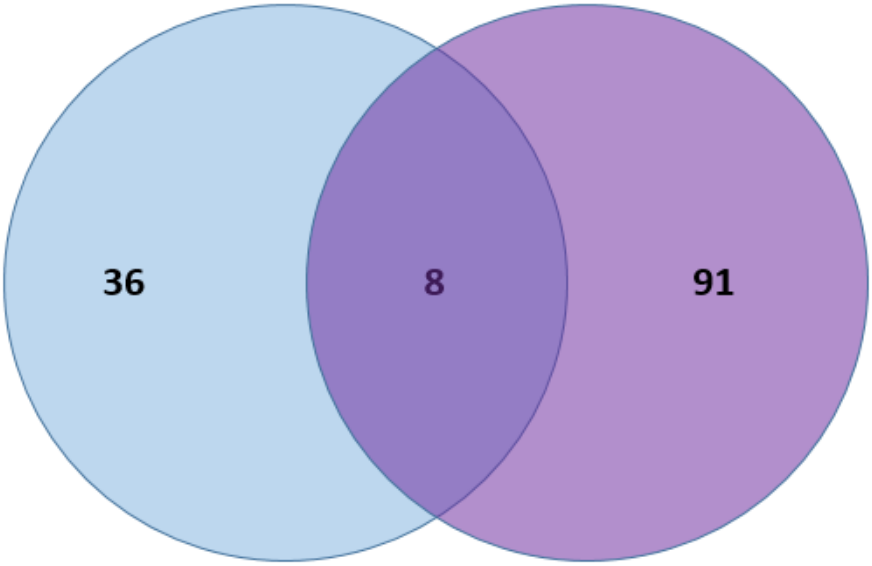

Stress granule proteins co-purified with Pab1 under glucose conditions by Richardson et al. 2012.	Stress granule proteins co-purified with Pab1 under glucose conditions in this thesis
Pab1	Pab1
Tif4631	Tif4631
Tif4632	Tif4632
Xrn1	Xrn1
Slf1	Ded1
Pub1	Tif1/Tif2

Figure 19: Comparative Analysis: Pab1 protein interaction network in this thesis vs. Richardson et al. 2012. The mChIP procedure used in this thesis is able to maintain some SG and translational protein interactions throughout the purification process, similar to the dataset published by Richardson, Denis et al. 2012.

3.3.2 NuA4 and GD Remodels the Pab1-TAP Interactome

Glucose deprivation remodels the Pab1 interactome

Upon shift to GD, SG proteins, Ded1, Tif4631, and Tif1/Tif2 maintained interactions with Pab1 but did not increase in co-purification compared to glucose replete conditions. This is expected as many of the core SG proteins are involved in translation and thus are expected to co-purify with Pab1 under normal conditions. However, the protein interaction dataset shows that there is an overall change in the Pab1-TAP protein interaction network upon shift to GD conditions (**Figure 20A**). Notably, translational proteins Fun12, Tif4632, Clu1, Rpg1, and Gcd11 increase co-purification with Pab1-TAP by at least 2 fold upon shift to GD (**Figure 20A**). As SGs represent sites that sequester mRNA and translational machinery in a non-translating state upon stress, this increase in co-purification of translational proteins with Pab1-TAP upon GD is not surprising. Further, SG proteins Tif4632 and Xrn1 increased co-purification with Pab1-TAP by at least 2 fold upon shift to GD (**Figure 20A**). Interestingly, nucleoproteins Ecm16, Nsr1, Nop56, and Nop58 were all enriched at least four fold under GD compared to glucose replete conditions (**Figure 20A**). These results identify potential novel GD SG associated proteins or may indicate that these proteins change protein levels upon exposure to GD stress.

Deletion of *EAF1* impacts the Pab1 GD interactome

I next asked how deletion of *EAF1* impacts the Pab1-TAP interactome in GD conditions (**Figure 20B**). Remarkably, a shift in co-purification of metabolic proteins in the Pab1-TAP NuA4 mutant interactome was observed upon GD (**Figure 20B**). Under GD conditions, the average total peptide count increased at least 3-fold for metabolic proteins implicated in the fatty acid biosynthesis (FAB) pathway (Fas1, Acc1, Pdc1, Ura2 and Adh1) in the *eaf1*Δ mutant compared to the wild type protein interaction network (**Figure 20B**). In fact, metabolic protein Acc1was

enriched 7-fold in the Pab1-TAP *eaf1Δ* interactome compared with the Pab1-TAP wild type (**Figure 20B**). This drastic change in co-purification of FAB proteins in NuA4 mutants implicates NuA4 as a potential regulator of this essential pathway. Most intriguingly, as Acc1 and acetyl-CoA are implicated in SG formation, further study is required to determine if NuA4 is influencing GD SG formation through modulation of Acc1.

A.

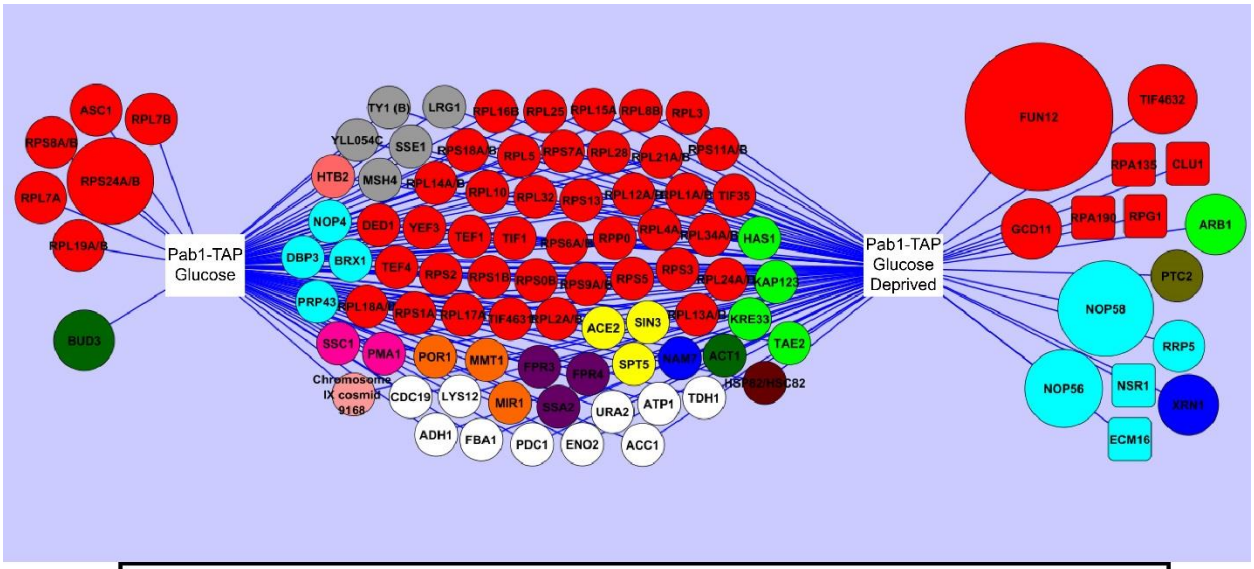
Pab1-TAP Glucose
Pab1-TAP Glucose Deprived
ASC1
RPL7B
RPS8A/B
RPS24A/B
RPL7A
RPL19A/B
BUD3
TY1 (B)
LRG1
RPL16B
RPL25
RPL15A
RPL8B
RPL3
YLL054C
SSE1
RPS18A/B
RPL5
RPS7A
RPL28
RPL21A/B
RPS11A/B
HTB2
MSH4
RPL14A/B
RPL10
RPL32
RPS13
RPL12A/B
RPL1A/B
TIF35
NOP4
DED1
YEF3
TEF1
TIF1
RPS6A/B
RPP0
RPL4A
RPL34A/B
HAS1
DBP3
BRX1
TEF4
RPS2
RPS1B
RPS0B
RPS9A/B
RPS5
RPS3
RPL24A/B
KAP123
PRP43
RPL18A/B
RPS1A
RPL17A/B
TIF463
RPL2A/B
ACE2
SIN3
RPL13A/B
KRE33
SSC1
PMA1
POR1
MMT1
FPR3
FPR4
SPT5
NAM7
ACT1
TAE2
Chromosome IX cosmid 9168
CDC19
LYS12
MIR1
SSA2
URA2
ATP1
TDH1
HSP82/HSC82
ADH1
FBA1
PDC1
ENO2
ACC1
FUN12
TIF4632
RPA135
CLU1
GCD11
RPA190
RPG1
ARB1
PTC2
NOP58
RRP5
NOP56
NSR1
XRN1
ECM16
Protein Processing
Ribosome Biogenesis
rRNA Processing
Cytoskeleton
Translation
Metabolism
Transcription
Metal/Ion Transport
mRNA Processing
Chromatin
Chaperone
Protein or Organelle Transport
Unknown/Other
Signalling

B.

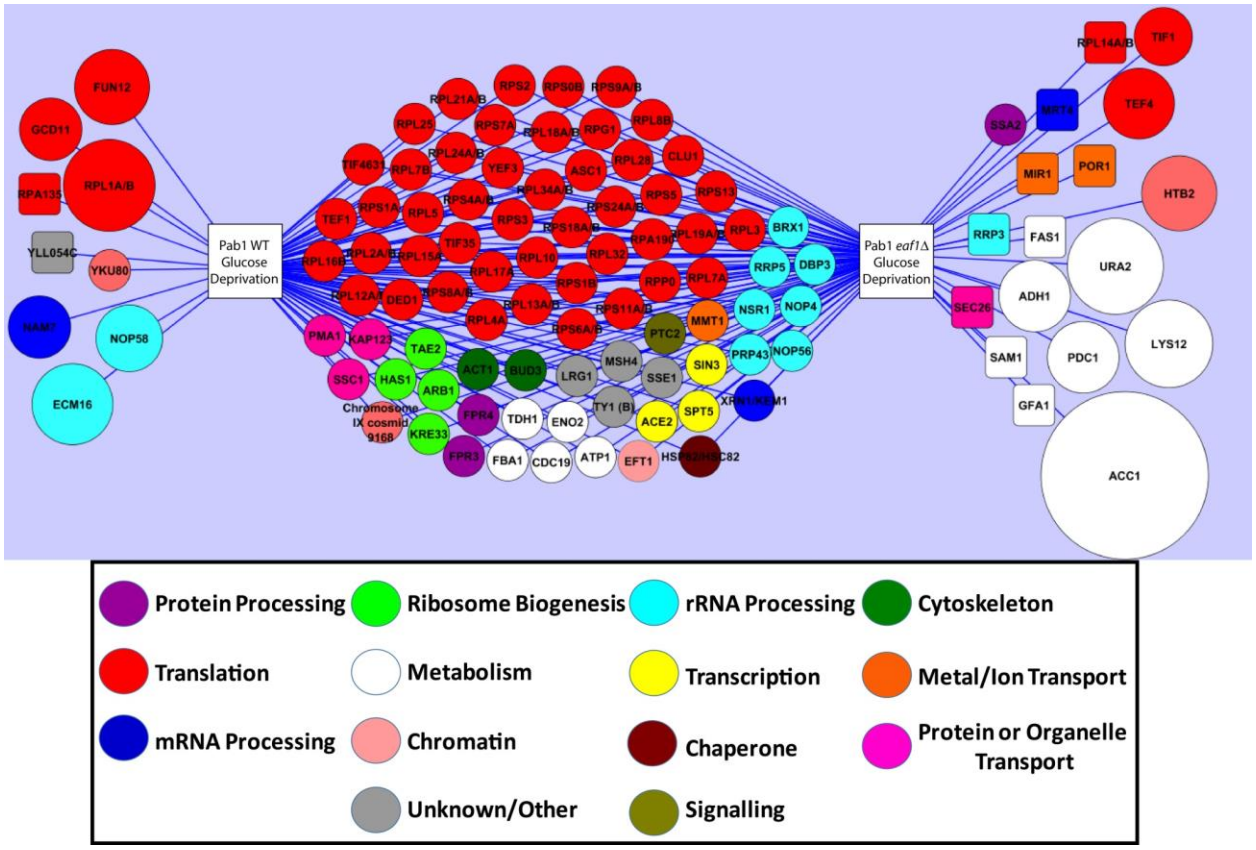

Figure 20: NuA4 and glucose deprivation remodel the Pab1-TAP interactome. Exponential phase (+glucose) wild type (WT, YKB1194) and *eaf1*Δ (YKB1229) cells expressing Pab1-TAP were harvested both before and after 30 minutes of GD. 20 mg of protein was used for the Modified Chromatin Immunopurification (mChIP). Images representative of 2 replicates. **Figures A and B** represent analysis from the same dataset. Protein targets were sorted to centre body of interactome (connecting to both source nodes) if change in peptide count was less than a 2-fold difference between the two conditions being compared (Glucose vs. GD or wild type vs. *eaf1*Δ). Protein targets were sorted to exterior of interactome (connecting to 1 source node) if 1.) the protein was only found in one of the conditions being compared or 2.) the peptide count for a protein was at least 2-fold greater in one of the conditions being compared. Protein targets possess a square node if only found in 1 of the conditions being compared. Size of protein node represents the fold increase in peptide count in one condition being compared vs the other **A.** Glucose Deprivation remodels the Pab1 interactome. Upon GD, Pab1-TAP co-purifies increasingly with core GD SG proteins as well as nucleoproteins. **B.** NuA4 remodels the GD Pab1 interactome. Upon GD, Pab1-TAP NuA4 mutant has an enrichment in co-purification with metabolic proteins; specifically the fatty acid biosynthesis pathway proteins (Acc1, Fas1, Pdc1, Adh1).

3.3.3 Acc1 co-purifies with Pab1 in NuA4 mutants

We next sought to confirm the results of our Pab1 interactome and asked if Pab1-TAP could co-purify Acc1-GFP and if NuA4 impacts this interaction. Exponential-phase wild type and *eaf7Δ* cells expressing both Acc1-GFP and Pab1-TAP from their endogenous loci were harvested before and after 10 minutes of GD. As deletion of *EAF1* possesses severe fitness defects, *eaf7Δ* is used in the following experiments to confirm data and to eliminate the possibility that phenotypes are a reflection of *eaf1Δ* growth defects. The co-IP between Pab1 and Acc1 in *eaf7Δ* cells was reproducible using western blot analysis (**Figure 21**). In addition, work by David Czosniak (MSc student in the Baetz lab) has shown that Esa1-TAP (NuA4 catalytic subunit) can co-purify Acc1 and that this interaction increases upon GD (personal communication), further suggesting that NuA4 may impact Acc1.

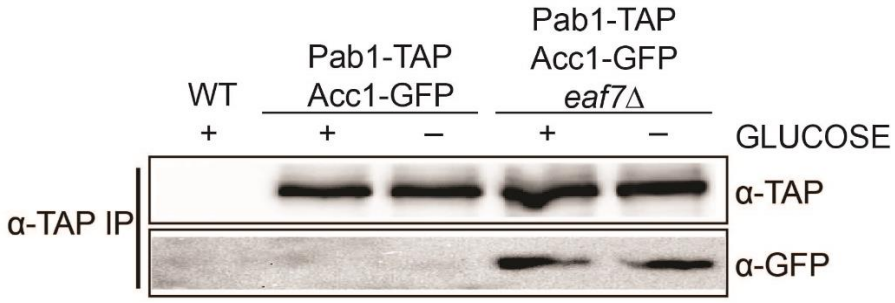

Figure 21: Acc1 co-purifies with Pab1 in NuA4 mutants. Exponential-phase (+ glucose) wild type (WT, YKB4129) and *eaf7Δ* (YKB4130) cells expressing both Acc1-GFP and Pab1-TAP were harvested before and after 10 minutes of GD. 10mg of protein used for IP [80% used for Co-IP blot; 5% used for Pab1-TAP IP blot]. Image representative of 3 independent experiments. Antibodies indicated on figure.

3.3.4 NuA4 does not impact Acc1 protein levels or gene expression

Purifying Acc1 using standard yeast lysis techniques resulted in a high degree of variability in protein levels within the WCE between replicates. As an alternative means to determine total Acc1 protein level, TCA lysis protocol was employed as previously described (Kao and Osley 2003). TCA extraction is an effective form of lysis as it precipitates all proteins out of solution allowing a more comprehensive analysis of WCE to be completed. As TCA solution is highly acidic, it dissociates immediately in a water solution, binding with the hydrophilic water molecules. This non-specifically forces all cellular proteins to form hydrophobic aggregates with themselves, rather than the occupied water molecules, thus pushing them out of solution as precipitate.

Whole cell extracts were prepared from exponential phase wild type, *eaf7Δ,* and *eaf1Δ* cells expressing Acc1-GFP both before and after 10 minutes of GD. Using TCA lysate procedure, we do not see a change in Acc1-GFP protein levels in NuA4 mutants when compared to wild type cells (**Figure 22A**). In agreement, RT-qPCR determined that NuA4 mutants, *eaf1Δ* and *eaf7Δ,* do not significantly impact *ACC1* gene expression (**Figure 22B**). Further, though there is a decrease in *ACC1* gene expression upon GD in all strains, this reduction is not significant. Microarray data further indicates that Acc1 gene expression is not regulated by NuA4 (Lindstrom 2006).

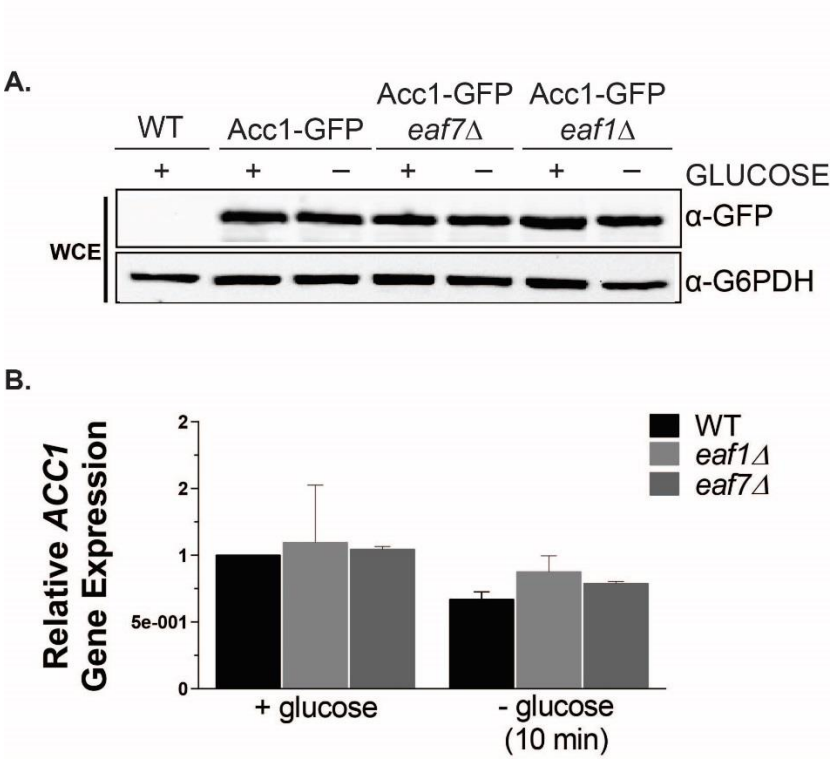

Figure 22: NuA4 does not impact Acc1 protein levels or gene expression Exponential-phase (+ glucose) wild type (WT, YKB3954), *eaf7Δ* (YKB3930), and *eaf1Δ* (YKB3929) cells expressing Acc1-GFP harvested both before and after 10 minutes of GD. **A.** Deletion of *EAF1* or *EAF7* does not impact Acc1 protein levels using the TCA lysis protocol. Cells were lysed by TCA extraction and 10ul of protein was resolved by SDS-PAGE followed by Western blot analysis using the indicated antibodies. Image representative of 3 independent experiments. **B.** Deletion of *EAF1* or *EAF7* does not significantly impact *ACC1* gene expression. Graph representative of 6 biological replicates from 2 independent experiments. 2 endogenous control primer sets used for normalization. Samples compared to WT glucose sample [value =1] (Significance determined using Two Way ANOVA* $p<0.05$).

3.3.5 NuA4 impacts Acc1 localization within the cell

To determine whether NuA4 impacts the localization of Acc1, wild type, *eaf7Δ,* and *eaf1Δ* cells expressing Acc1-GFP were analyzed via microscopy both before and after 10 minutes of GD. In glucose media, wild type Acc1-GFP form rod-shapes previously characterized as cytoplasmic punctate (**Figure 23**) (Brecker et al. 2013, Huh, Falvo et al. 2003, Tkach et al. 2012). In contrast, in *eaf1Δ* cells, almost every cell possesses a diffuse Acc1-GFP localization. Approximately 55% of the *EAF7* mutant cells possess a diffuse localization while a small proportion contains very large Acc1 foci (**Figure 23**). Upon 10 minutes of GD, all strain types display diffuse Acc1 localization within the cell (**Figure 23**). These results demonstrate that both NuA4 and the cellular metabolic state is influencing Acc1 localization within the cell.

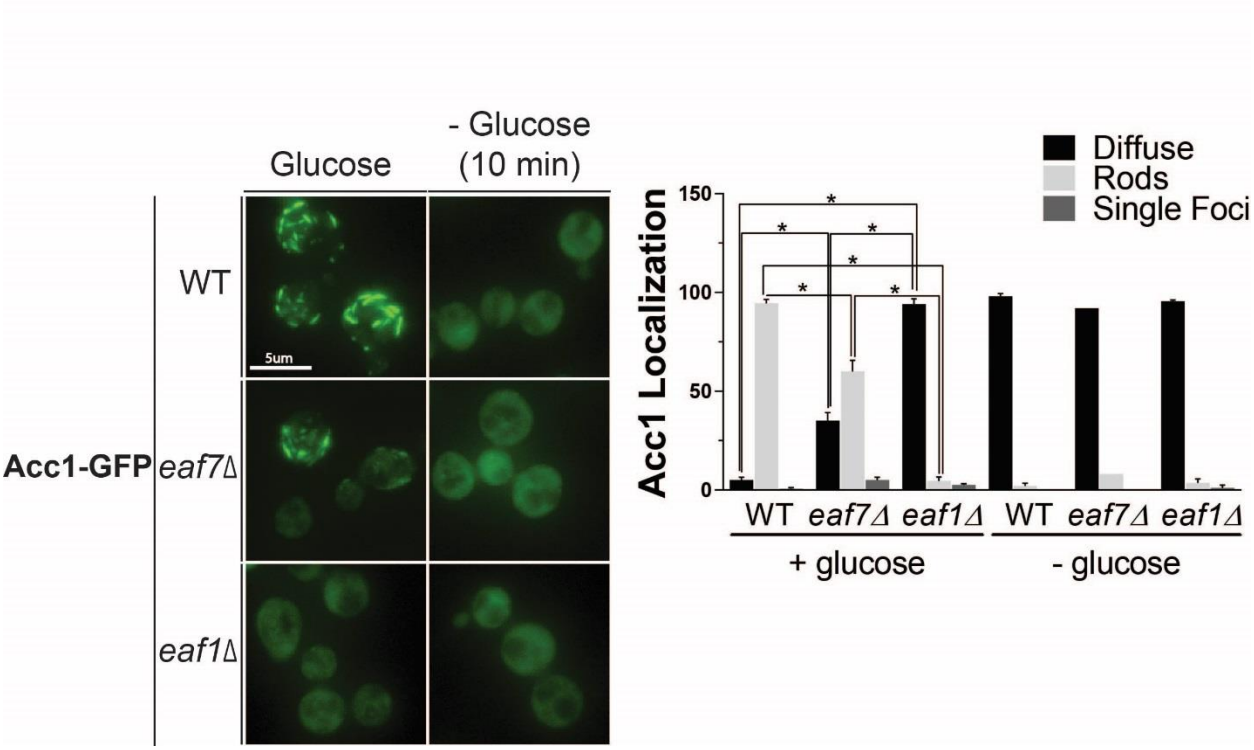

Figure 23: NuA4 and glucose availability impacts Acc1 localization within the cell. Exponential-phase (+ glucose) wild type (WT, YKB3954), *eaf7Δ* (YKB3930), and *eaf1Δ* (YKB3929) cells expressing Acc1-GFP from its endogenous loci were harvested and visualized by microscopy both before and after 10 minutes of GD. Localization (Acc1-GFP) was determined in three independent experiments with minimum of 100 cells per replicate. In glucose conditions, wild type Acc1-GFP form rod-shapes. NuA4 mutants possess a diffuse localization of Acc1-GFP, with the *eaf7Δ* possessing some very large punctate (larger but much less than WT). In GD conditions, all cell types possess a diffuse localization of Acc1-GFP. Graph indicates the average percent of cells in each localization +/- standard deviation (Significance determined using Two Way ANOVA * $p<0.05$).

3.3.6 *esa1-ts* alters Acc1 localization upon shift to 37°C

To corroborate the data that implicates NuA4 in the regulation of Acc1 localization, *esa1-ts* was used to determine how loss of Esa1 catalytic activity impacts Acc1 localization. Exponential phase wild type and *esa1-ts* cells expressing Acc1-GFP were harvested both before and after a shift to 37°C (1 hr and 2hr). Similar to *EAF1* and *EAF7* deletion mutants, upon shift to 37°C, Acc1-GFP localization becomes diffuse in *esa1-ts* cells (**Figure 24**). Together his data further supports NuA4 as a regulator of Acc1.

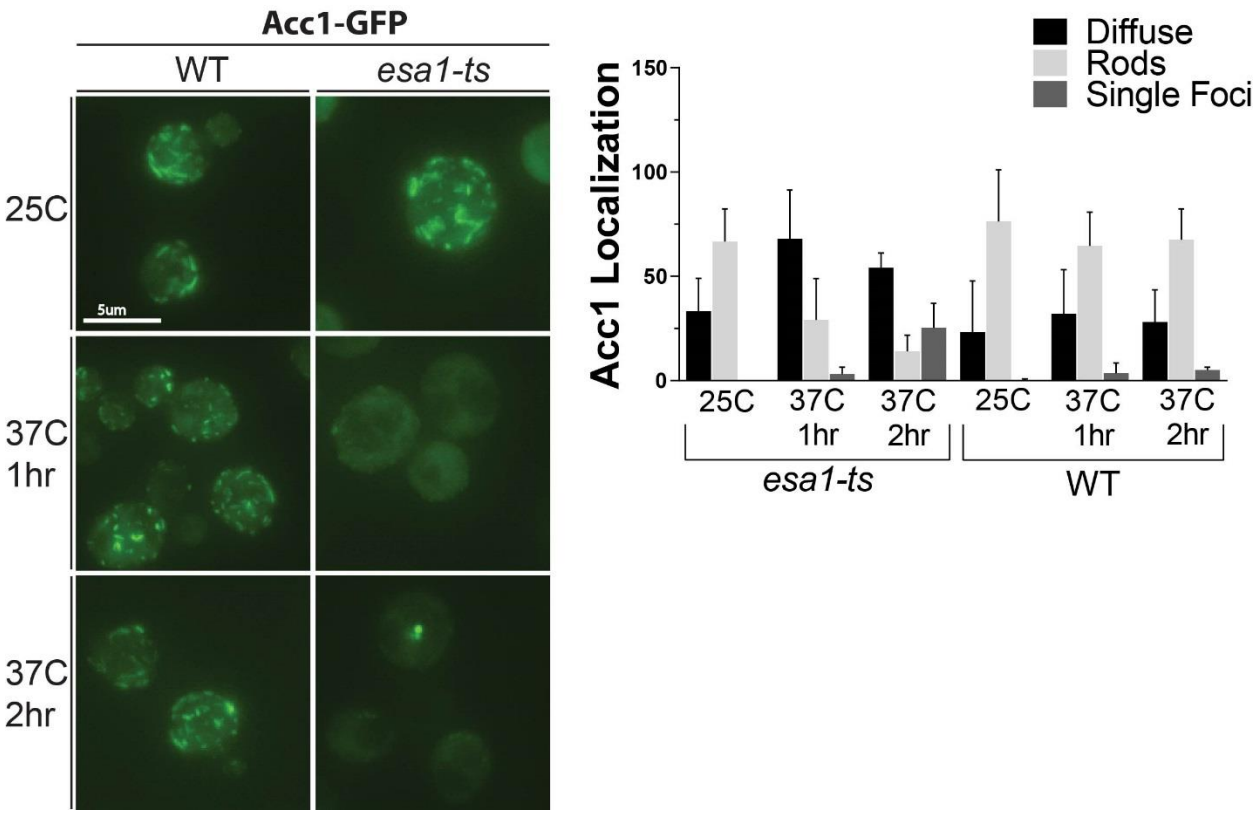

Figure 24: *esa1-ts* mutant impacts Acc1 localization. Exponential-phase (+ glucose) wild type (WT, YKB3954) and *esa1-ts* (YKB4115) cells expressing Acc1-GFP were visualized via microscopy both before and after a shift to 37°C (1 hr, 2hr). At the non-permissive temperature Acc1-GFP localization becomes diffused in *esa1-ts* cells. Graph represents quantification of results. Localization (Acc1-GFP) were determined in three independent experiments with minimum of 100 cells per replicate. Graph indicates the average percent of cells in each localization +/- standard deviation.

3.3.7 Acc1-GFP does not co-localize with mitochondria.

To assess if Acc1-GFP rods co-localize with mitochondria, yeast expressing Acc1-GFP were stained with MitoTracker Red CMXRos (catalog no. M-7512, Invitrogen). In addition to wild type cells, NuA4 mutants were also screened to determine if change in Acc1 localization occurs because of a defect in mitochondrial structure. Exponential-phase wild type, *eaf7Δ*, and *eaf1Δ* cells expressing Acc1-GFP were incubated with 100nM MitoTracker Red for 30 minutes prior to visualization. Acc1-GFP rods seen in wild type cells does not appear to co-localize with the MitoTracker Red (**Figure 25**). This suggests that Acc1-GFP rod structures are distinct from the mitochondria. Further, though existing literature demonstrates that mitochondrial localized proteins co-purify with NuA4 (Mitchell, Huard et al. 2013), and that many mitochondrial proteins are acetylated (Choudhary, Kumar et al. 2009, Downey, Johnson et al. 2015, Henriksen, Wagner et al. 2012) the mitochondrial structure as detected by MitoTracker are not discernably different between wild type and NuA4 mutant cells. This suggests that NuA4 does not impact the gross structure of the mitochondria. Characterization of Acc1 localization is essential to determining the role of NuA4 on Acc1 regulation. Further study will help determine if NuA4 is impacting the fitness of the organelle that Acc1 interacts with, or if NuA4 is affecting Acc1 directly.

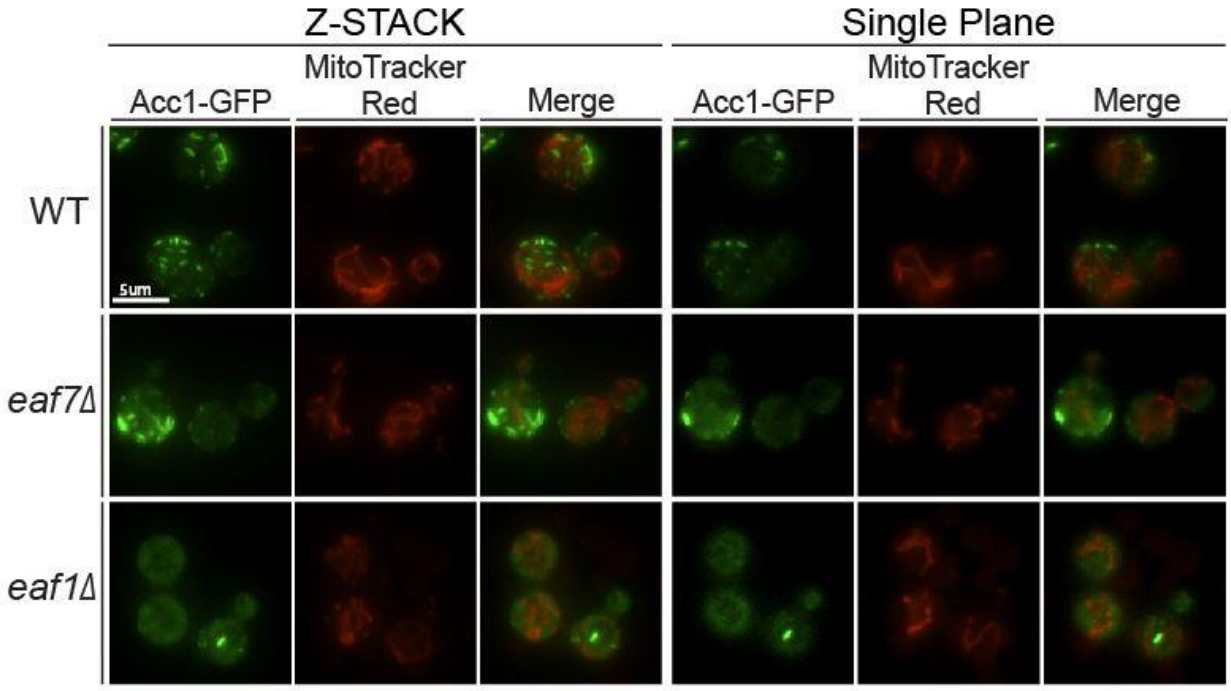

Figure 25: Acc1 does not co-localize with mitochondria in wild type or NuA4 mutant cells. Exponential-phase (+ glucose) wild type (WT, YKB3954), *eaf7Δ* (YKB3930), and *eaf1Δ* (YKB3929) cells expressing Acc1-GFP were harvested and visualized for microscopy following a 30 minute incubation with 100nM MitoTracker Red. Images were obtained from three independent experiments with minimum of 100 cells per replicate.

3.3.8 NuA4 impacts the acetylation of purified Acc1 *in-vivo*

Given the physical interaction between NuA4 and Acc1 and the reported acetylations on Acc1 (Henriksen, Wagner et al. 2012, Downey, Johnson et al. 2015), I next sought to determine if NuA4 impacts Acc1 acetylation levels. To determine whether acetylation of Acc1 is regulated by NuA4, wild type, *eaf7Δ*, and *eaf1Δ* cells expressing Acc1-GFP were harvested both before and after 10 minutes of GD. Acc1-GFP was purified and western blot analysis with anti-acetyl-antibodies was performed. Confirming acetylome studies (Henriksen, Wagner et al. 2012, Downey, Johnson et al. 2015), acetylation was detected on Acc1-GFP purified from wild type cells and while not significant, I do reproducibly detect an increase in Acc1 acetylation after GD (**Figure 26**). Acetylation on Acc1-GFP was reduced in both *eaf1Δ* and *eaf7Δ* cells, with *eaf1Δ* cells displaying a significant reduction compared to WT cells (**Figure 26**). In contrast to wild type cells, increased acetylation of Acc1 was not detected upon GD in either *eaf1Δ* or *eaf7Δ* cells (**Figure 26**).

We have shown that both the *in-vivo* acetylation state and cellular localization of Acc1 is dependent on NuA4. Taken together, these results characterize Acc1 as a potential novel target of NuA4.

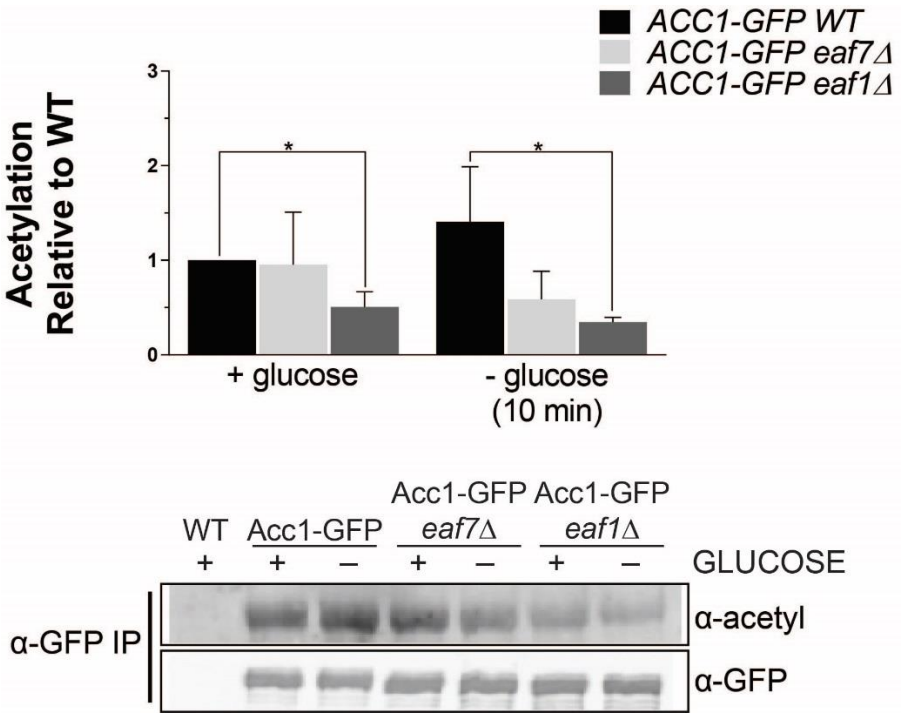

Figure 26: NuA4 impacts the acetylation of purified Acc1 *in-vivo*. Exponential-phase (+glucose) wild type (WT, YKB3954), *eaf7Δ* (YKB3930), and *eaf1Δ* (YKB3929) cells expressing Acc1-GFP were harvested both before and after GD (10 minutes). 10 mg of WCE was used for Immunoprecipitation (IP) which was resolved by SDS-PAGE [80% used for acetyl blot; 4% used for Acc1-GFP IP blot] and western analysis performed using the indicated antibodies. Image is representative of 3 replicates. Quantification of 3 western blots completed using image J. Acetylation levels measured relative to wild type (+ glucose). (Significance determined using Two Way ANOVA * $p<0.05$).

4. DISCUSSION

Despite the strengthening association between SG assembly and disease (Ginsberg, Galvin et al. 1998, Nonhoff, Ralser et al. 2007, Arimoto, Fukuda et al. 2008, Fournier, Gareau et al. 2010, Ito and Suzuki 2011, Fournier, Coudert et al. 2013, Thedieck, Holzwarth et al. 2013), the mechanisms regulating SG dynamics remain uncharacterized. My project further implicates KATs/KDACs and establishes acetyl-CoA in the regulation of GD SG dynamics. In addition, the results in this thesis characterize Acc1 as a novel target of NuA4. As Acc1 influences acetyl-CoA levels within the cell, and as acetyl-CoA impacts SG formation, this work has potentially uncovered a mechanism by which NuA4 regulates GD SG dynamics.

The role of KATs and KDACs in glucose deprived stress granule formation

Though it was previously shown that NuA4 impacts GD SGs at 10 minutes (**Figure 4**), I determined that NuA4 mutant *eaf7Δ* possess a delay in SG assembly rather than a complete inhibition of GD SG formation (**Figure 10**). As there are minimal fitness defects in *eaf7Δ* cells (**Figure 11C**) (Deutschbauer, Jaramillo et al. 2005), this result suggests that the delay in SG formation is not a result of cell sickness. One possible explanation for the *EAF7* mutant delay in GD SG formation is that another KAT may have the ability to compensate for the loss of *EAF7* function. In agreement with this hypothesis, Gcn5, a KAT implicated in the regulation of many stress response genes (Huisinga and Pugh 2004, Li and Shogren-Knaak 2009, Xue-Franzen, Henriksson et al. 2013, Gaupel, Begley et al. 2015), was determined to play a role in GD SG regulation. Though *gcn5Δ* cells do not display a significant reduction in GD SG assembly, the *eaf7Δgcn5Δ* double mutant shows a significant reduction in GD SG formation when compared to not only wild type cells but the single KAT mutants as well (**Figure 11A & B**). As the percentage of cells that form GD SGs remain reduced throughout a 60 minute GD time course in

eaf7Δgcn5Δ cells, it suggests that other KATs could not compensate for the loss of *EAF7* and *GCN5*, suggesting NuA4 and Gcn5 as the primary KATs regulating GD SG assembly. Further, it was determined that the *RPD3* deletion mutant rescues NuA4 and *GCN5* mutant defects in GD SG formation **(Figure 13)**.

The implication of KATs/KDACs in SG regulation is supported by existing literature (Buchan, Kolaitis et al. 2013, Kwon, Zhang et al. 2007, Choudhary, Kumar et al. 2009, Henriksen, Wagner et al. 2012, Mitchell, Huard et al. 2013). However, these studies in combination with the data presented in this thesis demonstrate that KAT/KDAC regulation of SG formation is stress and organism specific. For instance, work in this thesis implicates Rpd3 in SG inhibition upon GD in yeast (**Figure 13**). A study by Kwon, Zhang et al. 2007 demonstrates an opposing role for lysine deacetylases by defining HDAC6 as a critical component for the formation of SGs in mammals under heat, arsenite, carbonyl cyanide m-chlorophenylhydrazone, and UV stress. Further, while this thesis implicates Gcn5 in SG formation upon GD, studies by Buchan, Kolaitis et al. 2013 recognize Gcn5 as an inhibitor of SG assembly under non-stressed conditions. An increase in SG formation was not observed under non-stressed conditions in *GCN5* mutant strains within this thesis. This may be due to the fact that Buchan, Kolaitis et al. 2013 transformed a Pab1-GFP expressing centromere plasmid into their strains while this thesis used cells that expressed endogenously tagged Pab1-GFP. Despite this difference, these results highlight the importance of characterizing KAT/KDAC regulation of stress granule formation on a stress specific basis, highlighting the dynamic and complex nature of this post-translational modification.

How do KAT and KDACs regulate stress granule formation?

Pab1 is a core SG protein found in GD SGs (Hoyle, Castelli et al. 2007) and is known to both co-purify with and be acetylated *in-vitro* by NuA4 (Mitchell, 2013). Could Pab1 be the target

mediating NuA4 regulation of SG formation? In agreement with the result that *eaf7Δ* cells display a delay rather than a complete inhibition of stress granule formation, the single deletion mutants of *EAF7* and *GCN5* did not show a change in acetylation or protein levels of Pab1. *eaf7Δgcn5Δ* double mutant cells however, show a significant reduction the protein levels and acetylation of Pab1 compared to wild type cells (**Figure 12/13C**). Previous Master's student Jennifer Takuski demonstrated that NuA4 regulates GD SGs independently of Pab1 protein level regulation (personal communication and MSc Thesis J.Takuski). This suggests that, though NuA4 and Gcn5 are regulating Pab1 protein levels, this regulation is not impacting GD SG formation. Further, while deletion of *RPD3* rescued the GD SG defect of *eaf7Δgcn5Δ* cells (**Figure 13A**), it did not rescue the decrease in acetylation of Pab1 in these cells (**Figure 13C**). Potentially, this result suggests that KAT/KDAC regulation of GD SG formation occurs via a mechanism independent of Pab1 acetylation. Alternatively, NuA4/Gcn5-dependent acetylation of Pab1 may contribute to GD SG formation while Rpd3 rescues *eaf7Δgcn5Δ* GD SG defects through an independent pathway. Further studies discerning the biological impact of specific Pab1 acetylation sites will be necessary to determine whether NuA4 and Gcn5 acetylation of Pab1 regulates GD SG formation or other aspects of Pab1 function.

Does cellular acetyl-CoA levels regulate glucose deprived stress granule dynamics?

As cellular levels of acetyl-CoA reflect glucose availability (Zhang, Galdieri et al. 2013) (and see **Figure 5**) and are also implicated in the regulation KAT activity (Takahashi, McCaffery et al. 2006, Galdieri and Vancura 2012), we asked if changes in cellular acetyl-CoA are responsible for the misregulation of GD SG formation. We determined that the addition of 100mM exogenous acetate significantly reduces GD SG formation in wild type and *icl1Δ* cells (**Figure**

14). As *icl1Δ* is necessary for acetate to be turned into glucose via the glyoxylate cycle, acetate conversion to glucose is not the mechanism by which acetate suppresses GD SG formation. Further, we are able to show that acetate treatment of yeast for 10 minutes increased cellular acetyl-CoA levels 1.8 fold compared to untreated cells (**Figure 14A**). Thus, as exogenous acetate is at least partially converted to acetyl-CoA (Cai, Sutter et al. 2011), this work suggests that acetyl-CoA may be the metabolite suppressing GD SG. In agreement, inhibiting Acc1 activity, which increases cellular acetyl-CoA (**Figure 17C**) (Vancura 2012), reduces GD formation (**Figure 17E**), while decreasing acetyl-CoA pools in *acs1Δ* mutants, significantly increases SG formation compared to wild type cells (**Figure 18A**). Taken together, the genetics and acetate treatment suggest that acetyl-CoA is a regulator of the GD SG response. However, exogenous acetate was able to significantly reduce GD SG formation in *acs1Δ* cells (**Figure 18C**). This suggests either that exogenous acetate is suppressing GD SG formation independently of the acetate conversion to acetyl-coA, or that Acs2 is compensating for the loss of Acs1. As the essential Acs2 protein is functionally redundant with Acs1, the former scenario is likely. Unfortunately, upon temperature shift to 37^{o}C, SGs are not present in GD wild type or *acs2-ts* cells (**Appendix A: Figure S1**), precluding the direct testing of this hypothesis. Further study must be completed to determine the impact of Acs2 as well as Acs1 and Acs2 together, on GD SG assembly and GD SG inhibition via acetate.

How is acetate supressing glucose deprived stress granules?

Surprisingly we determined that exogenous acetate does not require NuA4 and/or Gcn5 in order to suppress GD SG formation **(Figure 16).** Therefore, if acetate/acetyl-CoA is suppressing GD SG through the increased KAT activity, it is likely not doing it through NuA4 or Gcn5. However, as *eaf7Δgcn5Δ* double mutant does not form SG even at 60 minutes GD (**Figure 11B**),

it is unlikely that another KAT can compensate for NuA4 and Gcn5 defects. Alternatively, acetate/acetyl-CoA could be suppressing GD SG through both KAT-dependent and independent pathways, and the further reduction displayed upon acetate treatment of *eaf7Δgcn5Δ* cells reflects only the KAT-independent pathways. More likely, the impact of acetate/acetyl-CoA on GD SGs may be occurring independent of or downstream of KAT regulation though a yet to be determined mechanism. Further study and characterization of NuA4 and acetate treatment on SGs is essential in determining a precise mechanism of regulation.

Is NuA4 impacting glucose deprived stress granule formation via regulation of Acc1 and acetyl-CoA levels?

Interestingly, deletion of *EAF1* remodelled the Pab1-TAP interactome in GD conditions (**Figure 20B),** highlighting potential SG proteins whose localization or protein levels are impacted by the presence or absence of NuA4. A shift toward metabolic proteins in the Pab1 NuA4 mutant interactome was observed (**Figure 20B**). Metabolic protein Acc1, implicated in reducing levels of Acetyl-CoA by conversion to malonyl-CoA, had one of the highest peptide counts in the *eaf1*Δ Pab1-TAP interactome but was almost absent in the wild type protein interaction network upon GD. This result highlights Acc1 as a potential target of NuA4. Work by David Czosniak determined that Esa1-TAP (NuA4 KAT) co-purifies Acc1 and that this interaction increases upon GD, further increasing a potential connection between NuA4 and Acc1 (personal communication). I determined, that while NuA4 does not impact *ACC1* gene expression or Acc1-GFP protein levels as assessed by TCA lysis (**Figure 22A/B**), microscopy analysis indicate that NuA4 does impact Acc1-GFP protein localization (**Figure 23/24**). In glucose media, Acc1-GFP in wild type cells form rod-shapes, previously characterized as cytoplasmic punctates (**Figure 23**) (Brecker et al. 2013, Huh, Falvo et al. 2003, Tkach et al. 2012). This localization

pattern was lost in NuA4 mutants (**Figure 23**). Rather, almost 100% of *eaf1Δ* cells and 50% of *eaf7Δ* display a diffused localization of Acc1 (**Figure 23**). This data was further verified using *esa1-ts* mutants. *esa1-ts* mutants at permissive temperature (25^{o}C) possessed rod-shaped oligomers of Acc1 as expected (**Figure 24**). However, upon shift to 37^{o}C, Acc1 display an increasing percentage of cells with a diffuse localization (**Figure 24**). This data suggests that localization of Acc1 is dependent on NuA4 catalytic activity. As Acc1 localization determines overall protein activity within mammalian cells (Kim, Moon et al. 2010), it is possible that NuA4's impact on Acc1 localization regulates Acc1 activity in yeast.

Given the physical interaction between NuA4 and Acc1 and the reported acetylations (Henriksen, Wagner et al. 2012, Downey, Johnson et al. 2015), I next sought to determine if NuA4 impacts the *in-vivo* acetylation state of Acc1. Interestingly, western blot analysis indicate a decrease in Acc1 acetylation in both *eaf1Δ* and *eaf7Δ* cells, with *eaf1Δ* cells displaying a significant reduction compared to WT cells (**Figure 26**). The abovementioned result highlights a potential mechanism in which NuA4 may be influencing Acc1 protein localization within the cell. More specifically, acetylations have been detected on conserved lysine residues 1764 in the carboxyl-transferase domain and 2034 in the binding pocket of the carboxyl-transferase domain (Henriksen, Wagner et al. 2012, Downey, Johnson et al. 2015). These lysine residues are located in the region implicated in the second step of acetyl-CoA carboxylation, and thus acetylation of these sites could impact overall Acc1 activity. Further, acetylation has been shown to enhance protein aggregation (Cohen et al. 2011, Cohen 2015, DiMauro 2014, Yousefi 2015). Thus a loss of acetylation on Acc1 may be responsible for the loss of Acc1 protein aggregation seen in NuA4 mutants. In mammals, Acc1 aggregation represents sites of Acc1 activity (Kim, Moon et al. 2010), thus if analogous to humans, diffuse localization of Acc1 in NuA4 mutants may

contribute to a loss of Acc1 activity. In agreement, preliminary work completed by Dr. Sylvain Huard demonstrates that acetyl-CoA levels are increased in *eaf7Δgcn5Δ* strains compared to WT cells (personal communication). Thus, further study characterizing the mechanism in which NuA4 impacts Acc1 and further defining the impact that this regulation has on Acc1 activity is required. As Acc1 reduces levels of acetyl-CoA by conversion to malonyl-CoA, these mechanisms not only provide insight into how NuA4 regulates Acc1 but potentially GD SG assembly as well. Major questions that need to be answered to further define the relationship between NuA4, Acc1, and GD SG formation include; 1.) Determining the impact that GD has on acetyl-CoA levels within the cell. 2.) If there is a change in acetyl-CoA levels – is this occurring through Acc1 or NuA4? 3.) If Acc1 and NuA4 are regulating the changes in Acetyl-CoA how is this happening? Does acetylation or localization of Acc1 impact its activity?

5. CONCLUSION

This thesis further defined the role of KATs/KDACs as well as acetyl-CoA in SG dynamics. I determined that in addition to NuA4, the lysine acetyltransferase Gcn5 is implicated in GD SG formation. In an antagonistic role, lysine deacetylase Rpd3 was determined to play a role in GD SG disassembly or inhibition. I also determined that cellular acetyl-CoA, a co-factor necessary for KAT activity, serves as a regulator of GD SG assembly. Further, I was able to define acetyl-CoA Carboxylase (Acc1) as a potential novel target of NuA4. As Acc1 influences acetyl-CoA levels within the cell, and as acetyl-CoA impacts SG formation, my work has potentially uncovered a mechanism by which NuA4 regulates GD SG dynamics (**Figure 27**). Though this thesis of work begins to characterize the role of KATs/KDACs, Acc1, and acetyl-CoA in GD SG regulation, further study is essential to understanding the complete regulatory mechanism involved.

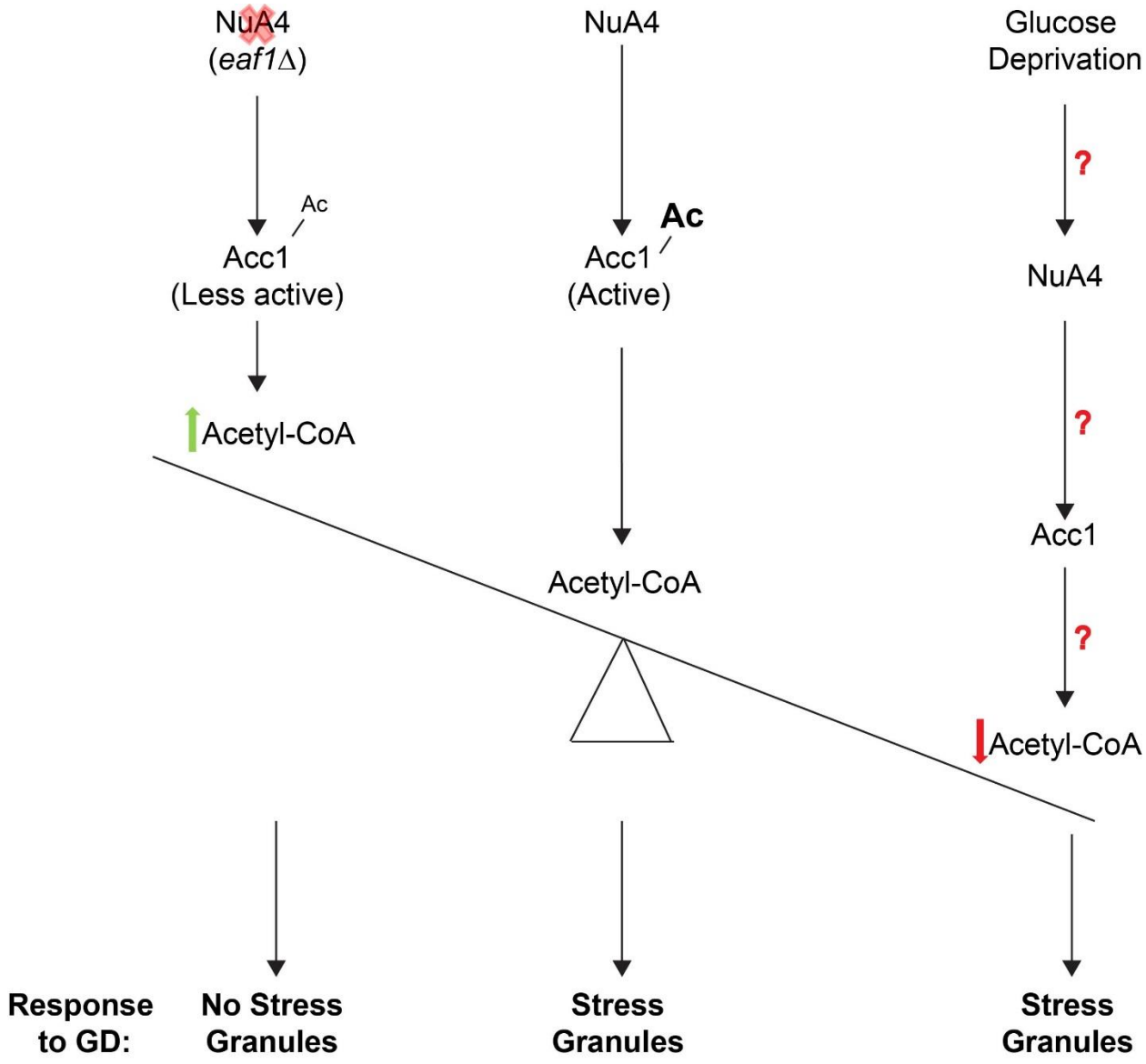

Figure 27: Working model of NuA4 and Acc1 regulation of glucose deprived stress granules.

6. REFERENCES

Arany Z et al. (1994). “E1A-associated p300 and CREB-associated CBP belong to a conserved family of coactivators.” Cell **77**(6): 799-800

Allard, S., et al. (1999). "NuA4, an essential transcription adaptor/histone H4 acetyltransferase complex containing Esa1p and the ATM-related cofactor Tra1p." EMBO J **18**(18): 5108-5119.

Arimoto, K., et al. (2008). "Formation of stress granules inhibits apoptosis by suppressing stress-responsive MAPK pathways." Nat Cell Biol **10**(11): 1324-1332.

Auger, A., et al. (2008). "Eaf1 is the platform for NuA4 molecular assembly that evolutionarily links chromatin acetylation to ATP-dependent exchange of histone H2A variants." Mol Cell Biol **28**(7): 2257-2270.

Bernstein, B. E., et al. (2000). "Genomewide studies of histone deacetylase function in yeast." Proc Natl Acad Sci U S A **97**(25): 13708-13713.

Biswas, D., et al. (2008). "Different genetic functions for the Rpd3(L) and Rpd3(S) complexes suggest competition between NuA4 and Rpd3(S)." Mol Cell Biol **28**(14): 4445-4458.

Boudreault, A., et al. (2003). "Yeast enhancer of polycomb defines global Esa1-dependent acetylation of chromatin." Genes Dev **17**(11): 1415-1428.
Brengues, M., et al. (2007). "Accumulation of polyadenylated Mrna, Pab1p, eIF4E, and eIF4G with P-bodies in Saccharomyces cerevisiae." Mol Biol Cell 11(7): 2592-2602

Brecker, M., et al. (2013). "A novel single-cell screening platform reveals proteome plasticity during yeast stress responses. J Cell Biol **200**(6): 839-850.

Buchan, J. R., et al. (2013). "Eukaryotic stress granules are cleared by autophagy and Cdc48/VCP function." Cell **153**(7): 1461-1474.

Buchan, J. R., et al. (2008). "P bodies promote stress granule assembly in Saccharomyces cerevisiae." J Cell Biol **183**(3): 441-455.

Buchan, J. R., et al. (2010). "Analyzing P-bodies and stress granules in Saccharomyces cerevisiae." Methods Enzymol **470**: 619-640.

Buchan, J. R. and R. Parker (2009). "Eukaryotic stress granules: the ins and outs of translation." Mol Cell **36**(6): 932-941.

Burgess et al. (1999). "GCN5-dependent histone H3 acetylation and RPD3-dependent histone H4 deacetylation have distinct, opposing effects on IME2 transcription, during meiosis and during vegetative growth, in budding yeast." Mol Cell **96**(12): 6835-6840.

Cai, L., et al. (2011). "Acetyl-CoA induces cell growth and proliferation by promoting the acetylation of histones at growth genes." Mol Cell **42**(4): 426-437.

Candau, R., et al. (1996). "Identification of human proteins functionally conserved with the yeast putative adapters *ADA2* and *GCN5*." Mol Cell Biol **16**:593-602.

Candau, R., et al. (1997). "Histone acetyltransferase activity and interaction with ADA2 are critical for *GCN5* function *in-vivo*." EMBO J **16**:555-565.

Carlson, M., et al. (1981). "Mutants of yeast defective in sucrose utilization." Genetics **98**(1): 25-40.

Castellani, R. J., et al. (2011). "A novel origin for granulovacuolar degeneration in aging and Alzheimer's disease: parallels to stress granules." Lab Invest **91**(12): 1777-1786.

Chang, C. S. and L. Pillus (2009). "Collaboration between the essential Esa1 acetyltransferase and the Rpd3 deacetylase is mediated by H4K12 histone acetylation in Saccharomyces cerevisiae." Genetics **183**(1): 149-160.

Cheng X., et al. (2015). "Eaf1 links the NuA4 Histone Acetyltransferase Complex to Htz1 Incorporation and Regulation of Purine Biosynthesis." Cell **14**(6):535-544.

Chittuluru, J. R., et al. (2011). "Structure and nucleosome interaction of the yeast NuA4 and Piccolo-NuA4 histone acetyltransferase complexes." Nat Struct Mol Biol **18**(11): 1196-1203.

Choudhary, C., et al. (2009). "Lysine acetylation targets protein complexes and co-regulates major cellular functions." Science **325**(5942): 834-840.

Choy, J. S., et al. (2001). "Yng2p-dependent NuA4 histone H4 acetylation activity is required for mitotic and meiotic progression." J Biol Chem **276**(47): 43653-43662.

Clarke, A. S., et al. (1999). "Esa1p is an essential histone acetyltransferase required for cell cycle progression." Mol Cell Biol **19**(4): 2515-2526.

Cohen. TJ., et al. (2011). The acetylation of tau inhibits its function and promotes pathological tau aggregation. Nat Commun. 2:252

Cohen. TJ., et al. (2015). An acetylation switch controls TDP-43 function and aggregation propensity. Nat Commun. 6:5845

Deutschbauer, A. M., et al. (2005). "Mechanisms of haploinsufficiency revealed by genome-wide profiling in yeast." Genetics **169**(4): 1915-1925.

DiMauro, MA., et al. (2014). "Acetylation of Gly1 and Lys2 promotes aggregation of human yD-crystallin." Biochemistry. **53**(46):7269:7282.

Downey, M., et al. (2015). "Acetylome profiling reveals overlap in the regulation of diverse processes by sirtuins, gcn5, and esa1." Mol Cell Proteomics **14**(1): 162-176.

Dudley, A. M., et al. (2005). "A global view of pleiotropy and phenotypically derived gene function in yeast." Mol Syst Biol **1**: 2005 0001.

Ficarro, S.B., et al. (2002). "Phosphoproteome analysis by mass spectrometry and its application to *Saccharomyces cerevisiae*. Nat Biotechnol (**20**):301-305.

Fournier, M. J., et al. (2013). "Inactivation of the mTORC1-eukaryotic translation initiation factor 4E pathway alters stress granule formation." Mol Cell Biol **33**(11): 2285-2301.

Fournier, M. J., et al. (2010). "The chemotherapeutic agent bortezomib induces the formation of stress granules." Cancer Cell Int **10**: 12.

Galdieri, L. and A. Vancura (2012). "Acetyl-CoA carboxylase regulates global histone acetylation." J Biol Chem **287**(28): 23865-23876.

Gareau, C., et al. (2011). "p21(WAF1/CIP1) upregulation through the stress granule-associated protein CUGBP1 confers resistance to bortezomib-mediated apoptosis." PLoS One **6**(5): e20254.

Gaupel, A. C., et al. (2015). "Gcn5 Modulates the Cellular Response to Oxidative Stress and Histone Deacetylase Inhibition." J Cell Biochem.

Ghaemmaghami, S., et al. (2003). "Global analysis of protein expression in yeast." Nature **425**(6959): 737-741.

Ginsberg, S. D., et al. (1998). "RNA sequestration to pathological lesions of neurodegenerative diseases." Acta Neuropathol **96**(5): 487-494.

Gregoretti, I. V., et al. (2004). "Molecular evolution of the histone deacetylase family: functional implications of phylogenetic analysis." J Mol Biol **338**(1): 17-31.

Grousl, T., et al. (2009). "Robust heat shock induces eIF2alpha-phosphorylation-independent assembly of stress granules containing eIF3 and 40S ribosomal subunits in budding yeast, Saccharomyces cerevisiae." J Cell Sci **122**(Pt 12): 2078-2088.

Henriksen, P., et al. (2012). "Proteome-wide analysis of lysine acetylation suggests its broad regulatory scope in Saccharomyces cerevisiae." Mol Cell Proteomics **11**(11): 1510-1522.

Hilliker, A., et al. (2011). "The DEAD-box protein Ded1 modulates translation by the formation and resolution of an eIF4F-mRNA complex." Mol Cell **43**(6): 962-972.

Hoyle, N. P., et al. (2007). "Stress-dependent relocalization of translationally primed mRNPs to cytoplasmic granules that are kinetically and spatially distinct from P-bodies." J Cell Biol **179**(1): 65-74.

Huang, J. and S. Tan (2013). "Piccolo NuA4-catalyzed acetylation of nucleosomal histones: critical roles of an Esa1 Tudor/chromo barrel loop and an Epl1 enhancer of polycomb A (EPcA) basic region." Mol Cell Biol **33**(1): 159-169.

Huh, W. K., et al. (2003). "Global analysis of protein localization in budding yeast." Nature **425**(6959): 686-691.

Huisinga, K. L. and B. F. Pugh (2004). "A genome-wide housekeeping role for TFIID and a highly regulated stress-related role for SAGA in Saccharomyces cerevisiae." Mol Cell **13**(4): 573-585.

Ito, D. and N. Suzuki (2011). "Conjoint pathologic cascades mediated by ALS/FTLD-U linked RNA-binding proteins TDP-43 and FUS." Neurology **77**(17): 1636-1643.

Kao, C. F. and M. A. Osley (2003). "In vivo assays to study histone ubiquitylation." Methods **31**(1): 59-66.

Keogh, M. C., et al. (2006). "The Saccharomyces cerevisiae histone H2A variant Htz1 is acetylated by NuA4." Genes Dev **20**(6): 660-665.

Kim, C. W., et al. (2010). "Induced polymerization of mammalian acetyl-CoA carboxylase by MIG12 provides a tertiary level of regulation of fatty acid synthesis." Proc Natl Acad Sci U S A **107**(21): 9626-9631.

Kim, G.W., et al. (2010). "Dietary, metabolic, and potentially environmental modulation of the lysine acetylation machinery." I J Cell Biol. **2010**:632739

Kim, K. H., et al. (1989). "Role of reversible phosphorylation of acetyl-CoA carboxylase in long-chain fatty acid synthesis." FASEB J **3**(11): 2250-2256.

Kim, N. C., et al. (2013). "VCP is essential for mitochondrial quality control by PINK1/Parkin and this function is impaired by VCP mutations." Neuron **78**(1): 65-80.

Klass, D. M., et al. (2013). "Quantitative proteomic analysis reveals concurrent RNA-protein interactions and identifies new RNA-binding proteins in Saccharomyces cerevisiae." Genome Res **23**(6): 1028-1038.

Kremer, S. B. and D. S. Gross (2009). "SAGA and Rpd3 chromatin modification complexes dynamically regulate heat shock gene structure and expression." J Biol Chem **284**(47): 32914-32931.

Krogan, N. J., et al. (2004). "Regulation of chromosome stability by the histone H2A variant Htz1, the Swr1 chromatin remodeling complex, and the histone acetyltransferase NuA4." Proc Natl Acad Sci U S A **101**(37): 13513-13518.

Kwon, S., et al. (2007). "The deacetylase HDAC6 is a novel critical component of stress granules involved in the stress response." Genes Dev **21**(24): 3381-3394.

Lambert, J. P., et al. (2010). "Defining the budding yeast chromatin-associated interactome." Mol Syst Biol **6**: 448.

Lambert, J. P., et al. (2009). "A novel proteomics approach for the discovery of chromatin-associated protein networks." Mol Cell Proteomics **8**(4): 870-882.

Lee, K. K. and J. L. Workman (2007). "Histone acetyltransferase complexes: one size doesn't fit all." Nat Rev Mol Cell Biol **8**(4): 284-295.

Li, S. and M. A. Shogren-Knaak (2009). "The Gcn5 bromodomain of the SAGA complex facilitates cooperative and cross-tail acetylation of nucleosomes." J Biol Chem **284**(14): 9411-9417.

Li, X. et al. (2014). "Overproduction of fatty acids in engineered *Saccharomyces cerevisiae."* Biotech and Bioeng. 111(9): 1841-1852.

Lin, Y. Y., et al. (2009). "Protein acetylation microarray reveals that NuA4 controls key metabolic target regulating gluconeogenesis." Cell **136**(6): 1073-1084.

Lin, Y. Y., et al. (2008). "A comprehensive synthetic genetic interaction network governing yeast histone acetylation and deacetylation." Genes Dev **22**(15): 2062-2074.

Lindstrom, K. C., et al. (2006). "Isw1 functions in parallel with the NuA4 and Swr1 complexes in stress-induced gene repression." Mol Cell Biol **26**(16): 6117-6129.

Longtine, M. S., et al. (1998). "Additional modules for versatile and economical PCR-based gene deletion and modification in Saccharomyces cerevisiae." Yeast **14**(10): 953-961.

Lu, J. Y., et al. (2011). "Acetylation of yeast AMPK controls intrinsic aging independently of caloric restriction." Cell **146**(6): 969-979.

Lynen, F. (1959). "Participation of acyl--CoA in carbon chain biosynthesis." J Cell Comp Physiol **54**: 33-49.
Miller, Luke (2010). "Analyzing Gels And Western Blots With Imagej. " *lukemiller.org.* Web.

Mitchell, L., et al. (2013). "mChIP-KAT-MS, a method to map protein interactions and acetylation sites for lysine acetyltransferases." Proc Natl Acad Sci U S A **110**(17): E1641-1650.

Mitchell, L., et al. (2008). "Functional dissection of the NuA4 histone acetyltransferase reveals its role as a genetic hub and that Eaf1 is essential for complex integrity." Mol Cell Biol **28**(7): 2244-2256.

Mitchell, L., et al. (2011). "Regulation of septin dynamics by the Saccharomyces cerevisiae lysine acetyltransferase NuA4." PLoS One **6**(10): e25336.

Neuwald et al. (1997). " GCN5-related histone N-acetyltransferases belong to a diverse superfamily that includes the yeast SPT10 protein." Trends Biochem Sci. 22(5): 154-155.

Nonhoff, U., et al. (2007). "Ataxin-2 interacts with the DEAD/H-box RNA helicase DDX6 and interferes with P-bodies and stress granules." Mol Biol Cell **18**(4): 1385-1396.

Obermayer, M. L., F. (1976). "Structure of biotin enzymes." Trends Biochem Sci. **1**: 169-171.

Oliver, S. S. and J. M. Denu (2011). "Dynamic interplay between histone H3 modifications and protein interpreters: emerging evidence for a "histone language"." Chembiochem **12**(2): 299-307.

Perez-Martin, J. et al. (1998). " Mutations in chromatin components suppress a defect of Gcn5 protein in Saccharomyces cerevisiae." Mol Cell Biol **18**(2): 1049-1054.

Polevoda, B. and F. Sherman (2002). "The diversity of acetylated proteins." Genome Biol **3**(5): reviews0006.

Reifsnyder et al. (1996). "Yeast SAS silencing genes and human genes associated with AML and HIV-1 Tat interactions are homologous with acetyltransferases." Nat Genet 14(1): 42-49.

Richardson, R., et al. (2012). "Mass spectrometric identification of proteins that interact through specific domains of the poly(A) binding protein." Mol Genet Genomics **287**(9): 711-730.

Rossetto, D., et al. (2014). "Eaf5/7/3 form a functionally independent NuA4 submodule linked to RNA polymerase II-coupled nucleosome recycling." EMBO J **33**(12): 1397-1415.

Roth, S. Y., et al. (2001). "Histone acetyltransferases." Annu Rev Biochem **70**: 81-120.

Sachs, A. B., et al. (1987). "A single domain of yeast poly(A)-binding protein is necessary and sufficient for RNA binding and cell viability." Mol Cell Biol **7**(9): 3268-3276.

Sandmeier, J. J., et al. (2002). "RPD3 is required for the inactivation of yeast ribosomal DNA genes in stationary phase." EMBO J **21**(18): 4959-4968.

Shirra, M. K., et al. (2001). "Inhibition of acetyl coenzyme A carboxylase activity restores expression of the INO1 gene in a snf1 mutant strain of Saccharomyces cerevisiae." Mol Cell Biol **21**(17): 5710-5722.

Shore, D. (2000). "The Sir2 protein family: A novel deacetylase for gene silencing and more." Proc Natl Acad Sci U S A **97**(26): 14030-14032.

Sinha, H., et al. (2008). "Sequential elimination of major-effect contributors identifies additional quantitative trait loci conditioning high-temperature growth in yeast." Genetics **180**(3): 1661-1670.

Smith, J. S., et al. (2002). "SIR2 family of NAD(+)-dependent protein deacetylases." Methods Enzymol **353**: 282-300.

Steger, D. J., et al. (1998). "Purified histone acetyltransferase complexes stimulate HIV-1 transcription from preassembled nucleosomal arrays." Proc Natl Acad Sci U S A **95**(22): 12924-12929.

Swisher, K. D. and R. Parker (2010). "Localization to, and effects of Pbp1, Pbp4, Lsm12, Dhh1, and Pab1 on stress granules in Saccharomyces cerevisiae." PLoS One **5**(4): e10006.

Takahashi, H., et al. (2006). "Nucleocytosolic acetyl-coenzyme a synthetase is required for histone acetylation and global transcription." Mol Cell **23**(2): 207-217.

Tehlivets, O., et al. (2007). "Fatty acid synthesis and elongation in yeast." Biochim Biophys Acta **1771**(3): 255-270.

Teixeira, D., et al. (2005). "Processing bodies require RNA for assembly and contain nontranslating mRNAs." RNA **11**(4): 371-382.

Thedieck, K., et al. (2013). "Inhibition of mTORC1 by astrin and stress granules prevents apoptosis in cancer cells." Cell **154**(4): 859-874.

van den Berg. M.A. and HY Steensma (1995). " ACS2, a Saccharomyces cerevisiae gene encoding acetyl-coenzyme A synthetase, essential for growth on glucose." Eur J Biochem **231**(3): 704-713.

Vogelauer M., et al. (2000). "Global Histone acetylation and deacetylation in yeast." Nature **408**(6811): 495-498.

Wang, Q., et al. (2010). "Acetylation of metabolic enzymes coordinates carbon source utilization and metabolic flux." Science **327**(5968): 1004-1007.

Witters, L. A. and T. D. Watts (1990). "Yeast acetyl-CoA carboxylase: in vitro phosphorylation by mammalian and yeast protein kinases." Biochem Biophys Res Commun **169**(2): 369-376.

Woods, A., et al. (1994). "Yeast SNF1 is functionally related to mammalian AMP-activated protein kinase and regulates acetyl-CoA carboxylase in vivo." J Biol Chem **269**(30): 19509-19515.

Yang, XJ., et al. (2004). " Lysine acetylation and the bromodomain: a new partnership for signaling." Bioessays **26**(10): 1076-1087.

Xu, W., et al. (1998). "Mammalian *GCN5* and *P/CAF* acetyltransferases have homologous amino-terminal domains important for recognition of nucleosomal substrates." Mol Cell Biol **18**:5659-5669.

Xue-Franzen, Y., et al. (2013). "Distinct roles of the Gcn5 histone acetyltransferase revealed during transient stress-induced reprogramming of the genome." BMC Genomics **14**: 479.

Yi, C., et al. (2012). "Function and molecular mechanism of acetylation in autophagy regulation." Science **336**(6080): 474-477.
Yousefi, R., et al. (2015). "Asprin-mediated acetylation induces structural alteration and aggregation of bovine pancreatic insulin." J Biol Mol 21: 1-34

Zhang, H., et al. (2004). "The Yaf9 component of the SWR1 and NuA4 complexes is required for proper gene expression, histone H4 acetylation, and Htz1 replacement near telomeres." Mol Cell Biol **24**(21): 9424-9436.

Zhang, M., et al. (2013). "The yeast AMPK homolog SNF1 regulates acetyl coenzyme A homeostasis and histone acetylation." Mol Cell Biol **33**(23): 4701-4717.

7. APPENDIX A: Supplemental Data

7.1 S1: Wild type, *acs1Δ* and *acs2-ts* cells possess a defect in glucose deprived stress granule formation at 37°C

To determine the impact that loss of acetyl-CoA synthetase function has on GD SG formation, SGs were measured in exponential-phase wild type, *acs2-ts*, and *acs2-tsacs1Δ* cells expressing Pab1-GFP. Exponential phase cells were GD for 10 minutes following a 1 hour temperature shift to 37°C. 37°C represents a non-permissive temperature at which *ACS2* expression would be inhibited. Upon shift to 37°C, SGs are not present in GD cells of any strain types (**Figure S1**). This result suggests that the temperature shift somehow prevents the GD SG response. In an attempt to obtain loss of function of *ACS2* while avoiding inhibiting GD SG formation, a semi-permissive temperature of 33°C was used in **Figure 18**.

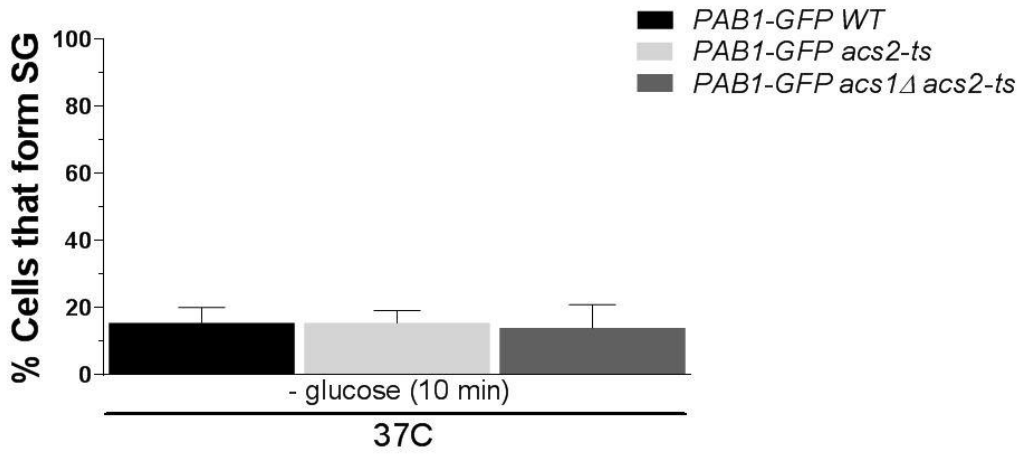

S1: Wild type, *acs1Δ* and *acs2-ts* cells possess a defect in glucose deprived stress granule formation at 37°C. Exponential phase cells were GD for 10 minutes following a 1 hour temperature shift to 37°C. Stress granules (Pab1-GFP) were manually quantified in three independent experiments with minimum of 100 cells per replicate. Data indicate the average percent of cells with SG foci +/- standard deviation.

7.2 S2: Pab1-TAP interactome dataset

In order to develop the Pab1-TAP protein interaction network, protein co-purifiers had to be analyzed and interpreted. The silver stain from replicate 1 shows a change in protein bands depending on condition and strain background (**Figure S2A**). Changes in bands on the silver stain provide primary evidence that NuA4 and GD are impacting the Pab1 interactome. This observation was confirmed via mass spectrometry analysis (**Full dataset found in Table A3**). Further, mass spectrometry analysis of silver stained bands indicated that proteins co-purified with Pab1 are acetylated (**Full dataset found in Table A2**). These acetylations represent sites that may be implicated in regulation of SG formation. Interestingly, Sin3, a component of Rpd3 was shown to be acetylated. As Rpd3 has been implicated in the GD SG response, acetylation of Sin3 may represent a mechanism of SG regulation.

A.

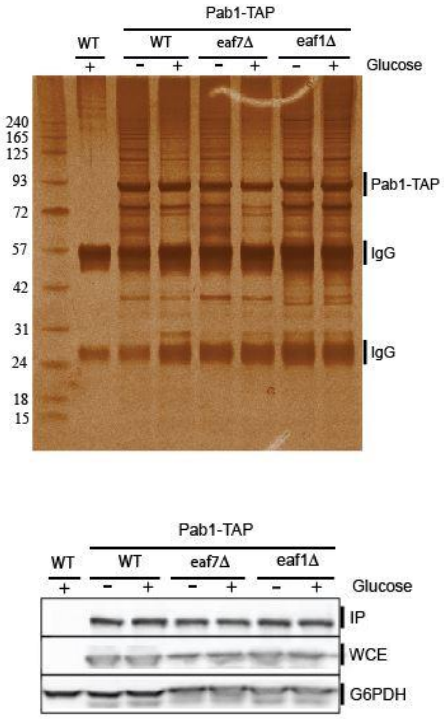
Pab1-TAP
WT
WT
eaf7Δ
eaf1Δ
+
- + - + - +
Glucose
240
165
125
93
72
57
42
31
24
18
15
Pab1-TAP
IgG
IgG
Pab1-TAP
WT
WT
eaf7Δ
eaf1Δ
+
- + - + - +
Glucose
IP
WCE
G6PDH

Table A2:

Protein	WT GD	WT Glucose+	*eaf1*Δ GD	*eaf1*Δ Glucose+
ALG5	K150	K150	K150	K150
ARP2			K367	
ASF2		K47	K47	
BUD3		K12	K12	
CBF5	K3		K3	K3
CBK1				K391
FPR4		K270	K270	
GYL1	K640	K640		K640
INP52	926	161	161	161
IRC20	K954		K954	
LTE1		K640 K642		
MMT1	K157	K157 K50	K157 K50	K157 K50
MSS2	K368	K368		
NAS2	K84	K84	K84	K84
NCE101			K11	K11
NMD2				K35
PAB1	K7	K7 K164	K7	K7
PRM8/9		K180		K180
SIN3	K940	K940	K940	K940
SPT23	k948		k948	
TAF5	K376	K376	K376	
TIF35	97/99			
TRM10	K282		K282	
YME2	K612 K618		K612 K618	K612 K618

Table A3:

Protein Name	WT GD R1	WT Glucose+ R1	*eaf1Δ* GD R1	*eaf1Δ* Glucose+ R1	WT GD R2	WT Glucose + R2	*eaf1Δ* GD R2	*eaf1Δ* Glucose+ R2
ACC1	0	0	18	10	1	1	7	1
ACE2	4	5	3	1	10	6	9	14
ACT1	5	0	6	11	6	15	10	18
ADH1	1	0	2	5	1	17	6	2
ALD6					0	6	0	0
ALG5	2	4	3	2				
ARB1	3	0	1	1	7	4	5	4
ARC1					0	0	2	0
ASC1	0	4	6	4	6	11	3	4
ATP1	0	0	2	2	0	4	0	0
ATP2					0	4	0	1
BAT1					0	5	0	0
BIK1	0	0	0	1	5	2	1	3
BMH1/2	0	0	0	1	0	2	1	4
BRX1	1	0	1	1	1	1	4	1
BUD3	0	1	1	3	2	6	2	2
CBF5	13	3	3	10	1	0	0	0
CDC19	2		2	4	2	38	7	0
CDC33	0	0	1	0	1	1	1	0
CDC48	0	0	2	1	0	0	1	0
CHC1	0	1	3	2	1	0	0	0
Chromosome IX cosmid 9168	2	1	0	4	1	3	1	2
CIC1	3	0	0	0				
CLB2	2	3	5	4				
CLU1	3	0	3	14	5	0	16	5
COY1					0	1	1	0
CTI6	0	0	1	3	1	0	0	0
DAM1					2	1	0	1
DBP2					0	2	7	5
DBP3	7	0	0	2	0	1	2	0
DBP8					0	0	3	0
DED1	12	4	8	14	8	9	12	8
DPS1					1	1	1	0
ECM16	2	0	0	2	2	0	1	0
EFB1					1	2	0	0

EFT1	4	1	9	10	3	16	2	4
ENO1					3	40	13	12
ENO2	5				3	49	13	12
FAS1	0	0	2	2	0	2	2	0
FBA1	1	0	1	1	0	10	3	0
FPR3	2	0	0	2	1	1	3	1
FPR4	3	0	0	2	1	2	3	1
FUN12	14	0	1	6	14	2	7	5
GAR1	2	1	1	1	0	1	1	1
GCD11	1	0	0	2	8	3	4	2
GFA1	0	0	2	2	0	0	2	1
GPM1					0	15	1	0
GUS1					0	0	2	0
GYL1					2	2	0	1
HAS1	1	0	0	1	0	1	4	0
HCA4	1	0	0	0	1	0	2	0
HEF3	4	2	7	7				
HHF1	3	0	0	1	0	0	0	4
HHT1	1	0	0	1	0	2	1	6
HSP42					1	0	2	0
HSP60					0	7	3	0
HSP82/HSC82	2	2	3	2	0	13	6	1
HTB2	3	1	11	4	0	0	1	3
HTZ1	1	0	0	0	0	2	0	7
ILV5					0	6	0	0
INM1	0	0	1	0	2	4	1	2
INP52					1	2	1	1
IRC20	0	0	1	0	1	1	0	0
KAP104	2	0	1	2	2	2	0	1
KAP123	3	0	3	0	0	1	1	0
KAR2					2	8	6	1
KIC1	0	0	0	3	2	0	2	2
KRE33	6	1	1	1	1	3	5	1
LRG1	3	7	15	4	4	4	5	1
LSP1					1	2	1	0
LYS12	1	0	3	0	0	1	5	2
LYS20	1	0	0	0	0	0	2	0
MDR1	1	1	0	1				
MET17					0	4	0	0
MET6					0	2	0	0
MIR1	0	0	3	0	0	2	1	0

MMT1	2	2	2	2	3	1	2	1
MRH1					1	0	2	0
MRT4	0	0	2	1	0	0	2	1
MSH4	5	1	4	0	5	3	3	6
NAB6	0	0	1	4	0	0	0	1
NAM7	7	3	3	2	1	1	0	2
NAS2	1	1	1	1				
NAT1					0	0	3	0
NEW1	1	0	0	0	3	2	5	4
NHP2	3	1	2	2				
NIP1	2	0	0	1	1	0	1	0
NOP1	8	0	2	5	6	1	5	1
NOP12	1	0	1	3	0	0	1	1
NOP4	2	0	1	1	0	0	0	2
NOP56	12	2	3	6	3	1	8	4
NOP58	15	1	4	8	4	2	2	2
NPL3	0	0	0	1	1	1	3	1
NSR1	3	0	0	1	1	0	4	1
OLA1	0	0	2	1	0	2	1	0
PAB1	87	101	83	107	129	144	129	180
PAC2					2	1	3	0
PDC1	1		2	5	1	37	6	2
PET9					1	7	2	0
PEX14	1	1	2	0				
PFK1	0	0	2	2	0	1	0	0
PGI1					0	8	1	0
PGK1	1				0	35	4	0
PIL1	0	0	0	1	2	6	5	2
PKC1	0	2	3	2				
PMA1	4	0	4	6	3	6	7	4
POR1	0	0	2	1	0	6	2	0
PRP43	9	1	0	4	1	2	3	2
PRT1					0	0	2	1
PSA1					0	3	0	0
PTC2	5	3	5	3	4	2	2	2
PWP1	2	0	1	2	0	0	0	1
PWP2	1	0	0	0	3	1	0	1
RBG1	1	0	0	0	4	0	1	1
RPA135	3	0	0	1	2	0	0	0
RPA190	4	0	0	1	1	0	3	1
RPF2	2	0	0	0	1	1	1	0

RPG1	2	0	2	2	5	0	8	4
RPL10	4	4	6	8	0	6	2	2
RPL11A/B	4	3	5	4	0	2	0	0
RPL12A/B	3	4	3	6	0	6	0	0
RPL13A/B	4	4	4	4	0	10	0	0
RPL14A/B	0	0	1	1	0	5	0	0
RPL15A	1	2	1	1	3	8	2	1
RPL16B	4	5	4	8	0	7	0	0
RPL17A	4	5	3	4	0	2	0	0
RPL18A/B	3	3	1	1	1	4	1	0
RPL19A/B	3	6	3	1	0	6	0	1
RPL1A/B	4	3	0	2	2	2	1	1
RPL20A/B	3	4	4	6				
RPL21A/B	2	3	3	1	0	3	0	0
RPL22A/B					0	3	0	0
RPL24A/B	1	0	0	1	0	2	0	0
RPL25	2	2	3	3	0	4	0	0
RPL27A/B	0	2	3	3	0	2	0	0
RPL28	2	3	1	2	0	3	0	0
RPL2A/B	3	4	5	3	12	12	6	6
RPL3	4	8	4	3	11	19	8	5
RPL30					0	4	0	0
RPL31A/B					0	4	0	0
RPL32	0	0	1	2	0	4	0	0
RPL33A/B	1	0	0	0	0	3	0	0
RPL34A/B	0	0	2	0	0	2	0	0
RPL4A	12	15	15	13	16	20	8	13
RPL4B					16	18	9	13
RPL5	0	2	7	5	6	11	7	3
RPL6A/B	3	4	6	5	0	2	0	0
RPL7A	5	12	8	9	8	18	7	6
RPL7B	3	12	8	10	8	17	7	5
RPL8B	2	4	6	5	8	16	4	5
RPL9A/B	1	4	3	3				
RPP0	7	5	9	10	13	17	11	9
RPS0B	5	6	11	5	5	11	5	7
RPS11A/B	3	3	3	3	0	4	0	0
RPS12					0	6	0	0
RPS13	0	0	5	3	0	7	0	0
RPS14A/B					0	3	0	0
RPS16A/B	0	0	0	1	0	4	0	0

RPS17A/B	0	1	1	2	0	2	0	0
RPS18A/B	1	1	1	2	0	6	0	0
RPS1A	5	7	7	8	8	16	7	3
RPS1B	6	8	10	11	10	20	7	4
RPS2	0	0	2	1	3	4	2	0
RPS20	0	0	4	4				
RPS23A/B	1	0	1	3	0	3	0	0
RPS24A/B	1	3	3	3	0	8	0	0
RPS25A/B	0	0	0	3	0	1	0	0
RPS26A/B	0	1	1	1	0	2	0	0
RPS28A/B					0	2	0	0
RPS3	10	16	17	13	18	21	12	7
RPS4A/B	4	10	12	6	7	12	7	3
RPS5	3	7	7	6	10	13	7	5
RPS6A/B	6	8	9	8	11	10	6	10
RPS7A	3	5	5	14	0	7	0	0
RPS8A/B	2	5	3	4	1	5	0	0
RPS9A/B	4	1	7	2	0	6	0	0
RRN5					0	2	1	1
RRP3	0	0	1	1	0	0	1	1
RRP5	10	5	3	9	5	2	6	3
SAH1					0	5	0	0
SAM1	0	0	2	2	0	2	2	0
SBP1	0	0	1	0	2	1	2	0
SCP160	0	0	1	0	0	0	2	0
SDA1					0	0	2	0
SEC14					0	0	2	0
SEC26	0	0	1	1	0	0	2	0
SIN3	1	0	2	1	0	2	0	2
SNP1	2	0	1	1				
SOV1	0	0	2	1				
SPH1	0	0	2	0	3	1	1	2
SPT5	1	0	0	4	1	1	2	1
SRO9					2	1	2	2
SSA2	8	3	5	3	11	18	18	10
SSA4					5	13	10	4
SSB1	24	16	23	24				
SSB2					19	38	48	30
SSC1	1	0	1	1	1	6	3	2
SSE1	1	0	1	2	1	2	0	1
SSZ1					0	0	2	0

STM1					1	2	0	0
SUI2	0	0	1	1	1	2	4	1
SUI3					1	0	3	0
SUP35					0	0	2	0
SUP45	3	3	4	5				
TAE2	0	0	0	2	0	0	1	2
TAF5					2	2	2	0
TDH1	3	0	3	2	2	24	0	0
TDH2					3	30	0	0
TEF1	13	5	13	19	15	38	57	22
TEF4	1	0	3	0	2	5	8	3
TFG1	1	0	0	0	0	0	0	2
TIF1	4	4	7	9	4	7	9	3
TIF34					2	0	6	0
TIF35	1	0	0	1	2	2	2	1
TIF4631	2	8	6	7	6	4	4	4
TIF4632	2	0	1	2	2	1	1	1
TRM10	0	0	0	1	2	0	1	0
TRS33/ARG4					0	2	1	3
TSA1/2					0	3	0	0
TY1 (B)	3	4	2	1	2	8	4	3
TYW1					0	2	0	1
UPC2					0	0	1	2
URA2	2	1	19	24	0	3	4	2
UTP10	2	2	0	1	0	0	3	0
UTP21					1	1	0	1
UTP7	2	0	0	2				
VMA5					0	0	3	0
VPS1					0	0	2	0
XRN1/KEM1	5	2	12	15	6	2	7	5
YEF3	12	5	16	16	15	19	42	14
YFR016C					7	3	2	4
YHB1					0	3	0	0
YKL107W					3	2	2	4
YKR011C	2	1	0	4				
YKU80	4	4	6	5	1	0	0	0
YLL054C	1	2	0	0	2	2	0	1
YLR419W	3	1	0	1	1	0	0	0
YME2	1	0	1	1				
YMR1					3	0	0	0
YMR134W	0	3	2	2	0	0	0	1

YND1					0	1	2	1
YRA1					0	0	2	0
YTA12	1	1	1	0	1	0	1	2
YWL134C					0	3	0	0

S2: NuA4 and glucose deprivation remodel the Pab1-TAP protein interaction network. **A.** Silver stain from replicate 1 that was sent for mass spectrometry analysis. Image representative of 2 replicates. Analysis of results can be found in **Figure 19/20**. **Table A2:** Proteins co-purified with Pab1 are acetylated. The following chart lists acetylation sites found from interactome mass spectrometry data sets. **Table A3:** Complete protein interaction network datasets for both replicates. Numbers representative of total peptide counts.

7.3 S3: *esa1-ts* alters Acc1 acetylation upon shift to 37°C

To determine the impact that Esa1 activity has on Acc1 acetylation, wild type and *esa1-ts* cells expressing Acc1-GFP were harvested both before and after a shift to 37°C (1 hr, 2hr, 3hr, and 4hr). Acc1-GFP was purified, and western blot analysis was completed using acetyl lysine antibodies. *esa1-ts* cells have a reduction in acetylation of Acc1 upon shift to 37°C (**Figure S3**), similar to both NuA4 mutants (**Figure 26**).

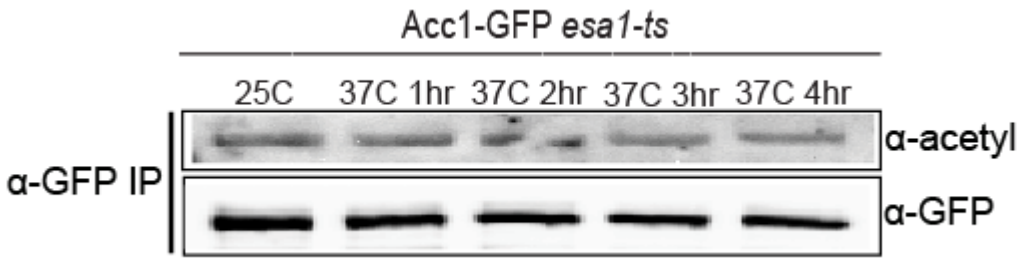

S3: *esa1-ts* alters Acc1 acetylation upon shift to 37°C Exponential-phase (+ glucose) wild type (YKB3954) and *esa1-ts* (YKB4115) cells expressing Acc1-GFP were harvested both before and after a shift to 37°C (1 hr, 2hr, 3hr, and 4hr). *esa1-ts* show a decrease in Acc1 acetylation upon shift to 37°C. 10mg of protein used for IP [80% used for acetyl blot; 10% used for Acc1-GFP IP blot]. Image representative of 2 independent experiments. Antibodies indicated on figure.

8. APPENDIX B

Table B4: Strain list

YKB	Auxotrophies	Reference
1079	*MATa his3Δ1 leu2Δ0 met15Δ0 ura3Δ0*	OpenBiosystems
3114	*MATa his3Δ1 leu2Δ0 met15Δ0 ura3Δ0* PAB1-GFP::HIS	GFP Collection
3336	*MATa his3Δ1 leu2Δ0 met15Δ0 ura3Δ0* PAB1-GFP::HIS *eaf7Δ::KAN*	This Study
4116	*MATa his3Δ1 leu2Δ0 met15Δ0 ura3Δ0* PAB1-GFP::HIS *gcn5Δ::KAN*	This Study
3341	*MATa his3Δ1 leu2Δ0 met15Δ0 ura3Δ0* PAB1-GFP::HIS *rpd3Δ::KAN*	This Study
4118	*MATa his3Δ1 leu2Δ0 met15Δ0 ura3Δ0* PAB1-GFP::HIS *eaf7Δ::KAN gcn5Δ::KAN*	This Study
4117	*MATa his3Δ1 leu2Δ0 met15Δ0 ura3Δ0* PAB1-GFP::HIS *gcn5Δ::NAT rpd3Δ::KAN*	This Study
4016	*MATa his3Δ1 leu2Δ0 met15Δ0 ura3Δ0* PAB1-GFP::HIS *eaf7Δ::KAN rpd3Δ::KAN*	This Study
4120	*MATa his3Δ1 leu2Δ0 met15Δ0 ura3Δ0* PAB1-GFP::HIS *eaf7Δ::KAN gcn5Δ::NAT rpd3Δ::KAN*	This Study
4019	*MATa his3Δ1 leu2Δ0 met15Δ0 ura3Δ0 icl1Δ::KAN*	OpenBiosystems
4010	*MATa his3Δ1 leu2Δ0 met15Δ0 ura3Δ0* PAB1-GFP::HIS *icl1Δ::KAN*	This Study
4047	*MATa* leu2Δ1::tTA-LEU2 trp1-63 ura3-52 tetO7ACC1	Shirra, Patton-Vogt et al. 2001
4048	*MATa* leu2Δ1::tTA-LEU2 trp1-63 ura3-52 tetO7ACC1 *CEN PAB1-GFP::URA3*	This Study
4022	*MATa his3Δ1 leu2Δ0 met15Δ0 ura3Δ0 acs1Δ::HIS3 acs2Δ::HygMX [pHT215, ACS2-Ts1-CEN-URA3]*	Takahashi, McCaffery et al. 2006
4121	*MATa his3Δ1 leu2Δ0 met15Δ0 ura3Δ0 acs1Δ::HIS3 acs2Δ::HygMX [pHT215, ACS2-Ts1-CEN-URA3]* PAB1-GFP::KAN	This Study
4020	*MATa his3Δ1 leu2Δ0 met15Δ0 ura3Δ0 acs2Δ::HygMX [pHT215, ACS2-Ts1-CEN-URA3]*	Takahashi, McCaffery et al. 2006
4122	*MATa his3Δ1 leu2Δ0 met15Δ0 ura3Δ0 acs2Δ::HygMX [pHT215, ACS2-Ts1-CEN-URA3]* PAB1-GFP::KAN	This Study
4132	*MATa his3Δ1 leu2Δ0 met15Δ0 ura3Δ0 acs1Δ::KAN* Pab1-GFP ::HIS	This Study
4154	*MATa his3Δ1 leu2Δ0 met15Δ0 ura3Δ0 acs1Δ::KAN*	OpenBiosystems
1194	*MATa ade2-101 his3Δ200 lys2Δ801 leu2Δ1 ura352 trp1Δ63* PAB1-TAP ::TRP	TAP Collection
1229	*MATa ade2-101 his3Δ200 lys2Δ801 leu2Δ1 ura352 trp1Δ63* PAB1-TAP ::TRP EAF7-MYC ::KAN *eaf1Δ ::KAN*	This Study
3701	*MATa ade2-101 his3Δ200 lys2Δ801 leu2Δ1 ura352 trp1Δ63* PAB1-TAP ::TRP eaf7*Δ ::KAN*	This Study
3934	*MATa ade2-101 his3Δ200 lys2Δ801 leu2Δ1 ura352 trp1Δ63* PAB1-TAP ::TRP ACC1-HA ::HIS	This Study

3933	*MATa ade2-101 his3Δ200 lys2Δ801 leu2Δ1 ura352 trp1Δ63* PAB1-TAP ::TRP ACC1-HA ::HIS eaf7*Δ ::KAN*	This Study
4129	*MATa ade2-101 his3Δ200 lys2Δ801 leu2Δ1 ura352 trp1Δ63* PAB1-TAP ::TRP ACC1-GFP ::HIS	This Study
4130	*MATa ade2-101 his3Δ200 lys2Δ801 leu2Δ1 ura352 trp1Δ63* PAB1-TAP ::TRP eaf7*Δ ::KAN* ACC1-GFP ::HIS	This Study
3954	*MATa his3Δ1 leu2Δ0 met15Δ0 ura3Δ0* ACC1-GFP::HIS	GFP Collection
3930	*MATa his3Δ1 leu2Δ0 met15Δ0 ura3Δ0* ACC1-GFP::HIS eaf7*Δ ::KAN*	This Study
3929	*MATa his3Δ1 leu2Δ0 met15Δ0 ura3Δ0* ACC1-GFP::HIS *eaf1Δ ::KAN*	This Study
4115	his3Δ200 leu2−3Δ112 trp1Δ1 ura3Δ52 ade2Δ101 ACC1-GFP::HIS *esa1ΔHIS3 esa1-L245P::URA3*	This Study
3984	*MATα his3Δ1 leu2Δ0 met15Δ0 ura3Δ0* FAS1-GFP::HIS PAB1-TAP::TRP	This Study
3985	*MATα his3Δ1 leu2Δ0 met15Δ0 ura3Δ0* FAS1-GFP::HIS PAB1-TAP::TRP eaf7*Δ ::KAN*	This Study
3983	*MATa his3Δ1 leu2Δ0 met15Δ0 ura3Δ0* FAS1-GFP::HIS	GFP Collection
4051	*MATa his3Δ1 leu2Δ0 met15Δ0 ura3Δ0* FAS1-GFP::HIS *eaf1Δ ::KAN*	This Study
3875	*MATa his3Δ1 leu2Δ0 met15Δ0 ura3Δ0* ESA1-TAP::HIS	TAP Collection
3292	*MATa his3Δ1 leu2Δ0 met15Δ0 ura3Δ0* eaf7*Δ ::KAN*	OpenBiosystems
3453	*MATa his3Δ1 leu2Δ0 met15Δ0 ura3Δ0* eaf1*Δ ::KAN*	OpenBiosystems

Table B5: Plasmid List

PKB	Other Name	Markers	Reference
PKB192	pRP1362	CEN PAB1-GFP::URA3	Brengues et al. 2007

9. CV

Meaghen Rollins

Education:

Master of Science 2015
- Department of Biochemistry, Microbiology and Immunology
- University of Ottawa
- Supervisor: Dr. Kristin Baetz

Honours Bachelor of Health Science with Minor in Biochemistry 2013
- Department of Health Sciences
- University of Ottawa
- Deans Honours List: 2009-2013

Research Experience:

Master Thesis 2015
- Department of Biochemistry, Microbiology and Immunology
- University of Ottawa
- Characterizing the role of NuA4 in glucose deprivation stress granule assembly and acetyl-CoA signaling in yeast

Summer Student Researcher 2013
- Department of Biochemistry, Microbiology and Immunology
- University of Ottawa

Summer Student Researcher 2012
- National Research Council-Plant Biotechnology Institute
- Saskatoon Saskatchewan
- Contributed to the Total Utilization Flax Genomics (TUFGEN) Program goal of increasing genetic knowledge of flax and improvement of seed and fibre traits.

Summer Student Researcher 2011
- Community Psychiatry Services
- St. Josephs Healthcare Hamilton
- Determining the effectiveness of the Dialectical Behavior Therapy Program for Clients with Borderline Personality Disorder

Presentations:

Department of Biochemistry, Microbiology and Immunology Seminar Day 2015
- University of Ottawa
- Presentation to Faculty Members (Staff and Students)

Department of Biochemistry, Microbiology and Immunology Poster Day 2014
- University of Ottawa
- Poster presentation to Faculty Members (Staff and Students)

Publications:

Barvkar VT, Pardeshi VC, Kale SM, et al. Genome-wide identification and characterization of microRNA genes and their targets in flax (linum usitatissimum) : Characterization of flax miRNA genes. Planta. 2013;237(4):1149-1161.

Academic Awards:

NSERC Canada Graduate Scholarship	2014- Present
University of Ottawa Excellence Scholarship	2014-Present
University of Ottawa Graduate Admissions Scholarship	2013- Present
University of Ottawa Undergraduate Admissions Scholarship	2009-2013
Andy Sheppard Memorial Award	2009
Michelle Kukta Award in Sciences	2009

Citizenship: Canadian